Unified Modeling of Filtration and Expression of Biological Sludge

Sørensen, Peter Borgen

Publication date:
1993

Document Version
Publisher's PDF, also known as Version of record

UNIFIED MODELING OF FILTRATION AND EXPRESSION OF BIOLOGICAL SLUDGE

PETER BORGEN SØRENSEN

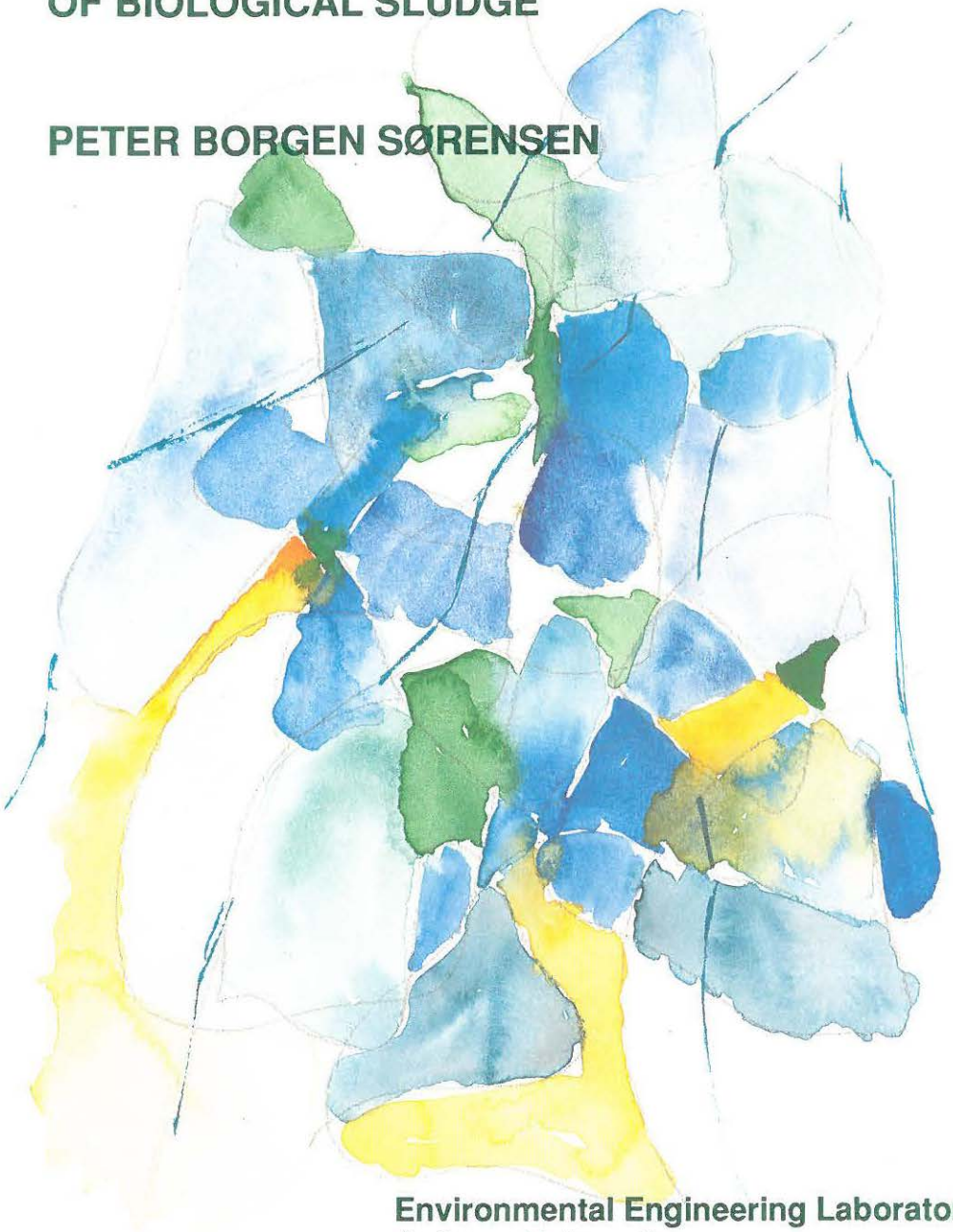

Environmental Engineering Laboratory
Aalborg University
Ph.D. Dissertation, 1992

UNIFIED MODELING OF FILTRATION AND EXPRESSION OF BIOLOGICAL SLUDGE

PETER BORGEN SØRENSEN

Environmental Engineering Laboratory
Aalborg University
Ph.D. Dissertation, 1992

Printed in Denmark by
Centertrykkeriet, Aalborg University, June 1993
ISBN 87-90033-00-0

The Environmental Engineering Laboratory Ph.D. Dissertation Series:

1. PER HALKJÆR NIELSEN. 1988. Svovlbrintedannelse i biofilm fra spildevandsledninger (Hydrogen sulfide formation in biofilm in sewers).

2. PER MØLDRUP. 1990 (minor updating 1993). New methods for modeling transport of water and solutes in soils.

3. SØREN OLE PETERSEN. 1991. Nedbrydning af flydende organisk affald i jord - med særligt henblik på anaerobe processer (Decomposition of liquid organic wastes in soil - with emphasis on anaerobic processes).

4. JACOB H. BRUUS. 1992. Filterability of wastewater sludge flocs.

5. JIMMY ROLAND CHRISTENSEN. 1992. A systematic approach to characterization of sludge conditioning and dewatering.

6. PETER BORGEN SØRENSEN. 1992. Unified modeling of filtration and expression of biological sludge.

UNIFIED MODELING OF FILTRATION AND EXPRESSION OF BIOLOGICAL SLUDGE

FORENET MODELERING AF FILTRATION OG UDPRESNING AF BIOLOGISK SLAM

Ph.D. Dissertation

Short-form thesis and overview

Five supporting papers

Peter Borgen Sørensen

1992

PREFACE

This dissertation is submitted as the requirements for the Doctor of Philosophy (Ph.D.) degree. The dissertation together with five supporting papers constitute the basis for the Ph.D. defense.

The Ph.D. study has been carried out at the Environmental Engineering Laboratory, Dept. of Civil Engineering, Aalborg University, Denmark. The study has been economic supported by The Danish Technical Research Council.

I would like to address my sincere thanks to my supervisor Professor Jens Aage Hansen Env. Eng. Lab., Aalborg University, for help and guidance and for establishing a good environment for research at the institute. Professor George Lee Christensen from Villanova University, USA is acknowledged for being responsible for a good beginning of my project during the first year, where he worked at the Aalborg University as guest professor. I will never forget the visit from the "Elmia Man". A study like this requires daily discussions for testing ideas, and I wish to express my sincere thanks to my colleague Jimmy Roland Christensen for the patient listening to confusing ideas during 3 1/2 years. I would also like to thank assistant professor Per Møldrup Env. Eng. Lab., Aalborg University for help and guidance in the final part of my study.

Aalborg, November 20, 1992

Peter B. Sørensen

LIST OF CONTENTS

Preface 3
Danish abstract (Dansk resume) 7
English abstract 11
Unified modeling of filtration and expression of biological sludge 15
1. Introduction 15
2. Governing equations for the solid/liquid system 17
3. Solution of the governing equations 21
3.1 Analytical solutions 21
3.2 Numerical solutions 25
4. Investigation of biological sludge dewatering 29
4.1 The compressibility of biological sludge solids 29
4.2 Skin formation as a result of extreme compressibility 31
4.3 Small scale solids migration in the filter cake during filtration 35
4.4 Dewaterability characterization by C_e and SRF 37
5. Conclusion 39
6. Notation 41
7. Literature 43
8. Supporting papers 47

DANSK RESUME (DANISH ABSTRACT)

Slamafvanding er en omkostningskrævende operation, dels i industrien, ved afvanding af f.eks. boremudder, havneslam og biomasse, og dels på de offentlige rensningsanlæg ved afvanding af biologisk slam. Praktisk drift og udformning af afvandingsudstyr bygger fortrinsvis på erfaring og empiri, og de opnåede resultater er ofte utilfredsstillende, f. eks. med hensyn til opnået tørstofindhold og kapacitet af et givet udstyr. Der eksisterer altså et stort behov for en teoretisk og teknisk udvikling, baseret på veldefinerede principper og lovmæssigheder, med henblik på opnåelse af forbedringer inden for slamafvanding.

De forskellige afvandingsformer kan groft opdeles i to hovedtyper efter hvilken drivende kraft for afvanding, der anvendes: (1) afvanding vha. gravitationskræfter (centrifugering, sedimentation og afdræning), og (2) afvanding vha. trykkræfter (tryk- og vakuumfiltre, kammerfilterpresser og sibånds presser). Kun afvanding med anvendelse af trykkræfter vil blive behandlet i det følgende.

Den teknisk videnskabelige beskrivelse af afvanding bygger i dette studie på et en-dimensionalt, to-fase (partikel/væske) system. Suspensionen (slammet) er afgrænset på den ene side af et filter medium, der kun er permeabel for væske, og på alle andre sider af impermeable barrierer. Ved afvandingen aflejres partiklerne på filtermediet og former en porøs struktur (filterkage). Så længe der er frie partikler tilstede i suspension, betegnes forløbet filtration. Når alle partikler er inkluderet i filterkagen, betegnes forløbet udpresning.

Ud fra lokal kontinuitet af væske, samt en forudsat lineær sammenhæng mellem væsketrykgradient og væskeflux, formuleres to styrende partielle differentialligninger. Væskefluxen er relateret til spændingen i den porøse struktur (kontakttrykket) vha. en kraftbalance mellem på den ene side det ydre tryk og på den anden side væsketryk og kontakttryk. To randbetingelser er

nødvendige, for en løsning af ligningsystemet og disse består af en beskrivelse af: (1) filterkageoverfladen, og (2) filtermediet. Randbetingelsen for kageoverfladen er formuleret som en aflejring af suspensionspartikler. Aflejringen sker med en rate, der er proportional med den væskeflux, der gennemstrømmer kageoverfladen. Ved udpresning er denne væskeflux nul, hvorfor der ingen kageopbygning foregår. Randbetingelserne ved filtermediet forudsætter lineær sammenhænge mellem væsketrykfald og væskeflux gennem filtermediet (filtratflux). En løsning af dette ligningssystem behøver to funktionelle sammenhænge, der beskriver egenskaber i den porøse struktur, der opbygger filterkagen. Begge disse er forudsat alene relateret til kontakttrykket; den ene vedrører vandindholdet og den anden flow modstanden. Store ændringer i vandindhold og flowmodstand ved en given ændring i kontakttrykket svarer til en stor kompressibilitet.

De partielle differentialligninger kan løses analytisk, hvis filtration og udpresning beskrives som separate fænomener og nogle ekstra begrænsninger indføres. Specifikt for filtration kan der derved udledes en simpel sammenhæng for filtratflux, udfra hvilken den såkaldte specifikke filtermodstand (SRF) defineres som en konstant parameter, der er omvendt proportional med filtratfluxen. For udpresning kan der ligeledes udledes sammenhænge for filtratfluxen, fra hvilken en konstant parameter i form af den såkaldte modificerede konsolideringskoefficient (C_e) defineres. Men, de hidtil kendte analytiske løsninger for udpresning dækker udelukkende situationer, hvor kompressibiliteten er lav eller moderat. Der er derfor med dette arbejde udviklet en semi-analytisk løsning, der gælder for udpresning under forudsætning af høj kompressibilitet. Med de restriktive beregningsforudsætninger og fordi filtration og udpresning i praksis ikke kan adskilles har dette komplette sæt analytiske løsninger dog begrænset praktisk anvendelighed.

For at undgå de forenklende begrænsninger, der er forbundet med analytiske løsninger, er der gennem tiden blevet udviklet en række numeriske løsningsmetoder. Disse har dog bibeholdt

adskillelsen af filtration og udpresning som to separate forløb, hvilket begrænser deres anvendelighed. En forenet numerisk model for beskrivelse af både filtration og udpresning er derfor blevet udviklet. Ved en integrering af differentialligningen, der beskriver de lokale flowforhold, er modellen gjort effektiv, også i tilfælde hvor flowmodstanden i filterkagen udviser meget store variationer grundet stor kompressibilitet. Den udviklede numeriske model, suppleret med den analytiske løsning for filtration, er blevet brugt til at identificere to basale fænomener, der er relevante ved afvanding af biologisk slam.

Det første fænomen er identificeret vha. laboratoriemålinger for både filtration og udpresning, der samstemmende viser, at biologisk slam udviser en så ekstrem stor kompressibilitet, at den ikke kan kvantificeres. Denne ekstreme kompressibilitet betyder dannelse af en slags hud oven på filtermediet. Denne hud optager næsten hele det tryk, der påtrykkes ved afvandingen, og betyder, at filtratfluxen bliver uafhængig af størrelsen af dette tryk. Derudover bevirker huddannelsen, at vandindholdet i filterkagen bliver uforholdsmæssig stort, også efter lang tids udpresning. Dette kan forklare hvorfor tørstof indholdet i en filterkage formet af biologisk slam i praksis sjældent overstiger 25-30 %.

Det andet basale fænomen for afvanding af biologisk slam er blevet identificeret vha. laboratorie målinger for filtration, der viser en flowmodstand, der med tiden vokser så hurtigt, at stigningen ikke alene kan skyldes kageopbygning og kompression. Denne ekstra tilvækst i flowmodstand kan forklares med udgangspunkt i partikel/væske konceptet, hvor biologisk slam i visse tilfælde kan betragtes som bestående af to partikelfraktioner i to forskellige størrelsesordner. Dels store partikler i form af slamflokke og dels små partikler, mest bestående af frie bakterier. Under filtration bygger de store partikler filterkagen op, mens de små partikler trænger ind i filterkagestrukturen og tilstopper denne. En sådan mulig tilstopning bryder med forudsætningerne bag de styrende ligninger da flowmodstanden i sådanne

tilfælde ikke er alene er relateret til kontakttrykket, men også til mængden af småpartikler, der er aflejret i den porøse struktur. En mere generel formulering af de styrende ligninger for at inkludere tilstopnings mekanismen synes nærmest umulig for biologisk slam grundet den høje kompressibilitet. For at få tilstopnings mekanismen kvantificeret, er der derfor blevet udviklet en empirisk metode til beskrivelse af fænomenet.

De analytiske løsninger af de styrende ligninger kan anvendes til afvandingskarakterisering med konstanterne C_e og SRF. Men, specifikt for biologisk slam betyder både den høje kompressibililtet og tilstopningsmekanismen i filterkagen, at der rejses begrundet tvivl om troværdigheden af begge disse konstanter. Kompressibiliteten for biologisk slam er så stor, at den analytiske løsning bag parameteren C_e er ugyldig, hvilket betyder at C_e er ubrugelig som karakteriseringsparameter for afvanding af biologisk slam. SRF regnes for uafhængig af det valgte filtermedie, hvilket er en problematisk forudsætning, fordi den hud, som dannes lige over filtermediet er så tynd at dens areal må afhænge af overfladestrukturen på filtermediet. Derfor vil filtratfluxen og dermed også SRF afhænge af det valgte filtermedie. Samtidig vil en tilstopningsmekanisme i filterkagen betyde, at værdien af SRF vokser under filtration. Dermed kan SRF ikke regnes som en konstant, der karakteriserer filtrationsmodstanden.

Der er med det foreliggende arbejde opnået en betydelig forbedring af det eksisterende modelapparat for filtration og udpresning. Denne forbedring er opnået ved: (1) en forening af filtration og udpresning i en samlet beskrivelse, og (2) en direkte løsning af de styrende ligninger uden andre forudsætninger end dem, der ligger til grund for det basale partikel/-væske system. Specielt i forbindelse med afvandingen af biologisk slam er to basale fænomener identifiseret: (1) en ekstrem høj kompressibilitet af den porøse struktur resulterende i et lavt tørstofindhold i filterkagen, og (2) en tilstopning af den porøse struktur ved penetrering af småpartikler, der resulterer i nedsat filtratflux.

ENGLISH ABSTRACT

Dewatering is a costly operation in both industry, e.g. when dewatering drilling mud, harbor sludge or biomass, and at municipal wastewater treatment plants when dewatering biological sludges. In practice, design and operation of dewatering equipment are mostly based on empirical knowledge, and normally results are not satisfactory, e.g. in terms of cake solids or capacity of equipment. Thus, there is a need for theoretical and technical developments to improve dewatering performance, based on better scientific knowledge and well defined principles and rules.

Separation can be divided into two categories according to the type of driving dewatering force involved: (1) separation by gravity forces (centrifugation, sedimentation, and drainage), and (2) separation by pressure forces (pressure and vacuum filters and belt presses). However, the present study has been confined to dewatering by use of pressure forces.

The technically scientific description of sludge dewatering is based on a one-dimensional, two-phase (solid/liquid) system. The suspension (the sludge) is bounded on one side by a filter medium, permeable only for liquid and on all the other sides by impermeable barriers. During dewatering solids are deposited on the filter medium gradually forming a porous solid structure (filter cake). As long as solids in suspension are present above the filter cake, the dewatering phenomenon is defined as filtration. When all solids are forming a cake, the dewatering phenomenon is defined as expression.

Two governing partial differential equations are formulated based on local continuity of liquid and an assumed linear relationship between the liquid pressure gradient and the liquid flux. The liquid flux is related to the contact pressure in the porous solid structure by a force balance between, on one side, the applied pressure and on the other side the liquid pressure and

contact pressure. Two boundary conditions are needed to solve the governing equations: (1) at the cake surface, and (2) at the filter medium. At the cake surface the deposition rate of solids is assumed proportional to the liquid flux entering the cake surface. During expression this flux is equal to zero and all solids are included in the cake. Through the filter medium a linear relationship is assumed between liquid pressure drop and liquid flux (filtrate flux). A solution of the governing equations requires two functional relationships describing the solid structure forming the cake. Both are assumed to be only a function of the contact pressure, one regarding liquid content and the other flow resistance. Large changes in liquid content and flow resistance for a given change in contact pressures means a high degree of compressibility.

Analytical solutions of the governing equations are available if filtration and expression are described separately and additional restrictions are introduced. Specifically for filtration it is possible to derive a simple relationship for the filtrate flux based on which the so-called specific resistance to filtration (SRF) is defined, as a constant parameter, which is inversely proportional to the filtrate flux. It is also possible to derive analytical relationships for the filtrate flux in case of expression based on which the so-called modified consolidation coefficient (C_e) is defined as a constant parameter. However, so far all analytical solutions for expression are based on an assumption of low or moderate compressibility. Therefore, a semi-analytical relationship has been derived to describe the filtrate flux during expression in which high compressibility is assumed. The practical use of these analytical solutions is, however, limited due to the restrictive assumptions and the calculatory distinction between filtration and expression.

In order to avoid the restrictive assumptions needed in the analytical solutions, several kinds of numerical solution techniques have been suggested. However, these methods still consider filtration and expression separately and, as a conse-

quence, their use is limited. Therefore, a unified numerical model describing both filtration and expression is developed. An integration of the differential equation describing the local flow conditions makes the model effective, also in cases where the flow resistance changes drastically due to a high compressibility. This numerical model and the analytical solution for filtration have been used to identify two important phenomenons relevant for biological sludge dewatering.

The first phenomenon was identified by laboratory measurements of both filtration and expression, which showed that the degree of compressibility of biological sludge solids is extremely high; in fact so high that it is impossible to determine the actual degree. Such extreme compressibility results in formation of a skin just above the filter medium. This skin accounts for a liquid pressure drop nearly equal to the applied pressure and results in a filtrate flux independent on the magnitude of the applied pressure. Furthermore, the skin formation results in a relatively high liquid content in the filter cake, even after a long period of expression. This can explain why the dry matter content of biological sludge filter cakes normally is below 25-30 %.

The second basic phenomenon was identified by laboratory measurements of filtration showing an increase in flow resistance during filtration which was to large to be explained only by cake formation and compression. This additional increase in flow resistance can be explained using the solid/liquid concept, by which biological sludges under some circumstances can be considered as a suspension in which the solids exist in two sizes of different orders in magnitudes. Sludge flocs are defined as large scale solids, while small scale solids are constituted by free bacteria. The large scale solids form the cake during filtration, while the small scale solids penetrates the cake structure and blind the pores. Such blinding phenomenon conflicts with the assumptions for the governing equations, because, in this case, the flow resistance is not only a function of contact

pressure but also a function of the amount of small scale solids deposited in the porous structure. The high compressibility makes a more general formulation of the governing equations for including the blinding mechanism nearly impossible. Therefore, an empirical approach is developed in order to quantify the blinding mechanism.

The analytical solutions of the governing equations normally provide a useful characterization of dewaterability by the constants C_e and SRF. But, in the case of biological sludge dewatering the application of both constants become questionable due to extremely high compressibility as well as due to blinding. The extreme compressibility of biological sludge solids prohibits an analytical solution for derivation of C_e and, therefore, the parameter C_e should not be used in case of biological sludge dewatering. SRF is normally considered independent of the choice of filter medium, which seems a questionable assumption in case of biological sludge dewatering, because the skin formed above the filter medium is so thin that the area is significantly affected by the geometry of the filter medium surface. Therefore, the filtrate flow and, consequently, SRF depends on the choice of filter medium. Furthermore, the blinding phenomenon results in an increasing SRF value during filtration and is as such not a constant parameter characterizing the resistance to filtration.

In the present study, improvements are obtained in modeling filtration and expression by: (1) a unification of filtration and expression in one description, and (2) a solution of the governing equations only based on the assumptions inherent the basic solid/liquid system. In the special case of biological sludge dewatering, two basic phenomenons are identified: (1) extremely high compressibility of the sludge solids forming the cake resulting in a low dry matter content in the finale cake, and (2) blinding of the porous structure in the cake and medium due to small-scale solids penetration resulting in a reduced filtrate flux.

UNIFIED MODELING OF FILTRATION AND EXPRESSION OF BIOLOGICAL SLUDGE

Short-form thesis and overview

1. INTRODUCTION

Solid/liquid suspensions are generated as a result of both industrial production, e.g. in form of drilling mud, harbor sludge or biomass, and at municipal wastewater treatment plants in form of biological sludges. Often a costly separation (dewatering) operation is applied in order to increase the solid content. In practice, design and operation of dewatering equipment are mostly based on empirical knowledge, and results are normally not satisfactory, e.g. in terms of cake solids or capacity of equipment. Thus, there is a need for theoretical and technical developments to improve dewatering performance, based on better scientific knowledge and well defined principles and rules.

In order to establish such well defined principles and rules a physical system is defined. This system consists of a solid-/liquid mixture in which the solids are either in free suspension or packed closely together. The solid/liquid separation implies a movement of solids and liquid with different velocities. Friction occurs between solids and liquid and, therefore, a driving force is needed for the separation to take place. The commonly used separation operations can be divided in two categories related to the type of driving force involved:

1. Separation by gravity forces, where both solid movement through liquid and liquid movement though a porous solid structure are involved. This type of separation includes centrifugation, sedimentation, and drainage.

2. Separation by pressure, where an external force is applied resulting in a liquid flow through a solid porous structure. This type of separation includes vacuum and pressure filters as well as belt presses.

Separation by use of an applied pressure (denoted pressure dewatering) is investigated in this study and a two phase solid/liquid system is used in the basic description.

The key factor in pressure dewatering is the liquid volume contained in the solid/liquid system, which may be defined relative to the cross-sectional area, as a function of time ($\Theta(t)$). Improvements in solid/liquid separation mean minimizing $\Theta(t)$. The volume of liquid released from the solid/liquid system per cross-sectional area is denoted the filtrate volume ($V(t)$), which is related to $\Theta(t)$ by

$$V(t) = \Theta(0) - \Theta(t) \tag{1}$$

where t is time, and $\Theta(0)$ the initial liquid content. Minimizing $\Theta(t)$ mean maximizing $V(t)$. The filtrate flux ($u_m(t)$) is defined by

$$u_m(t) = \frac{dV}{dt} \tag{2}$$

Therefore, a description of the dewatering phenomenon for obtaining operation improvements is given by a determination of $u_m(t)$ for maximizing $V(t)$. It is the object in this dissertation to establish this relationship.

Considered as a one-dimensional phenomenon, the suspension is bounded on one side by a filter medium permeable for only liquid and on all the other sides impermeable barriers. During the dewatering process, a cake is gradually formed above the filter medium. In the cake, the solids are pressed together to form a solid porous structure. As long as free solids are present, the process is called filtration. When all the solids are forming a cake, the process is called expression.

2. GOVERNING EQUATIONS FOR THE SOLID/LIQUID SYSTEM

In order to determine $u_m(t)$ basic equations describing the local properties in the filter cake are derived and the following assumptions made.

1. Dimensions:
   - The phenomenon can be described by one dimensional considerations.
2. Continuity:
   - No mass transport between solids and liquid.
   - No changes in solid or liquid density.
3. Flow description:
   - Laminar (Darcyan) liquid flow.
4. Force balance:
   - No gravity forces in the filter cake.
   - No initial forces.

The formulation of the equations can be either in absolute space coordinates (distance from filter medium), or relative to the position of the solids (material coordinates). Formulation of the governing equations relative to the solid structure (material coordinates) make them simple, because the velocity of solids in the material coordinate system is zero and the only flow is that of the liquid relative to solids. A material coordinate system expressed as volume of solids per cross section area between a given position in the cake and the filter medium (w) is chosen. In the literature a mass related material coordinate system is often based on mass of solids instead of volume of solids. But these are equivalent formulations as long as the density of the solids is assumed constant. In the material coordinate system, it is convenient to express the liquid content as void ratio (e) equal to volume of liquid per volume of solids. In the material coordinate system the relation between e and the liquid flux (u) by continuity is

$$\frac{\partial e}{\partial t}=\frac{\partial u}{\partial w} \tag{3}$$

where u is defined positive towards the medium.

The liquid flux in the filter cake (u) is given by

$$u=\frac{1}{\mu\alpha}\frac{\partial p_l}{\partial w} \tag{4}$$

where μ is the liquid viscosity, α is the flow resistance (specific resistance), and p_l is the liquid pressure. p_l is related to the contact pressure (p_s) by

$$P=p_l+p_s \tag{5}$$

where P is the applied pressure.

The boundary condition at the cake/medium interface is formulated by the liquid flux through the filter medium (u_m), which is equal to the filtrate flux and given by

$$u_m=\frac{p_{lm}}{\mu R_m} \tag{6}$$

where p_{lm} is the liquid pressure (p_l) at the cake/medium interface, and R_m the total flow resistance in the filter medium.

The boundary condition at the cake surface is different for filtration and expression. During filtration the cake surface is open for liquid flow and the change in cake thickness is given by

$$\frac{dw_c}{dt}=\frac{u_{wc}}{e_s-e_0} \tag{7}$$

where w_c is cake thickness in material coordinates, u_{wc} the liquid flux (u) entering the cake surface, e_s the void ration in the suspension, and e_0 the void ratio at the cake surface during filtration. During expression w_c is constant and u_{wc} equal to zero.

Eqs. 3, 4, 5, 6 and 7 represent the basic description of the defined physical system. The parameters P, e_s and e_0 are assumed to be known. Five equations are established but nine dependent variables introduced, i.e. e, u, p_s, p_l, μ, α, u_m, R_m, and w_c. Therefore, four extra equations are needed. These are found through four functional relationships.

1. The void ratio (e) is only a function of contact pressure (p_s)
   => $e(p_s)$
2. The specific resistance (α) is only a function of contact pressure (p_s)
   => $\alpha(p_s)$
3. The liquid flow is Newtonian
   => μ=constant
4. The medium resistance is constant in time
   => R_m=constant

The relationships $e(p_s)$, $\alpha(p_s)$, μ and R_m need to be quantified in order to obtain equations. The functions $e(p_s)$ and $\alpha(p_s)$ describe basic solids properties and are denoted constitutive functions.

The functions $e(p_s)$ and $\alpha(p_s)$ are basically different in their behavior. The void ratio (e) is a decreasing function of the contact pressure (p_s) and the smallest possible value is zero for a totally collapsed porous structure containing no liquid (at infinite high p_s values). In contrast the specific resistance (α) is an increasing function of p_s and will reach infinite values at infinitely high p_s at a totally collapsed and closed porous structure, see Table 1.

Constitutive function	Trend for increasing p_s	Value for $p_s \rightarrow \infty$
$e(p_s)$	decreasing	0
$\alpha(p_s)$	increasing	∞

Table 1. The basic behavior of the constitutive functions.

The degree of compressibility is defined relative to the trend of the constitutive functions. A high degree of compressibility is associated with large changes in functional values.

The literature shows no attempts to determine $e(p_s)$ deterministically. The so-called Kozeny-Carmen relationship could be used to determine $\alpha(p_s)$, but, experimental results show that the description is questionable for pressure dewatering (Tiller, 1975). Therefore, $e(p_s)$ and $\alpha(p_s)$ need to be estimated empirically through functional relationships.

In this study power law functions are chosen according to Tiller and Leu (1980):

$$(1-\varepsilon)=(1-\varepsilon_0)\,(1+\frac{p_s}{p_a})^{\beta} \tag{8}$$

$$\alpha=\alpha_0\,(1+\frac{p_s}{p_a})^{n} \tag{9}$$

where the porosity (ε) is related to e by $e=\varepsilon/(1-\varepsilon)$. In this way, 5 empirical constants are introduced. ε_0 and α_0 have a physical meaning in describing the situation where the solids are just in contact and $p_s=0$ (corresponding to the conditions at the cake surface during filtration); p_a is a scaling factor; and β and n are form constants. It is noticed that Eq. 8 does not satisfy e equal to zero for infinite p_s. Therefore, Eq. 8 should be used with caution to avoid negative e values. As a control Eq. 8 can be rewritten

$$\beta<\frac{\ln(1+e_0)}{\ln(1+\frac{P}{p_a})} \tag{10}$$

where $1+e_0=1/(1-\varepsilon_0)$. β must satisfy Eq. 10 in order to avoid negative e values.

3. SOLUTION OF THE GOVERNING EQUATIONS

3.1 Analytical solutions

Analytical solutions of the governing equations are available if filtration and expression are described separately and additional, sometimes restrictive, assumptions made.

Filtration

In the analytical cake filtration theory (CFT) the following additional assumptions are made (Ruth, 1946) to obtain a solution:

1) Uniform u profile in the filter cake.
2) No sedimentation of suspension solids on the filter cake surface.

Use of these additional assumptions gives

$$u_m = \frac{P}{SRF' \mu C' V + R_m \mu} \tag{11}$$

where

$$SRF' = \frac{P - p_{sm}}{\int_0^{p_{sm}} \frac{1}{\alpha} dp_s} \tag{12}$$

C′ is deposited cake solid volume per unit filtrate volume; SRF′ denotes the specific resistance to filtration; and p_{sm} is the contact pressure at the cake/medium interface. The relationship between u_m and V is given by Eq. 2.

Due to the compressible behavior of the filter cake structure, it is not immediately clear that C′ is a constant. However, using the two additional assumptions mentioned above it can be shown that C′ becomes a constant if $p_{sm} << P$ (Tiller, 1975).

Bockstal et al. (1985) suggested a modification of CFT for cases where C′ is non-constant due to sedimentation of suspension solids on the filter cake surface. They assumed a constant Stoke settling velocity (v_s) of solids. The amount of solids deposited on the cake surface due to filtration was estimated from the

suspension concentration and the filtrate volume. Adopting the notation used in this dissertation, they derived the equation

$$u_m=\frac{P}{\mu\left(\frac{\mu}{2P}(c'SRF')^2 v_s V^2+SRF'c'V+R_m\right)} \qquad (13)$$

where c' is the volume fraction of solids in the suspension. It is noticed that normally a mass related material coordinate system is used to derive the relationships in Eqs. 11, 12 and 13. However, the density of solids (ρ_s) is assumed constant and, therefore, the corresponding parameter values are related (' for volume basis) as follows

$$SRF=SRF'\cdot\frac{1}{\rho_s}\ ,\quad C=C'\cdot\rho_s\ ,\quad c=c'\cdot\rho_s \qquad (14)$$

Expression

Several analytical solutions have been suggested in case of expression.

Shirato et al. (1970) defined the so-called modified coefficient of consolidation as

$$C_e=\frac{-1}{\mu\alpha}\frac{dp_s}{de} \qquad (15)$$

In the analytical expression theory (Shirato, 1986) additional assumptions are necessary for obtaining an analytical solution to the governing partial differential equations:

1) C_e is a constant.
2) No medium resistance (R_m=0).
3) Constant applied pressure (P=constant).

Using assumption 1), Eqs. 3, 4 and 5 give

$$\frac{\partial e}{\partial t}=C_e\frac{\partial^2 e}{\partial w^2} \qquad (16)$$

Two analytical solutions of Eq. 16 are available using assumption

2) and 3) and related to two different initial conditions.

Assuming an initial e profile where $e<e_0$ the solution to Eq. 16 is (Shirato, 1986)

$$V=\frac{4w_c}{\mu\alpha\pi C_e}\sum_{N=1}^{\infty}A_N[1-\exp(-B_N t)] \tag{17}$$

where

$$A_N=\frac{1}{(2N-1)}\left[\frac{2P}{(2N-1)\pi}-\frac{1}{w_c}\int_0^{w_c}p_{s0}\sin\left(\frac{(2N-1)\pi\tau}{2w_c}\right)d\tau\right]$$

and

$$B_N=\frac{(2N-1)^2\pi^2 C_e}{4w_c^2}$$

where p_{s0} is the local contact pressure in relation to the initial e profile. Using Eq. 2, Eq. 17 can be rewritten

$$u_m=\frac{4w_c}{\mu\alpha\pi C_e}\sum_{N=1}^{\infty}A_N B_N \exp(-B_N t) \tag{18}$$

Assuming an initial sinusoidal liquid pressure profile the solution to Eq. 16 is (Shirato, 1986)

$$V=\frac{2w_c P}{\mu\alpha\pi C_e}\left[1-\exp\left(-\frac{\pi^2 C_e t}{4w_c^2}\right)\right] \tag{19}$$

Using Eq. 2, Eq. 19 can be rewritten

$$u_m=\frac{P\pi}{2\mu\alpha w_c}\exp\left(-\frac{\pi^2 C_e}{4w_c^2}t\right) \tag{20}$$

A sinusoidal liquid pressure profile is a good approximation in case of filter cake expression associated with moderately compressible solids (Shirato, 1986).

A semi-analytical solution for filter cake expression is derived (Sørensen et al. a) by assuming:

1) Eqs. 8 and 9 is valid.
2) No medium resistance ($R_m=0$).
3) Strongly convex e profile (extremely high solids compressibility, n>>1 in Eq. 9).

as

$$u_{m,j+1}=\frac{2p_a}{\mu w_c \alpha_0 (1-n)}\left(\left[1+\frac{P}{p_a}\right]^{1-n}-\left[(1-\varepsilon_0)\left(1+e_0-\frac{\Delta t}{w_c}\sum_{N=0}^{j} u_{m,N}\right)\right]^{-\frac{1}{\beta}(1-n)}\right) \quad (21)$$

where $u_{m,j}$ is the filtrate flux at time step j and Δt the time step used in a numerical integration. The initial condition is

$$u_{m,0}=\frac{2p_a}{\mu w_c \alpha_0 (1-n)}\left(\left[1+\frac{P}{p_a}\right]^{1-n}-1\right) \quad (22)$$

The term $[1+P/p_a]^{1-n}$ is close to zero for extremely compressible solids (n>>1), which makes the $u_m(t)$ relationship independent of the actual value of the applied pressure. A short time period of expression has to elapse before Eq. 21 is valid (Sørensen et al. a).

The analytical solution methods are summarized in table 2.

Phenomenon	Reference	Initial conditions	Additional assumptions
Filtration	Ruth (1946)	Suspension	-$R_m=0$* -P=constant* -uniform u profile -no sedimentation of suspension solids on the cake surface
	Bockstal et al. (1985)	Suspension	-$R_m=0$* -P=constant* -uniform u profile -constant settling velocity of suspension solids on the cake surface
Expression	Shirato (1986)	$e<e_0$	-$R_m=0$ -P=constant -C_e=constant
	Shirato (1986)	Cease of filtration	-$R_m=0$ -P=constant -C_e=constant -initial sinusoidal p_l profile (moderately compressibility)
	Sørensen et al., a	Cease of filtration	-$R_m=0$ -Eqs. 8 and 9 valid -strongly convex e profile (extremely high compressibility)

* If SRF is considered as a constant.

Table 2. Summary of analytical solutions for pressure dewatering modeling.

3.2 Numerical solutions

Numerical modeling methodologies are necessary in order to avoid the restrictive, additional assumptions needed in the analytical solutions. Several numerical models have been proposed.

Constant pressure filtration

Several numerical models have been suggested for the special case of constant pressure filtration, where the medium resistance and the sedimentation of solids on the filter cake surface are disregarded. These assumptions make it possible to transform the partial differential equations into an ordinary one and this can be done according to two different principles. Firstly, the transformation is possible using the so-called similarity variable, if the average e value in the cake is assumed constant and the filtrate volume is assumed proportional to $t^{1/2}$. This was

exploited in numerical filtration models by Atsumi and Akiyama (1975) using material coordinates and Wakeman (1978) applying absolute coordinates. Atsumi and Akiyama (1975) solved the resulting ordinary differential equation by a method of moments, while Wakeman used a Runge-Kutta-Nystrom algorithm. Secondly, the transformation of the partial differential equations into an ordinary differential equation is possible if the e value in the filter cake during filtration is assumed to be a unique function of the ratio between the distance to the filter medium and cake thickness (quasi stationary assumption). This was done in a numerical model by Yeh (1985) formulated in material coordinates and he solved the ordinary differential equation by weighted residuals. Instead of transforming the partial differential equations into an ordinary one they are solvable using the Kehoes method if the formulation is done in material coordinates, this was suggested by Tosun (1986).

Expression

Expression in the case of an initially uniform e profile has been modelled numerically by Satoh and Atsumi (1970), Shirato et al. (1971), and Risbud (1974). Satoh and Atsumi (1970) divided the expression phenomenon up into two stages, an early stage in which the total liquid pressure drop across the filter cake is constant, and an later stage in which the total liquid pressure drop decreases. For both periods the resulting equations were solved by a method of moments. Both Shirato (1971) and Risbud (1974) used a finite difference method for solving the governing partial differential equations. A numerical model for expression in case of an initially non-uniform e profile, related to cease of filtration, was presented by Yeh (1985) using the CFT for obtaining the necessary initial conditions. He used the methods of weighted residuals to solve the governing partial differential equations. All four expression models were formulated in material coordinates.

Unified filtration/expression

The local conditions in the filter cake are the same for filtration and expression. It would, therefore, be reasonable and useful to develop one combined description of the physical system in a unified numerical model. That was first done by Wells and Dick (1989) formulating mass balance and flow equations for both liquid and solids. They disregarded the sedimentation of suspension solids on the cake surface. However, their formulation of the equations in absolute coordinates made the numerical calculations unnecessary troublesome due to deformation of the porous matrix. Using material coordinates, the deformation problem is avoided which simplifies the equations (Sørensen et al. a). Both Wells and Dick (1989) and Sørensen et al. (a) used a finite difference technique as solution methodology for the governing equations. But, Sørensen et al. (a) modified the method by integration of the Darcyan flow equation between the spatial grid points in the solution scheme. By this integration, the average specific resistance between the grid points is estimated as the true mean value, also for very compressible solids where the specific resistance exhibits large changes between the grid points. This modification results in a much better description of dewatering of very compressible solids compared to the conventional finite difference method used by Wells and Dick (1989).

The research concerning numerical pressure dewatering modelling is summarized in Table 3.

Phenomenon	Reference	Coordinate system	Initial conditions	Solution method for the governing equations
Constant pressure filtration * and **	Atsumi and Akiyama (1975)	Material	Suspension	Transformation by similarity variable/solution by method of moment
	Wakeman (1978)	Absolute	Suspension	Transformation by similarity variable/solution by Runge-Kutta-Nystrom
	Yeh (1985)	Material	Suspension	Transformation by quasi stationary assumption/Solution by method of weighted residuals
	Tosun (1986)	Material	Suspension	Kehoes method
Expression	Satoh and Atsumi (1970)	Material	Uniform e profile	Method of moment
	Shirato et al. (1971)	Material	Uniform e profile	Finite Difference
	Risbud (1974)	Material	Uniform e profile	Finite Difference
	Yeh (1985)	Material	Cease of filtration	Method of weighted residuals
Unified filtration**/expression	Wells and Dick (1989)	Absolute	Suspension	Finite Difference
	Sørensen et al. (a)	Material	Suspension	Modified Finite Difference

* Disregarding medium resistance
** Disregarding sedimentation of suspension solids on the cake surface.

Table 3. Summary of numerical one-dimensional pressure dewatering modelling.

4. INVESTIGATION OF BIOLOGICAL SLUDGE DEWATERING

Dewatering of inorganic suspensions has been studied and analyzed by a large number of investigators, while only a few have performed theoretically well based studies in dewatering of biological sludges. Often the only parameter used for characterizing dewaterability is SRF which at best considers the filtrate flux during filtration properly. An even more simple dewatering parameter is frequently used: the capillary suction time (CST). The CST apparatus determines the time interval needed extracting a certain filtrate volume by capillary suction of a specific filter paper. However, the filter paper resistance in the CST apparatus is so high that it will often be difficult to characterize the dewaterability of the sludge cake (Christensen et al. 1993). There is consequently a need for improved characterization of biological sludge dewaterability.

In the following an investigation of the basic mechanisms governing the pressure dewatering of biological sludges will be performed. The sludge type used is activated sludge taken from low loaded wastewater treatment plants having nutrient removal.

4.1 The compressibility of biological sludge solids

In order to investigate the compressibility of biological sludge solids the pressure apparatus applied by Christensen et al. (1993) is used to perform filtration experiments. A polyelectrolyte conditioned sludge is filtered using different values of applied pressure (P) and the filtrate flux (u_m) is measured as a function of filtrate volume per cross-sectional area (V). Sample results are shown in Figure 1.

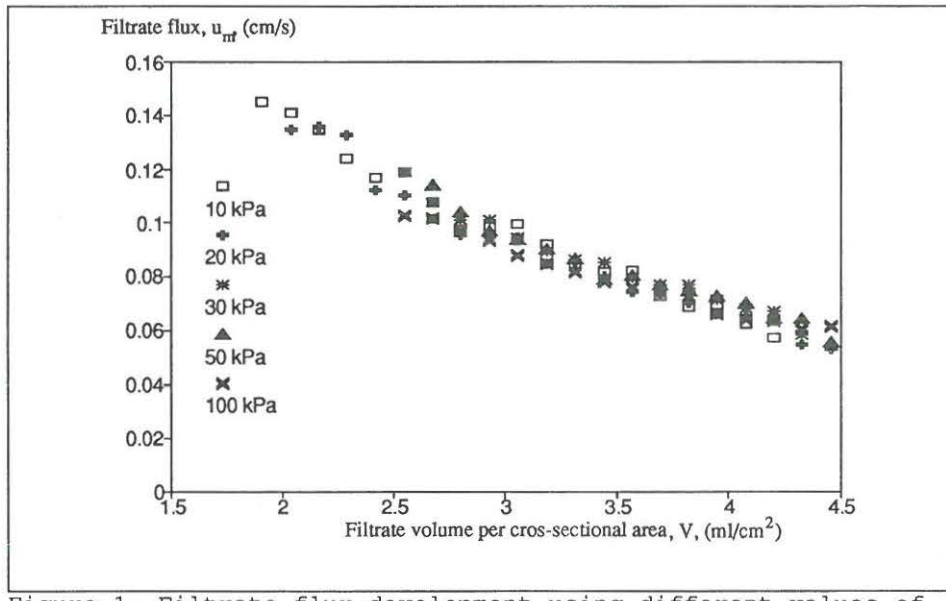

Figure 1. Filtrate flux development using different values of applied pressure for polyelectrolyte conditioned biological sludge.

In case of in-compressible solids Eq. 11 predicts u_m to be proportional to P. However, from Figure 1 it appears, that u_m is virtually independent of P. In order to explain this independence it is necessary to reconsider the influence on u_m of the constitutive functions $e(p_s)$ and $\alpha(p_s)$, which in case of compressible solids may change drastically and thereby influence u_m due to a changed porous structure of the filter cake. A possible relationship between u_m and P based on e and α was suggested by Sørensen and Hansen using the CFT and assuming zero medium resistance

$$\frac{\partial u_m}{\partial P} = \frac{e_s - (e)_{p_s=P}}{\mu V (\alpha)_{p_s=P}} \qquad (23)$$

Use of the relationships in Table 1 and Eq. 23 reveals that

$$\lim \frac{\partial u_m}{\partial P} \rightarrow 0 \quad for \quad P \rightarrow \infty \tag{24}$$

$$\frac{\partial u_m}{\partial P} > 0 \tag{25}$$

So, as P increases, u_m becomes less and less sensitive to the actual value of P. This tendency is more and more marked as the degree of compressibility increases. Also, it is impossible for u_m to decrease as P increases, no matter how compressible the cake is. Therefore, a high degree of compressibility is identified by a filtrate flux independent of the applied pressure. The independence between u_m and P in Figure 1 seems, therefore, to be a result of a high degree of compressibility. It is important to notice that the independence between u_m and P in Figure 1 makes it impossible by these measurements to predict the actual degree of compressibility. It is only possible to predict the minimum degree for obtaining the independence between u_m and P.

A method for determining the n value in Eq. 9 was developed by Tiller and Yeh (1987) using the CFT and assuming zero medium resistance and n>1. Sørensen and Hansen applied this method to the data shown in Figure 1 and the n value for obtaining the independence between u_m and P was determined to be 5 or greater (for p_a=5 kPa). This n value is so high that the polyelectrolyte conditioned biological sludge is denoted extremely compressible (Sørensen and Hansen).

The use of power laws as constitutive functions for such high values of n has never been verified. However, no better form of constitutive functions has been suggested.

4.2. Skin formation as a result of extreme compressibility

Model calculations in this work for pressure dewatering of extremely compressible solids show uniform liquid pressure profile in the filter cake and the total liquid pressure drop taking place in a thin layer immediately above the filter medium.

This is interpreted as a skin formation between the filter cake and the filter medium. During filtration skin formation was reported by Tiller and Green (1973) for latex particles and by Bierck and Dick (1990) for biological sludges. This skin formation was also demonstrated during expression by numerical model calculations and constitutive parameters in Eq. 8 and 9 expressing extremely compressible solids (Sørensen et al. a). This investigation predicted extreme compressibility to result in a liquid pressure in the filter cake which is nearly constant in time and equal to the applied pressure (P), even after a long period of expression. This prediction was investigated by Sørensen and Hansen using an experimental device for filtration and expression. The liquid pressure below the piston was shown to be constant during expression of polyelectrolyte conditioned sludge. The numerical model predictions and the laboratory measurements are in accordance and the unaffected liquid pressure during expression seems, therefore, to be a consequence of the skin formation above the filter medium and the result of extremely high compressibility of the sludge solids.

The skin formation results in a high liquid content in the filter cake during filtration and prevents the liquid from flowing out of the cake structure during expression. The skin formation is, therefore, a reasonable explanation for the relatively low final dry matter content in biological sludge cakes (<25-30 %) observed in practice, even when a longer period of expression is applied.

The existence of the skin is illustrated by calculating the profile of liquid pressure (p_l) or contact pressure (p_s) in the filter cake just above the filter medium. This can be done using an equation relating the absolute distance from the filter medium (x) to the contact pressure (p_s) by using the CFT and Eqs. 8 and 9 (Leu, 1981). If the skin is defined to take up 90 % of the total liquid pressure drop across the cake the skin thickness (x_{90}) can be estimated by modifying this equation as

$$x_{90}=x_c\left(1-\frac{\left(1+\frac{0.1\cdot P}{p_a}\right)^{1-n-\beta}-1}{\left(1+\frac{P}{p_a}\right)^{1-n-\beta}-1}\right) \qquad (26)$$

where x_c is the filter cake thickness. From Eq. 26 it is seen that the skin thickness (x_{90}) is linearly related to the filter cake thickness (x_c), and also a function of the value of the applied pressure (P), and the degree in compressibility (the value of β and n). The skin thickness (x_{90}) is calculated as a function of the applied pressure (P) for the extremely compressible fictitious suspensions suggested by Sørensen et al. (a) (n=5, β=0.5, p_a=5 kPa) where the total cake thickness (x_c) is chosen to be equal to 1 cm, see Figure 2.

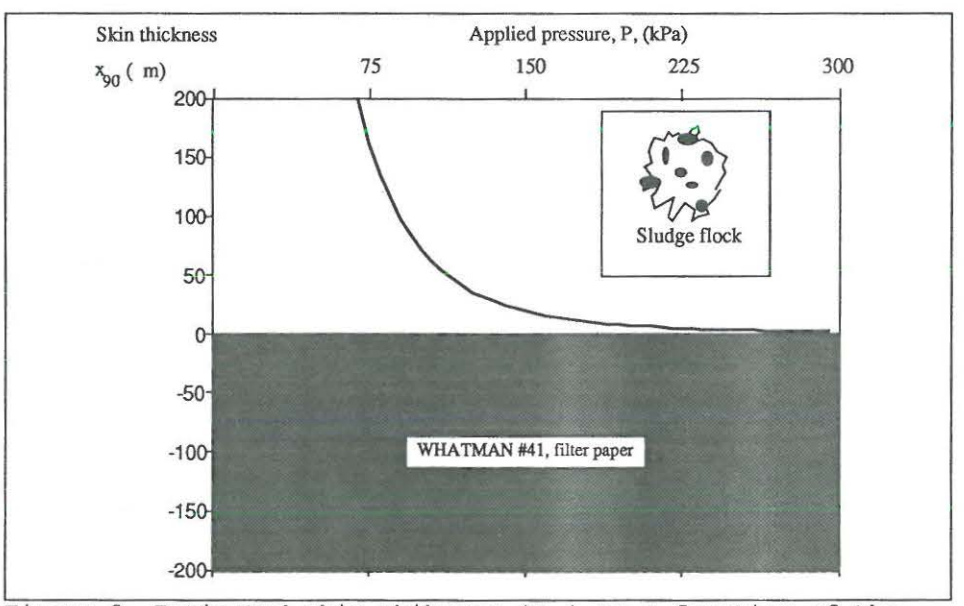

Figure 2. Estimated skin thikness (x_{90}) as a function of the applied pressure (P), using Eq. 26.

The thickness of the filter paper used as filter medium in Figure 1 (Whatman #41) is illustrated in Figure 2 and it is seen that the skin thickness generally is much smaller than the thickness

of the filter paper. Skin thicknesses of a magnitude below 10 µm seems likely.

In the literature attempts have been made to correlate the so-called particle size distribution of biological sludge solids to dewatering performance, typically through SRF laboratory characterization. The particle size measured by a Micro Trac apparatus on a typical, unconditioned biological sludge shows a mean size of the sludge solids around 80-100 µm (Bruss et al.). Such sludge solid size is illustrated in Figure 2 and it is so large that the solids forming the skin must be much smaller. Therefore, it seems impossible to relate the size of the sludge suspension solids directly to dewatering performance. However, the size and numbers of so-called small scale solids of a magnitude of about 1 µm, equal to the size of free bacteria, are more likely to have an effect on pressure dewatering performance.

The skin thickness seems so small that its shape must be affected by the filter paper surface. An investigation of the real shape of the skin could be interesting, but also extremely difficult. A possible picture of the cake/medium interface in Figure 2 is illustrated in Figure 3 and indicates that the separate description of medium and cake properties, as made in the governing equations, is questionable in case of biological sludge dewatering modeling.

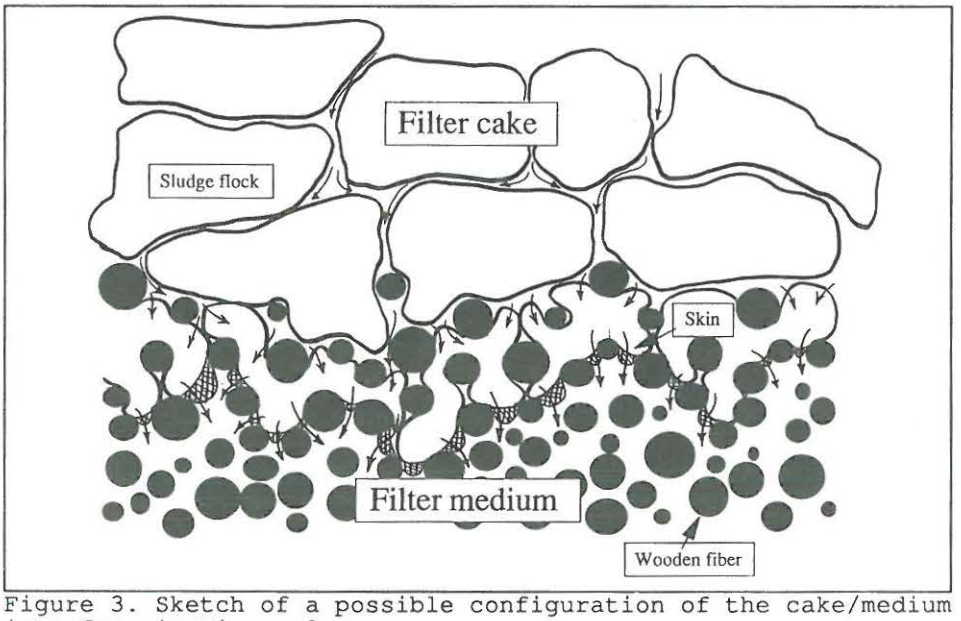

Figure 3. Sketch of a possible configuration of the cake/medium interface in Figure 2.

4.3 Small scale solids migration in the filter cake during filtration

Sørensen et al. (b) showed that during anaerobic storage of biological sludges a decrease in filterability was accompanied by concave filtration plots relating dt/dV (equal to $1/u_m$) and V during filtration. A similar tendency was shown by Novak et al. (1988). The following explanations for such kind of non-linear filtration plots are suggested in relation to Eq. 11:

1. Sedimentation of suspension solids on the filter cake surface simultaneous with filtration and resulting in a increasing C′ value in time.

2. Blinding of the porous structure in the filter cake or medium due to migration of small scale solids and resulting in an increasing SRF or R_m value in time.

Concave filtration plots were attributed to sedimentation by Bockstal et al. (1985) and to blinding by Notebaert et al. (1975); Tiller et al. (1981); Leu and Tiller (1983); Novak et al. (1988), Sørensen et al. (b). The blinding mechanism conflicts with the basic assumption concerning the specific resistance (α) to be a function of only p_s and R_m to be constant in time. Due to the deformation of the cake solid structure a deterministic description of the blinding mechanism will result in a very complicated theory. The blinding mechanism has, therefore, only been investigated empirically by all the investigators mentioned.

A systematic and empirical analysis of concave filtration plots was carried out by Sørensen et al. (b) using a polynomium of arbitrary order. A regression analysis showed that the non-linear behavior could be completely described by

$$\frac{dt}{dV}=a_2V^2+a_1V+a_0 \tag{27}$$

Eq. 13, which describes filtration and simultaneous sedimentation, can be rewritten to the same form as Eq. 27. Therefore, sedimentation of suspension solids on the filter cake surface could be the explanation to the concave filtration plots. However, extensive investigations reject the sedimentation hypothesis and the blinding mechanism seems to be more reasonable (Sørensen et al. b).

In order to characterize the influence of blinding, the filtrate volume (V_b) at which the ratio between resistance due to blinding and resistance due to unblinded cake is unity was estimated using Eq. 27 (Sørensen et al. b)

$$V_b=\frac{a_1}{a_2} \tag{28}$$

After about one week of anaerobic storage, though, the blinding influence was shown to be nearly constant for unconditioned sludge yielding a V_b value of about 2 ml/cm^2.

The derivation of V_b is based on the assumption that the resistance associated with blinding and unblinded cake structure, respectively, can be separated by Eq. 27. This is a rather unproven assumption and therefore V_b must be considered an interesting concept rather than a real number characterizing the actual physical system. However, the correlation between the number of small scale solids and a_2 was much better than the same correlation for a_1, which indicates some physical reality behind V_b, Sørensen et al. b.

Considering filtration of polyelectrolyte conditioned sludge, it occurs that the parameter a_2 in Eq. 27 decreases as the polymer dose increases. The quantity $a_2=0$ seems to be useful for identification of the optimal dosages of conditioning chemicals (Christensen and Sørensen). The quantity $a_2=0$ in relation to sludge conditioning can be physically explained as the situation where all small scale solids are coagulated by conditioning chemicals.

4.4 Dewaterability characterization by C_e and SRF

Two dewaterability characterization parameters are defined by analytical solutions of the governing partial differential equations. The modified coefficient of consolidation (C_e) as obtained from Eqs. 17, 18, 19 and 20, and the specific resistance to filtration (SRF) as obtained from Eqs. 11 and 14. In case of biological sludge dewatering the solid compressibility is high. Therefore, the assumptions of constant C_e governing Eqs. 17, 18, 19 and 20 are not valid, and C_e should not be used to characterize dewatering of biological sludge.

SRF is often used as the only dewatering characterization parameter for biological sludge. However, SRF characterize only the magnitude of the filtrate flux during filtration and not the liquid content in the cake or the filtrate flux during expression. Therefore, SRF is insufficient to give a complete characterization of the dewatering operation (Sørensen et al. a).

The distinction between cake and medium properties in the basic solid/liquid system is reflected in Eq. 11 and the value of SRF is, thereby, assumed independent of the geometry of the filter medium. but due to the a skin formation as illustrated in Figure 3, the SRF value may be directly affected by the surface geometry of the filter medium. This hypothesis is supported by measurements done by Tosun et al. showing a dependency between SRF and the type of filter medium.

SRF will normally be proportional to the applied pressure (P) due to the high compressibility and from a theoretical view point it is impossible for the SRF value to increase more than proportional to P (Sørensen and Hansen, b). However, the literature reports on cases of SRF increasing above proportionality to P. This illustrates the deficiency of SRF regarding dewatering characterization, rather than errors in the measurements reported. Furthermore, in case of blinding the SRF value increases during filtration because of the convex filtration plot. The SRF parameter is, therefore, in such situations, not a constant characterizing the resistance to filtration.

5. CONCLUSION

A unified numerical pressure dewatering model has been established. It seems useful, in theoretical and practical situations, because it handles data from both filtration and expression as they actual appear from laboratory experiments and full-scale operation.

Biological sludge from wastewater treatment has been specifically studied. On the one hand the model developed gives satisfactory dewatering description when assuming extremely high compressibility of sludge solids. I.e. the model seems able to predict pressure dewatering if the sludge solids can be characterized correctly regarding compressibility. On the other hand, solid compressibility has been identified as a topic worthy of more research. The constitutive functions used in this work to characterize compressibility were derived by other researchers for less compressible solids and the extrapolations done need validation. More work to develop other and better methods of characterizing compressible solids may be necessary, before satisfactory modeling can be accomplished.

Pressure dewatering of biological sludge implies the formation of a thin skin over the filter medium. In this skin nearly all the liquid pressure drop takes place and it is a major reason why dewatering becomes time-consuming and renders sludge cakes low in dry matter content, e.g. 25-30 %. The skin identifies a very concrete technical challenge. Finding a way of breaking it may greatly enhance the rate of dewatering of biological sludge.

Blinding, i.e. penetration of small scale solids e.g. 1 μm, into the porous structure of the filter cake and the filter medium, seems a plausible explanation for maybe half the resistance to pressure dewatering of biological sludge. However, conditioning can partly eliminate blinding from influencing the dewatering performance and a totally elimination seems identical to the optimal dosage of conditioning chemicals.

The extensive use of SRF -specific resistance to filtration- in dewaterability characterization of biological sludges seems not justified due to: (1) the actual value is dependent on the choice of filter medium due to the skin formation, and (2) the blinding phenomenon prohibits a determination of a SRF value as a constant.

6. NOTATION

A_N	Coefficient in Eqs. 17, 18.
a_i	Coefficient in Eq. 27 for the term of degree i.
B_N	Coefficient in Eqs. 17, 18.
C	Deposited mass of cake solids on the filter cake surface per unit filtrate volume (kg/m^3).
C′	Deposited volume of cake solids on the filter cake surface per unit filtrate volume (m^3/m^3).
C_e	Modified consolidation coefficient (m^2/s).
c	Slurry concentration (kg/m^3).
c′	Volume fraction of suspension solids (m^3/m^3).
e	Volume of liquid per volume of solid (void ratio).
e_s	Void ratio of the suspension.
e_0	Void ratio when the solids are just in contact and $p_s=0$ (void ratio at filter cake surface during filtration).
j	Time step number.
N	Enumerator in Eqs. 17, 18 and 21.
n	Form factor for the compressibility with respect to specific resistance.
P	Applied pressure (Pa).
p_a	Scaling factor (Pa).
p_l	Liquid pressure taken as an average over the cross section area (Pa).
p_{lm}	Liquid pressure at the cake/medium interface (Pa).
p_s	Solid pressure (contact pressure) taken as an average over the cross section area (Pa).
p_{sm}	Contact pressure at the medium/cake interface (Pa).
p_{s0}	Initial contact pressure (Pa).
R_m	Total flow resistance in filter medium (1/m).
SRF	Specific Resistance to Filtration defined by mass related material coordinates (m/kg).
SRF′	Specific Resistance to Filtration defined by volume related material coordinates ($1/m^2$).
t	Time (s).
Δt	Time step used in the solution scheme (s).
u	Liquid flux relative to solids (m/s).

u_m	Liquid flux through the medium (filtrate flux), (m/s).
u_{wc}	Liquid flux through the cake surface (m/s).
V	Filtrate volume per unit cross-sectional area (m^3/m^2).
V_b	Filtrate volume per unit cross-sectional area at which the resistance from blinding equals the unblinded cake resistance (m^3/m^2).
v_s	Stoke settling velocity of solids (m/s).
w	Material coordinate (solid volume per cross section area) (m^3/m^2).
w_c	Total solid volume per cross section area in the filter cake (m^3/m^2).
x_c	Cake thickness in absolute coordinates, m.
x_{90}	Skin thickness in absolute coordinates (m).

Greek Letters

α	Specific resistance ($1/m^2$).
α_0	Specific resistance when solids are just in contact and $p_s=0$ (specific resistance at the cake surface during filtration) ($1/m^2$).
β	Form factor for the compressibility with respect to the porosity.
ε	Porosity.
ε_0	Porosity when solids are just in contact and $p_s=0$ (porosity at the cake surface during filtration).
Θ	Liquid volume in the solid/liquid system per cross-sectional area (m^3/m^2).
μ	Viscosity of liquid (kg/ms).
ρ_s	Density of the solids (kg/m^3).

Abbreviations

CFT	Cake filtration theory.
CST	Capillary suction time.
SRF	Specific resistance to filtration.

7. LITERATURE

Atsumi, K., and T. Akiyama (1975) "A Study of Cake Filtration - Formulation as a Stefan Problem", *J. Chem. Eng. Japan*, Vol. 8, No. 6, pp. 487-492.

Bierck, B.R., and R. I. Dick (1990) "In Situ Examination of Effects of Pressure Differential on Compressible Cake Filtration", *The International Association on Water Pollution Research and Control*, 1990 Sludge Management Conference at Los Angeles California.

Bockstal, F., F. Fouarge, J. Hermia and G. Rahier (1985) "Constant Pressure Cake Filtration with Simultaneous Sedimentation". *Filt. & Sep.*, **22**, pp. 255.

Bruss, J.H., Christensen, J.R., and Rasmussen, H:, "Anaerobic Storage of Activated Sludge: Effects on Conditioning and Dewatering Performance", *Wat. Sci. Tech.* (submitted June 1992).

Christensen, J.R., Sørensen, P.B., Christensen, G.L., Hansen J.Aa. (1993) "Mechanisms for Overdosing in Sludge Conditioning", *J. Env. Eng.*, ASCE, Vol. 119, No. 1, pp. XX-XX (in press)

Christensen, J.R. and Sørensen, P.B.,"Control of Polymer Sludge Conditioning", (Working paper, Env.Eng.Lab., Aalborg Uni.)

Leu, W. (1981)"Cake Filtration", Ph. D. Dissertation, Univ. of Houston.

Leu, W., and Tiller, F.M. (1983) "Experimental Study of the Mechanism of Constant Pressure Cake Filtration: Clogging of Filter Media", *Sep. Sci. Tech.*, Vol. 18, pp. 1351.

Notebaert, F.F., D.A. Wilms and A.A. Van Haute (1975) A New "Deduction with a Larger Application of The Specific Resistance to Filtration of Sludges", *Water Res.*, Vol. 9, pp. 667.

Novak, J.T., G.L. Goodman, A. Pariroo and J. Huang (1988) "The Blinding of Sludges During Filtration", *J. Water Pollut. Control Fed.*, **60**, pp. 206.

Risbud, H. M. (1974) "Mechanical Expression, Stress at Cake Boundaries, and New Compression-Permeability Cell,"Ph.D. Dissertation, Univ. of Houston.

Ruth, B. F. (1946) "Correlating Filtration Theory with Industrial Practice", *Industrial and Engineering Chemistry*, Vol. 38, No. 6, pp. 564-571.

Satoh, T., and K. Atsumi (1970) "Forced Expression of Liquid from Pasty Mixture of Liquid and Fine Solid Particles and its Numerical Solution by Method of Moments", *J. Chem. Eng. Japan*, Vol. 3, No. 1., pp. 92-98.

Shirato, M., T. Murase, H. Kato, and S. Fukaya (1970) "Fundamental Analysis for Expression under Constant Pressure", *Filt. & Sep.*, Vol. 7, pp. 277-282.

Shirato, M., T. Murase, M. Negawa, and H. Moridera (1971) "Analysis of Expression Operations", *J. Chem. Eng. Japan*, Vol. 4, No. 3, pp. 263-268.

Shirato, M., (1986) "Deliquoring by Expression - Theory and Practice", in *Progress in Filtration and Separation*, ed. by Wakeman, R.J, Elsevier Amstadam, pp. 181-287.

Sørensen, P.B., Moldrup, P., Hansen, J.Aa. (a) "Unified Filtration/Expression Modelling by Finite Differences", *AIChE J.* (for submission, November 1992).

Sørensen, P.B. and Hansen, J.Aa "Extreme Compressibility in Biological Sludge Dewatering", *Water Sci. Tech.* (accepted, October 1992).

Sørensen, P.B, Christensen, J.R., and Bruus, J.H. (b) "Effect of Small Scale Solids Migration in Filter Cakes during Filtration of Wastewater Solids Suspensions", *Wat. Env. Res.*, (for submission, November 1992).

Tiller, F. M., and T. C. Green (1973) "Role of Porosity in Filtration IX Skin Effect with Highly Compressible Materials", *AIChE J.* Vol. 19, No. 6., pp. 1266-1269.

Tiller, F.M. (1975) "Compressible Cake Filtration" in *Scientific Basis of Filtration*, ed. by Ives K.J., Noordhoff, London, pp. 315-397.

Tiller, F. M., and W. F. Leu (1980) "Basic Data Fitting in Filtration", *Journal of The Chinese Institute of Chemical Engineers*, Vol. 11, pp. 61-70.

Tiller, F.M., *et al.* (1981) "Clogging Phenomena in the Filtration of Liquefied Coal", *Chem. Eng. Progress*, **77**, 61.

Tiller, F. M. and C. S. Yeh (1987)"The Role of Porosity in Filtration, Part XI: Filtration Followed by Expression", *AIChE J.*, Vol. 33, No.8., pp. 1241-1256.

Tosun, I. (1986) "Formulation of Cake Filtration", *Chem. Eng. Sci.*, Vol. 41, No. 10, pp. 2563-2568.

Tosun, I., Yetis, U., Willis, M.S., and George G.C. "Specific Cake Resistance: Myth or Reality", *Wat. Sci. Tech.* (Submitted).

Wakeman, R. J. (1978) "A Numerical Integration of the Differential Equations Describing the Formation of and Flow in Compressible Filter Cakes", *Trans IChemE*, Vol. 56., pp. 258-265.

Wells, S. A., and R.I.Dick (1989) "Mathematical Modelling of Compressible Cake Filtration", *Proceedings of the 1989 Specialty Conference, Austin, Texas, July 10-12.*

Yeh, S. (1985) "Cake Deliquoring and Radial Filtration", *Ph. D. Dissertation, Univ. of Houston.*

8. SUPPORTING PAPERS

Paper no. I

Sørensen, P.B., Moldrup, P., Hansen, J.Aa. (a), "Unified Filtration/Expression Modelling by Finite Differences", American Institute of Chemical Engineers (for submission, February 1993).

Paper no. II

Sørensen, P.B. and Hansen, J.Aa, "Extreme Compressibility in Biological Sludge Dewatering", Water Science and Technology (accepted, October 1992).

Paper no. III

Sørensen, P.B, Christensen, J.R., and Bruus, J.H. (b), "Effect of Small Scale Solids Migration in Filter Cakes during Filtration of Wastewater Solids Suspensions", Water Environment Research, (for submission, December 1992).

Paper no. IV

Christensen, J.R., Sørensen, P.B., Christensen, G.L., Hansen J.Aa. (1993), "Mechanisms for Overdosing in Sludge Conditioning", Journal of Environmental Engineering, ASCE, Vol. 119, No. 1, pp. 159-171.

Paper no. V

Christensen, J.R. and Sørensen, P.B., "Control of Polymer Sludge Conditioning" (Working paper)

Unified Filtration/Expression Modelling by Finite Differences

I

UNIFIED MODELING OF FILTRATION AND EXPRESSION BY FINITE DIFFERENCES

P. B. Sørensen, P. Moldrup and J. AA. Hansen

Environmental Engineering Laboratory, Dept. of Civil Engineering, Aalborg University, Sohngaardsholmsvej 57, DK-9000 Aalborg, Denmark

KEYWORDS

numerical modeling, pressure dewatering, compressible solids, biological sludge, skin formation.

ABSTRACT

This study presents a numerical model for sludge dewatering, covering both filtration and expression. A simple and easy to solve model for the solid/liquid system is obtained by formulating the basic flux and continuity equations in material coordinates. A modified finite difference solution method is used. A precise determination of the flow resistance between the spatial node points in the solution scheme is obtained for even extremely compressible sludge types by integration of the liquid flux equation with respect to cake thickness. Model calculations show that the extreme compressibility typical for biological solids results in the formation of a skin above the filter medium. This skin becomes limiting to liquid release from the cake during expression. It is also shown that the degree of solid compressibility governs the void ratio profile in the filter cake. In the case of expression and extreme compressibility of solids, an approximate semi-analytical solution describing the measurable relationship between filtrate flux and time is derived. The numerical model for unified filtration and expression seems promising to further improve the understanding and control of dewatering of biological sludges as well as other porous media consisting of compressible solids.

INTRODUCTION

Mechanical dewatering is a costly operation in municipal wastewater treatment plants and many industries. Therefore, improvements in optimization are of great interest and must be based on the ability to correctly describe and model the dewatering mechanisms.

Sludge can be described physically as a solid/liquid mixture where the solids are either in free suspension or packed closely together. The purpose of mechanical dewatering is to separate solids and liquid through application of pressure, below or above atmosphere pressure. Considered as an one-dimensional phenomenon, the mixture is bounded on the one side by an impermeable barrier and on the other side by a filter medium, permeable only for liquid, Figure 1. During the dewatering operation, a cake is formed gradually above the filter medium. In the cake, the solids are pressed together to form a porous solid structure. As long as free solids are present, the operation is called **filtration**. When all the solids are forming a cake, the operation is called **expression**, Figure 1.

Physical considerations will include mass balance of liquid, force balance between applied pressure, contact pressure and liquid pressure, and considerations about the liquid flow (as flux or velocity) in the porous structure and the filter medium. From this, a **governing partial differential equation** for the solid/liquid system is formulated. The formulation can be either in absolute coordinates (distance from filter medium), Figure 1.a, or in material coordinates, i.e. relative to the position of the solids, Figure 1.b. In the governing equation, **constitutive functions** are needed to describe the local relationships between flow resistance, liquid content, and contact pressure in the filter cake. These relations must be established before the governing equation can be solved. The sensitivity of flow resistance and liquid content to contact pressure is denoted compressibility. It is the key factor in determining the basic behavior of the dewatering phenomenon. High compressibility means that flow resistance and liquid content are very sensitive to changes in contact pressure.

A number of analytical solutions for filtration and expression have been suggested. An analytical model that describes filtration and assumes constant liquid velocity through the cake was presented by Ruth (1946). However, the liquid velocity is not constant because of release of liquid from the porous structure due to local compression. Shirato et al. (1970) presented an analytical model for expression assuming both constant flow resistance and linear elastic behavior of the porous structure. Often, however, the deformation of the porous structure during expression is fairly large which causes the flow resistance to change and the elastic behavior to be nonlinear.

Analytical solutions are based on assumptions that are restrictive and sometimes conflicting with reality. In contrast, **numerical models** do not need these restrictive assumptions and may, therefore, be in better accordance with the actual sludge dewatering phenomenon. Several numerical models for filtration and expression have been proposed.

When only filtration is considered and when the liquid pressure drop across the cake is assumed constant (constant pressure filtration), it is possible to transform the governing partial differential equation into an ordinary differential equation, which may be simple to solve numerically. The constant liquid pressure drop across the cake implies constant applied pressure and insignificant filter medium resistance. The transformation of the partial differential equation into an ordinary one can be obtained according to two different principles. In the one case the transformation is possible if the average liquid content in the cake is assumed constant and the filtrate volume proportional to $t^{1/2}$. This was exploited in numerical filtration models by Atsumi and Akiyama (1975) using material coordinates and Wakeman (1978) applying absolute coordinates. It is noticed that Tosun (1986) showed a flaw in the development of the boundary condition at the cake surface in the governing equation derived by Wakeman (1978). In the other case, the liquid content in the filter cake is assumed a unique function of the ratio between distance to filter medium and cake thickness (quasi stationary situation). This was done in a

numerical model by Yeh (1985) and formulated in material coordinates. As an alternative to the transformations the so-called Kehos method can be applied to solve the governing partial differential equations using material coordinates (Tosun, 1986).

Expression in the case of initially uniform liquid content has been modeled numerically by Satoh and Atsumi (1970), Shirato et al. (1971), and Risbud (1974). A numerical model for expression was also presented by Yeh (1985) using the analytical filtration theory for obtaining the necessary initial conditions. All four expression models were formulated in material coordinates.

It is advantageous to combine filtration and expression in one unified numerical model, because local conditions regarding contact pressure, solid compressibility and flow resistance are identical in both cases. This was first done by Wells and Dick (1989) formulating mass balance and flow equations for both liquid and solids. However, their formulation of the equations in absolute coordinates made the numerical calculations troublesome due to the deformation of the solid cake structure. Using material coordinates, the deformation problem is avoided which simplifies the equations.

There seems to be a need for a numerically simple model based on a general physical formulation of filtration and expression and subject only to assumptions inherent in the basic flux and continuity equation for the solid/liquid system. In this study such numerical model is developed. A material coordinate system is used to obtain a simple and easy to solve model.

GOVERNING EQUATIONS

During the dewatering operation, the deformation of the cake causes a flow of both liquid and solids towards the medium. The accelerations are sufficiently small that the forces involved can be neglected. Formulation of the governing equations relative to the solid structure (material coordinates) makes them simple because the velocity of solids in the material coordinate system is zero and the only flow is that of liquid relative to solids. A one-dimensional material coordinate system (w) is chosen, ex-

pressing volume of solids per cross section area between a given position in the cake and the filter medium, Figure 1.b. In the literature, w is often defined as mass of solids instead of volume of solids which are equivalent formulations, given constant density of the solids. The porous structure is considered a continuum which allows an averaging of forces and liquid velocities over the cross section area.

In the material coordinate system, it is convenient to express the liquid content as void ratio (e) equal to volume of liquid per volume of solids. The liquid flux (u) is subsequently defined relative to the material coordinate system. The relation between e and u is by continuity

$$\frac{\partial e}{\partial t}=\frac{\partial u}{\partial w} \tag{1}$$

where u is defined positive towards the medium. It is noticed that $u=q-eq_s$, where q is the liquid flux and q_s is the solid flux, both relative to absolute coordinates.

The relative liquid flux is assumed Darcyan (Shirato et al., 1969),

$$u=\frac{1}{\mu\alpha}\frac{\partial p_l}{\partial w} \tag{2}$$

where μ is the liquid viscosity (assumed constant), α is the flow resistance (specific resistance), and p_l is the liquid pressure taken as an average over the cross section area. A contact pressure (p_s) describing the contact force between the solids is defined. If gravity is neglected, p_l and p_s are related to each other and the applied pressure (P) by

$$P=p_l+p_s \tag{3}$$

Combining Eqs. 2 and 3 and remembering that P is constant with respect to w gives

$$u=\frac{1}{\mu\alpha}\frac{\partial (P-p_s)}{\partial w}=\frac{-1}{\mu\alpha}\frac{\partial p_s}{\partial w} \tag{4}$$

It is assumed that α, p_s and e are related by unique constitutive functions.

The flux through the filter medium (u_m) is assumed Darcyan,

$$u_m=\frac{1}{\mu R_m}p_{lm} \tag{5}$$

where R_m is the total resistance in the medium (assumed constant), and p_{lm} is the liquid pressure at the cake/medium interface.

In case of filtration, the cake thickness expressed in material coordinates (w_c) needs to be determined. The void ratio in the suspension is denoted e_s and at the cake surface e_0. Both void ratios are assumed constant and the deposition of solids on the cake surface due to sedimentation is neglected. During the time increment dt, the filter cake is extended with a new cake segment of length dw_c. Hence, the segment dw_c goes from being in suspension at time t to being part of the filter cake at time t+dt. The volume of liquid released from the element dw_c during dt is equal to the liquid content in the element at time t minus the liquid content at time t+dt. Hence,

$$\int_t^{t+dt} u(w_c,\tau)\,d\tau=e_s dw_c-\int_{w_c}^{w_c+dw_c} e(w,t+dt)\,dw \tag{6}$$

When dt and dw_c are infinitesimal, Eq. 6 becomes

$$\frac{dw_c}{dt}=\frac{u_{wc}}{e_s-e_0} \tag{7}$$

where

$$u_{wc}=\frac{-1}{\mu\alpha_0}\left(\frac{\partial p_s}{\partial w}\right)_{w=w_c} \tag{8}$$

u_{wc} being the liquid flux and α_0 the specific resistance on the cake surface.

During expression, the cake includes the total volume of solids, so w_c is a constant equal to w_{tot} (see Figure 1.b) and u_{wc} is zero.

Eqs. 1-8 represent the description of the defined physical system. Eqs. 1 and 4 are the basic governing equations for liquid

continuity and flux. The presented partial differential equations can only be solved numerically due to the functional relationships between α, p_s and e which make Eq. 4 nonlinear and, also, due to the moving boundary at the cake surface during filtration and the non-constant boundary condition at the filter medium; both being depending on the main variables (e and u). A modified finite difference solution methodology is developed to solve these equations.

NUMERICAL MODEL

The finite difference (FD) solution method is chosen to solve the model equations as it is simple and physically comprehensible. In the FD solution scheme, the cake is divided into segments (grids). The orientation of the solution scheme is upward from the filter medium towards the cake surface.

The grids in the solution scheme are chosen so that the values of e and u are determined alternately by use of so-called displaced grids (Harlow and Welch, 1965), i.e., the neighbor points of an e point are u points, see Figure 2. Within the cake, 2I intervals of constant, equal length (Δw) are defined, separating the e and u points. A u point is placed both at the medium/cake interface and at the cake surface in order to calculate the change in cake thickness according to Eq. 7.

The continuity equation (1) is discretisized as a central space and time approximation of u around an e point, Figure 2. This gives the following FD approximation for e_I^{j+1},

$$e_I^{j+1}=e_I^j-\frac{\Delta t}{2\Delta w}(\overline{u}_{i+1/2}-\overline{u}_{i-1/2}) \qquad (9)$$

where

$$\overline{u}_{i+1/2}=\frac{1}{2}(u_{I+1/2}^{j}+u_{I+1/2}^{j+1}) \qquad (10)$$

and where the superscript j denotes time, the subscript i denotes cake distance (from the filter medium), and Δt is the time increment. The mean flux ($\overline{u}_{i+1/2}$) is chosen estimated by a simple

arithmetic mean value (Eq. 10). A more precise averaging is not needed because of relative small gradients in u during time.

In order to formulate the flow equation (4) in the solution scheme, the best central space estimate for $u_{i+1/2}^{j+1}$ is the average value between e_i^{j+1} and e_{i+1}^{j+1} (see Figure 2) represented by

$$u_{i+1/2}^{j+1}=\frac{1}{2\Delta w}\int_{\Delta w(2i-1)}^{\Delta w(2i+1)} u\,dw \tag{11}$$

Estimation of the average liquid flux between two node points by integration of the flow equation (11) with respect to cake distance is advantageous when the flow resistance shows significant variations. Such variations occur when the compressibility is high. The integration with respect to cake distance is denoted the integration method (IM) and is known from modeling water and solute transport in unsaturated soil systems (Moldrup et al., 1992; 1993). The IM also forms the basis in the analytical filtration theory (Ruth, 1946). Integration of Eq. 4 between e_i^{j+1} and e_{i+1}^{j+1} gives

$$\int_{\Delta w(2i-1)}^{\Delta w(2i+1)} u\,dw=\frac{1}{\mu}\int_{p_s(e_{i+1}^{j+1})}^{p_s(e_i^{j+1})}\frac{1}{\alpha}\,dp_s \tag{12}$$

where $p_s(e_i^{j+1})$ and $p_s(e_{i+1}^{j+1})$ are the contact pressures corresponding to e_i^{j+1} and e_{i+1}^{j+1}, respectively. Combining Eqs. 11 and 12 gives the final estimate for $u_{i+1/2}^{j+1}$,

$$u_{i+1/2}^{j+1}=\frac{1}{\mu 2\Delta\omega}\int_{p_s(e_{i+1}^{j+1})}^{p_s(e_i^{j+1})}\frac{1}{\alpha}\,dp_s \tag{13}$$

The contact pressure at the medium/cake interface (p_{sm}) is determined from Eqs. 3 and 5, where the filtrate flux (u_m) at time step j+1 is denoted $u_{1/2}^{j+1}$ in the solution scheme, i.e.,

$$p_{sm}=P-u_{1/2}^{j+1}\mu R_m \tag{14}$$

The contact pressure p_{sm} is subsequently used for estimation of $u_{1/2}^{j+1}$ as a forward space approximation by applying the IM between the medium and e_1^{j+1} (see Figure 2),

$$u_{1/2}^{j+1}=\frac{1}{\mu\Delta w}\int_{p_s(e_1^{j+1})}^{p_{sm}}\frac{1}{\alpha}\,dp_s \tag{15}$$

Cake surface during filtration

During filtration, the cake surface is moving continuously upward from the filter medium. This process has to be implemented in the solution scheme as a moving boundary condition. This is done by an expansion of the solution scheme by introduction of new node points as the calculation progresses. The solution scheme is divided into two zones; a main solution zone containing uniform space steps equal to Δw, and a cake surface layer of variable thickness ($\Delta w1$), see Figure 2.

For this purpose, the integer number I is defined as the greatest integer number which satisfies the two criteria $2I\Delta w<w_c$ and $\Delta w1$ equal to $w_c-2I\Delta w$. Hence, I is equal to the total number of grid points for e and u in the main solution zone. The value of $\Delta w1$ increases with time and when $\Delta w1\geq 2\Delta w$, the grid points for e_{I+1} and $u_{I+1 1/2}$ are included in the main solution zone and the I value is increased by one.

The change in surface layer thickness during one time step ($\Delta(\Delta w1)$) is determined by discretezation of Eq 7,

$$\Delta(\Delta w1)=\frac{\overline{u}_{I+1\ 1/2}}{e_s-e_0}\Delta t \qquad (16)$$

where $\overline{u}_{I+1 1/2}$ is estimated according to Eq. 10. The cake surface layer thickness at the next time step ($\Delta w1^{j+1}$) is determined from the old one ($\Delta w1^{j}$) by $\Delta w1^{j+1}=\Delta w1^{j}+\Delta(\Delta w1)$.

In order to avoid significant numerical errors, the time step (Δt) is adjusted so that $\Delta w1=2\Delta w$ is true before a new grid point is introduced. In practice, this is done using Eq. 16 and iterating until $\Delta(\Delta w1)=2\Delta w-\Delta w1^{j}$. After this, a new grid point is introduced in the main solution zone and the value of $\Delta w1^{j+1}$ is set to zero.

$\Delta w1$ is normally different from $2\Delta w$, and therefore the central space approximation for u between e_I^{j+1} and e_{I+1}^{j+1} will not be placed at the grid point for $u_{I+1/2}^{j+1}$, Figure 2. The u value at this grid point is estimated by making central approximations between e_I^{j+1} and e_{I+1}^{j+1} (to obtain ú) and between e_{I+1}^{j+1} and the cake surface where e is equal to e_0 (to obtain $u_{I+1 1/2}^{j+1}$) and, subsequently, by

making a linear approximation between ú and $u^{j+1}_{I+1\,1/2}$. This procedure gives the following equation for determination of $u^{j+1}_{I+1/2}$,

$$u^{j+1}_{I+1/2}=ú+(u^{j+1}_{I+1\,1/2}-ú)\frac{2\Delta w-\Delta w1^{j+1}}{2(\Delta w+\Delta w1^{j+1})} \tag{17}$$

where ú is determined by IM between e^{j+1}_{I} and e^{j+1}_{I+1},

$$ú=\frac{2}{\mu(2\Delta w+\Delta w1^{j+1})}\int_{p_s(e^{j+1}_{I+1})}^{p_s(e^{j+1}_{I})}\frac{1}{\alpha}dp_s \tag{18}$$

The void ratio e^{j+1}_{I+1} is determined from a mass balance for the liquid for the cake surface layer. Consider the interval $\Delta w1^{j+1}$ in Figure 2. The liquid content at time t is $e^{j}_{I+1}\Delta w1^{j}+e_s-\Delta(\Delta w1)$. At time t+Δt the liquid content is $e^{j+1}_{I+1}\Delta w1^{j+1}$. The difference must be equal to the amount of liquid that has moved deeper into the cake equal to $\bar{u}_{I+1/2}\Delta t$. From this mass balance, e^{j+1}_{I+1} is given by

$$e^{j+1}_{I+1}=\frac{e^{j}_{I+1}\Delta w1^{j}+e_s\Delta(\Delta w1)-\bar{u}_{I+1/2}\Delta t}{\Delta w1^{j+1}} \tag{19}$$

where $u_{I+1/2}$ is estimated using Eq. 10 and $u^{j+1}_{I+1\,1/2}$ is estimated as a backward space approximation between e^{j+1}_{I+1} and cake surface, see Figure 2, by use of the IM,

$$u^{j+1}_{I+1\,1/2}=\frac{2}{\mu\Delta w1^{j+1}}\int_{0}^{p_s(e^{j+1}_{I+1})}\frac{1}{\alpha}dp_s \tag{20}$$

where p_s equal to zero is used as the lower integration boundary according to the condition on the cake surface.

Cake surface during expression

During expression, the cake surface is fixed and the liquid flux at the cake surface (u_{wc}) is zero. I.e., w_c is a constant and equal to w_{tot}, u^{j+1}_{I} is equal to zero, and I needs to satisfy $2I\Delta w$ equal to w_{tot}.

INITIAL CALCULATION CONDITIONS

Filtration

At low medium resistance, an initial amount of cake equal to $2\Delta w$ is assumed to be deposited instantly and the initial liquid flux is assumed uniform through the cake ($u^0_{1/2}=u^0_{11/2}$). By using IM between the medium and e^0_1, $u^0_{1/2}$ is determined. Similarly, the use of IM between e^0_1 and the cake surface makes it possible to determine $u^0_{11/2}$. As these two integral equations are assumed equal, $p_s(e^0_1)$ is determined from

$$\int_0^{p_s(e^0_1)} \frac{1}{\alpha} dp_s = \int_{p_s(e^0_1)}^{p_{sm}} \frac{1}{\alpha} dp_s \qquad (21)$$

where p_{sm} is calculated from Eq. 14. The void ratio e^0_1 is then determined from $p_s(e^0_1)$ using the constitutive relationship.

At high medium resistance, $u^0_{1/2}$ is determined from Eq. 14 with $p_{sm}=0$ and during the calculations, the deposited cake is modelled using Eqs. 16-20. When $\Delta w1^{j+1}>2\Delta w$, Δt is adjusted until $\Delta w1=2\Delta w$ and the first grid point in the main solution zone is introduced by setting I=1.

If $u^0_{1/2}$ estimated by Eq 21 is larger than $u^0_{1/2}$ estimated by Eq. 14 with $p_{sm}=0$, the medium resistance is considered low. Otherwise, it is considered as high.

Expression

If e_s is smaller than e_0 corresponding to expression at the start of the simulation, the initial condition for modeling expression is the actual void ratio (e_s) and the liquid flux both equal to zero. The parameters I and Δw have to satisfy the criterion $2I\Delta w=w_{tot}$.

USE OF CONSTITUTIVE FUNCTIONAL RELATIONSHIPS

The constitutive functional relationships between α, p_s and e must be established before the numerical model becomes operational. In general, power law functions show fairly good agreement with measurements using a Compression-Permeability Cell for a variety of inorganic suspensions (Tiller, 1955). However,

filtration analyses of biological sludge show a compressibility so extreme that the use of the power law functions become problematic (Sørensen and Hansen). For better alternatives yet to be established the functional relationships are formulated as power law functions according to Tiller and Leu (1980):

$$(1-\varepsilon) = (1-\varepsilon_0)\,(1+\frac{p_s}{p_a})^{\beta} \tag{22}$$

$$\alpha = \alpha_0\,(1+\frac{p_s}{p_a})^{n} \tag{23}$$

where the porosity (ε) is related to e by $e=\varepsilon/(1-\varepsilon)$. In this way, 5 empirical constants are introduced where ε_0 and α_0 have a physical meaning describing the situation where the solids are in contact and $p_s=0$ (corresponding to the conditions at the cake surface during filtration), p_a is a scaling factor, and β and n are form constants which specify the degree of compressibility. The values of β and n are partly correlated so that a high value of β indicates a high value of n. However, the value of β has an upper limit due to the fact that ε must be positive for all value of p_s associated with the calculations.

Eqs. 22 and 23 are used in the integrated flow equations (Eqs. 13, 15, 18 and 20). For the cake/medium interface, Eqs. 14, 15, 22 and 23 yield

$$u_{1/2}^{j+1} = \frac{p_a}{\mu \Delta w \alpha_0 (1-n)} \left(\left[1+\frac{P - R_m \mu u_{1/2}^{j+1}}{p_a} \right]^{1-n} - \left[(1-\varepsilon_0)\,(1+e_1^{j+1}) \right]^{-\frac{1}{\beta}(1-n)} \right) \tag{24}$$

For the main solution zone of the cake, Eqs. 13, 22 and 23 for i=1,2...I yield

$$u_{i+1/2}^{j+1} = \frac{p_a (1-\varepsilon_0)^{-\frac{1}{\beta}(1-n)}}{\mu 2 \Delta w \alpha_0 (1-n)} \left(\left[1+e_i^{j+1} \right]^{-\frac{1}{\beta}(1-n)} - \left[1+e_{i+1}^{j+1} \right]^{-\frac{1}{\beta}(1-n)} \right) \tag{25}$$

For the interface between main solution zone and cake surface layer, Eqs. 18, 22 and 23 yield

$$\dot{u}=\frac{p_a(1-\varepsilon_0)^{-\frac{1}{\beta}(1-n)}}{\mu\alpha_0(\Delta w+\frac{1}{2}\Delta w1^{j+1})(1-n)}([1+e_I^{j+1}]^{-\frac{1}{\beta}(1-n)}-[1+e_{I+1}^{j+1}]^{-\frac{1}{\beta}(1-n)}) \quad (26)$$

For the cake surface, Eqs. 20, 22 and 23 yield

$$u_{I+1\,1/2}^{j+1}=\frac{2p_a}{\mu\alpha_0\Delta w1^{j+1}(1-n)}([(1-\varepsilon_0)(1+e_{I+1}^{j+1})]^{-\frac{1}{\beta}(1-n)}-1) \quad (27)$$

Eqs. 24-27 are not valid for n=1. To solve this problem, n equal to one is replaced by n equal to a value close to one (for example n=1.00001 instead of n=1). This does not affect the accuracy of the calculations.

CHOSEN NUMERICAL SOLUTION PROCEDURE FOR THE DESCRETISIZED EQUATIONS

The unknown values of e and u at time step j+1 are formulated as a vector X^{j+1} and Eqs. 9, 16, 17, 19, and 24-27 as a vector F'. Hence, the problem to solve is $F'(X^{j+1})=X^{j+1}$, equivalent to a solution of $F(X^{j+1})=F'(X^{j+1})-X^{j+1}=0$. To find the root for $F(X_{j+1})$, the Newton iteration method is chosen in which the Jacobean matrix (J) for F is determined. With k being the iteration number, the equation

$$J(X_k^{j+1})\Delta X=-F(X_k^{j+1}) \quad (28)$$

where ΔX is the estimated error on X_k^{j+1}, is solved followed by a correction equal to $X_{k+1}^{j+1}=X_k^{j+1}+\Delta X$. This is repeated until ΔX is acceptably small. The solution of Eq. 28 by elimination is easy because J is a diagonal matrix and, therefore, it is possible to use the so-called Double Sweep method (Cunge et al., 1980).

EVALUATION OF NUMERICAL ERRORS

Numerical errors can affect the calculation result, especially in the initial phase of the simulation. This is caused by two type of errors. First, for filtration at low medium resistance, the initial condition of uniform flow profile in the cake is not fully correct. Second, the gradients in the dependent variables (e and u) are largest in the beginning which introduces the most significant truncation errors.

The errors from the initial condition decrease as the calculation progresses and the numbers of calculation points increase. The errors become insignificant as soon as a few grid points have been introduced in the solution scheme.

The truncation errors can be characterized by the Diffusive Courant number (C_{rd}) defined for the well-known convection-dispersion equation (CDE) for one dimensional solute transport as

$$Crd=D\frac{\Delta t}{(\Delta z)^2} \qquad (29)$$

where D is the dispersion coefficient and z is distance. In the filtration /expression model, the mathematical analogy with D and z in the CDE can be identified by combination of Eqs. 1 and 4,

$$\frac{\partial e}{\partial t}=\frac{\partial}{\partial w}\left[\frac{-1}{\mu\alpha}\frac{\partial p_s}{\partial w}\right] \qquad (30)$$

Use of the Chain Rule gives

$$\frac{\partial e}{\partial t}=\frac{\partial}{\partial w}\left[\frac{-1}{\mu\alpha}\frac{dp_s}{de}\frac{\partial e}{\partial w}\right] \qquad (31)$$

Comparison between Eq 31 and the CDE reveals the identities

$$D\sim\frac{-1}{\mu\alpha}\frac{dp_s}{de}\ , \quad z\sim w \qquad (32)$$

It is noticed that D in the case of filtration/expression modelling (Eq 32) equals the so-called modified consolidation module (C_e), the latter defined by Shirato et al. (1970). By inserting Eqs. 22 and 23 in Eq. 32, D for the filtration/expression model equals

$$D \sim \frac{p_a (1-\varepsilon_0)^{\frac{1}{\beta}(n-1)}}{\mu \alpha_0 \beta} (1+e)^{\frac{1}{\beta}(n-1)-1} \qquad (33)$$

From a number of calculations using different values of n, β, e_s, and P, it was concluded that $Crd=D\Delta t/(\Delta w)^2$ should be smaller than about 5 m^2/s to avoid quantitatively important truncation errors.

MODEL VERIFICATION

It is possible to verify the presented numerical model using analytical models for filtration and expression.

During filtration, the average value for u ($\overline{u}_c$) can be determined using the IM on Eq. 4 between the filter medium and the cake surface

$$\overline{u}_c = \frac{1}{\mu w_c} \int_0^{p_{sm}} \frac{1}{\alpha} dp_s \qquad (34)$$

In case of filtration, excellent agreement between the average value of u calculated from the u values at the grid points in the numerical model and Eq. 34 was obtained for a wide range coefficient values (not shown).

In order to make a model verification in the case of expression, the values of n and β must be chosen so $\beta=n-1$, which makes the coefficient D (Eq. 33) a constant. An analytical solution to Eq. 31 in case of constant D is available (Shirato et al., 1970) for the initial condition of $e_s<e_0$ and the boundary condition of $R_m=0$. Excellent agreement between the numerical model and the analytical solution was obtained for a wide range of n and β values observing the relationship $\beta=1-n$ (not shown).

In this study, no verifications of the numerical model in relation to laboratory measurements have been carried out. Such verifications should to be carried out in future studies in order to fully investigate the validity of the defined solid/liquid model system and the applied constitutive functions. The constitutive functional parameters need to be measured before the numerical model can be verified. Direct measurement of these parameters is possible using a Compression-Permeability Cell but difficulties using this apparatus are reported by several

investigators, e.g. Risbud (1974). A better way for obtaining the necessary parameter values could be by direct calibration between a model and measured dewatering data. A calibration method using the porosity profiles in the filter cake during constant pressure filtration was suggested by Wakeman (1978). However, a such detailed measurement of the internal properties in the filter is difficult. A registration of filtrate volume as function of time is much more simple and, therefore, more attractive as a laboratory method. Tiller and Leu (1980) developed a calibration methodology that only requires measurements of the filtrate volume as function of time. However, they based the calibration method on the analytical filtration theory that assumes a uniform flow profile in the filter cake. A better way for obtaining the constitutive parameters could be by a direct calibration of the numerical model to measurements of filtrate volume as function of time obtained during both filtration and expression.

ANALYSIS OF DEWATERABILITY IN RELATION TO THE DEGREE OF COMPRESSIBILITY

The success of filtration/expression operation (dewaterability) depends on two factors. First, the filtrate flux (u_m) that determines the capacity of the dewatering machinery and, second, the final dry matter content in the filter cake. The common way to estimate dewaterability is by the so-called specific resistance to filtration (SRF) which only considers the flux of filtrate during filtration. The numerical model on the other hand is useful in order to analyze simultaneously how both factors affect the dewaterability during both filtration and expression.

Compressibility becomes the key mechanism in this analysis. The degree of compressibility is given by the values of n and β in Eqs. 22 and 23. The following 3 levels of compressibility are defined based on the value of n:

1. Low and moderately compressible, n<1 (Tiller and Yeh, 1987).
2. Highly compressible, n>1 (Tiller and Yeh, 1987).
3. Extremely compressible, n>>1 (Sørensen and Hansen).

The border between high and extreme compressibility is not well defined but n values for highly compressible solids are typically reported in the interval 1-2 (Tiller and Green, 1973; Tiller and Yeh, 1987).

Definition of two fictive suspensions

In order to asses the impact of compressibility on dewaterability, two fictive suspensions are considered, one with moderately and another with extremely compressible suspension solids.

For both suspensions the following parameter values are used: ε_0=0.9, p_a=5 kPa, P=100 Kpa, w_{tot}=0.01 m, e_s=12, $\mu=10^{-3}$ kg/ms and $R_m=10^{11}m^{-1}$. Moderately compressible solids are defined using β=0.15, n=0.6 and $\alpha=10^{13}$ m^{-2} (Leu, 1981) corresponding to a typical inorganic slurry. Extremely compressible solids are defined using β=0.5, n=5 and $\alpha_0=7\ 10^{11}$ m^{-2} where the value of α_0 is chosen so that the liquid fluxes during filtration are similar to those for moderately compressible solids. A value of n=5 for extremely compressibility was suggested by Sørensen and Hansen for a polyelectrolyte conditioned biological sludge using a filtration model developed by Tiller and Yeh (1987) to obtain agreement between measurements and calculations. A methodology for determining the value of β for extreme compressibility is unknown to the authors. But the magnitude of β is limited by the fact that ε much be positive for all values of p_s associated with the calculations. Eqs. 22 and 23 have never been verified for extreme compressibility. Therefore, the calculations in this study are useful only in order to investigate the general behavior of extreme compressibility.

Analyses of e and u profiles

In these analyses, the liquid flux relative to the solids u is given in material coordinates (w) while the liquid flux relative to absolute coordinates q and the void ratio (e) are given in absolute coordinates (x), i.e., as functions of the distance from the filter medium. Results from model calculations

are transformed from material into absolute coordinates by

$$x(w) = w + \int_0^w e\,dw \tag{35}$$

where the relationship between dx and dw is

$$\frac{dx}{dw} = (1+e) \tag{36}$$

Calculated values of u as a function of w are shown in Figure 3a for moderately compressible solids and in Figure 4a for extremely compressible solids. The corresponding values of q as a function of x are shown in Figure 3b for moderately compressible solids and in Figure 4b for extremely compressible solids. Curves for different times representing both filtration and expression are shown. Each curve represents the profile in the cake at the actual cake thickness. Therefore, the curves are expanding over a larger interval as the cake is getting thicker. The zero tendency for the u value at the cake surface (at the right end of each curve) in Figures 3a and 4a represents the change from filtration to expression. From the cake surface towards the medium, the value of both u and q increases due to the release of liquid from the cake structure being compressed.

The calculated e profiles for the moderately compressible suspension solids are shown in Figure 5. The value of the void ratio (e) at the cake/medium interface (x=0) decreases with time. This is due to the effect of the medium resistance which causes the contact pressure to increase during time. The duration of expression is rather small and a completely dewatered situation is reached after about 200 sec, where the e profile in the filter cake becomes uniform and is determined by a contact pressure equal to the applied pressure cf. Eq. 22.

The analogous e profiles for extremely compressible solids are shown in Figure 6. The e profile is convex during filtration and the values of e change drastically just above the filter medium which results in a relatively high liquid content in the filter cake at the end of filtration/expression. The time needed

for expression is so large that in praxis dewatering takes infinite time.

The p_l profiles for the extremely compressible solids in Figure 7 show an even more drastic pressure drop just above the filter medium. The liquid pressure in the cake is nearly constant in time, even after a long period of expression. This phenomenon was experimentally shown for a polyelectrolyte conditioned biological sludge by Sørensen and Hansen. This would suggest that in case of extremely compressible solids, it is a thin skin at the cake/medium interface and not the resistance of the whole porous structure that controls dewatering (release of liquid) during expression. The skin formation may be the reason why it is so difficult to obtain more than about 30 % dry matter content for biological sludge cakes, even when rather long periods of expression and high pressures are used. Skin formation was also reported by Tiller and Green (1973) in filtration of highly compressible latex particles and by Bierck and Dick (1990) in filtration of biological sludge.

It is important to point out that the parameter values were chosen so the filtrate fluxes for the two suspensions were nearly the same during filtration, i.e., a dewaterability characterization in form of specific resistance to filtration (SRF) will erroneously predict the dewaterability to be nearly the same for two different suspensions. In contrast, this more detailed study shows some important and basic differences between the two suspensions. The liquid content in the cake during filtration is highest for the extremely compressible solids. The filtrate flux during expression is highest for the moderately compressible solids until a completely dewatered situation is reached.

GENERAL BEHAVIOR OF THE e PROFILES DURING FILTRATION

A relationship that describes the shape of the e profile during filtration is derived using Eqs. 4, 32 and 36,

$$\frac{\partial e}{\partial x} = \frac{u}{(1+e)\,D} \tag{37}$$

Combining Eqs. 33 and 37 yields

$$\frac{\partial e}{\partial x} = \frac{u\mu\alpha_0\beta}{p_a(1-\varepsilon_0)^{\frac{1}{\beta}(n-1)}}(1+e)^{-\frac{1}{\beta}(n-1)} \qquad (38)$$

The value of e increases from the medium towards the cake surface. Therefore, if a filtration situation is considered and the u profile is assumed uniform, the following shapes of the e profile are evident from Eq. 38:

1. n<1, concave e profile (Figure 5).
2. n=1, linear e profile.
3. n>1, convex e profile (Figure 6).

Hence, according to Eq. 38 the shape of the e profile is independent of the value of β. If the non-uniform u profile is taken into account, the e profile becomes slightly convex for n=1, because u will be a decreasing function of the distance from the filter medium.

From this analysis it is seen that a general behavior of the e profile during filtration exists, and that the compressibility is the key parameter in controlling the shape of the e profile.

APPROXIMATE SEMI-ANALYTICAL SOLUTION FOR EXPRESSION OF EXTREMELY COMPRESSIBLE FILTER CAKES

An approximate semi-analytical solution describing the relationship between time and filtrate flux (u_m) in the case of expression can be derived for extremely compressible solids (n>>1). In case of expression, the u profile is more non-uniform than for filtration because, in contrast to filtration, the liquid flux at the cake surface (u_{wc}) is zero during expression. Therefore, it is seen from Eq. 38 that a convex e profile during filtration becomes increasingly convex when filtration ends and expression begins. Hence, a strongly convex e profile in the cake during expression can be assumed for extremely compressible solids.

The material coordinate system is chosen as reference. The space gradient of e in the material coordinate system is related to the space gradient of e with respect to absolute distance by

(cf. Eq. 36),

$$\frac{\partial e}{\partial w}=\frac{\partial e}{\partial x}\frac{dx}{dw}=\frac{\partial e}{\partial x}(1+e) \tag{39}$$

The e value is an increasing function from the filter medium toward the cake surface. Hence Eq. 39 shows that the e profile is less convex in the material coordinate system than in the absolute space coordinate system. However, if the compressibility is extremely high, the e profiles will still be strongly convex even in the material coordinate system. When the e profile is strongly convex, the values of e changes drastically just above the filter medium and are nearly constant in the rest of the filter cake. Therefore, the following assumption is valid for any location in the filter cake that is not very close to the filter medium,

$$\frac{\partial e}{\partial w}\approx 0 \;\Rightarrow\; \frac{\partial}{\partial t}\left[\frac{\partial e}{\partial w}\right]\approx 0 \tag{40}$$

Combining Eqs. 1 and 40 gives

$$\frac{\partial^2 u}{\partial w^2}\approx 0 \tag{41}$$

which predicts a linear u profile, i.e., a linear u profile is a consequence of a strongly convex e profile. This is in accordance with the calculated u profiles for the extremely compressible suspension, see Figure 4a, where the u profiles are linear except during the very early stages of the expression.

Assuming a linear u profile, the filtrate flux (u_m) can be determined from the average relative liquid flux in the cake ($\bar{u}_c$) by $\bar{u}_c=u_m/2$, i.e., $u_m=2\bar{u}_c$, because the relative liquid flux at the filter cake surface is zero. The parameter $\bar{u}_c$ is determined using the IM between the medium and cake surface using Eq. 4 which gives the following equation for the filtrate flux (u_m),

$$u_m=\frac{2}{\mu w_c}\int_{p_{s,wc}}^{P}\frac{1}{\alpha}dp_s \tag{42}$$

where the medium resistance is assumed equal to zero and $p_{s,wc}$ is the contact pressure at the filter cake surface. Use of Eq. 1 for

the linear u profile where the liquid flux at the cake surface is zero and the e profile is assumed strongly convex gives

$$\frac{de_{wc}}{dt}=\frac{u_m}{w_c} \tag{43}$$

where e_{wc} is the void ratio at the filter cake surface. A simple forward time discretization of Eq. 43 yields

$$e_{wc,\,j+1}=e_{wc,\,j}-\frac{\Delta t}{w_c}u_{m,\,j} \tag{44}$$

where j denotes the time step number. The void ratio at the filter cake surface when expression begins is e_0, and if $u_{m,0}$ denotes the initial condition (j equal to zero) for u_m when filtration ends and expression begins, Eq. 44 becomes

$$e_{wc,\,j+1}=e_0-\frac{\Delta t}{w_c}\sum_{s=0}^{s=j}u_{m,\,g} \tag{45}$$

where the time step Δt is assumed constant. Eq. 42 can be integrated analytically using Eqs. 22, 23 and 45, which gives the final equation for the filtrate flux at time step j+1,

$$u_{m,\,j+1}=\frac{2p_a}{\mu w_c\,\alpha_0\,(1-n)}\left([1+\frac{P}{p_a}]^{1-n}-[\,(1-\varepsilon_0)\,(1+e_{wc,0}-\frac{\Delta t}{w_c}\sum_{s=0}^{s=j}u_{m,\,g})\,]^{-\frac{1}{\beta}(1-n)}\right) \tag{46}$$

where $u_{m,0}$ is given by

$$u_{m,\,0}=\frac{2p_a}{\mu w_c\,\alpha_0\,(1-n)}\left([1+\frac{P}{p_a}]^{1-n}-1\right) \tag{47}$$

The derived solution for the filtrate flux (u_m) as a function of time (Eq. 46) is labelled semi-analytical because of the summation term in Eq. 46. It is recommended to use a Δt value around 1-10 sec in Eq. 46.

The term $[1+P/p_a]^{1-n}$ is normally close to zero because n>>1. This makes the filtrate flux (u_m) independent of the applied pressure (P), especially in the beginning of the expression period. Tiller and Yeh (1987) showed the same independence of u_m on P for filtration associated with high compressibility (n>1). A comparison between the semi-analytical solution (Eq. 46) and

the unified filtration model (Eqs. 9, 10, 24 and 25) is shown in figure 8 for the extremely compressible solids (defined earlier) and a reasonable good agreement is obtained. However, a poor agreement exists during the very early stages of the expression period where the u profile in the cake is non-linear.

The coincidence between the semi-analytical model and the unified numerical model is improved as the degree in compressibility is increased. Therefore, in the case of expression of extremely compressible solids, the filtrate flux as function of time can be adequately described by the presented simple semi-analytical solution (Eq. 46). One promising use of this could then be estimation of the constitutive parameters in Eqs. 22 and 23 by curve-fitting Eq. 46 to measured data for u_m as a function of time during filtration.

CONCLUSIONS

A unified model for filtration and expression of a solid/liquid suspension has been developed, assuming constant filter medium resistance and allowing for non-constant applied pressure. The model is able to simulate dewatering of extremely compressible suspensions such as biological sludges by an integration of the flux equation with respect to cake thickness. This eliminates numerical errors, even for large changes in flow resistance in the cake.

The model is not yet verified in relation to actual dewatering experiments because a good methodology for assessing the constitutive parameters is needed. A promising way to do this could be by direct calibration of the unified numerical model based on several series of measurements of filtrate volume as function of time for both filtration and expression.

The constitutive functions used have never been verified in case of extremely high solid compressibility, as in biological sludge, and this verification needs to be performed before the unified model can be used to describe biological sludge dewatering. If such a verification predicts the functions to be satisfactory then the constitutive parameters could be estimated by calibrating the semi-analytical solution using measured

relationships between time and filtrate flux during expression.

The suggested numerical model made it possible to analyze the influence of solid compressibility on dewaterability. In this way the specific resistance to filtration (SRF) was shown to be deficient in predicting dewaterability. This applies to both filtration and expression and combinations thereof.

Model calculations indicated that extreme solid compressibility results in the formation of a skin just above the filter medium. This skin is responsible for nearly all the liquid pressure drop across the cake. This implies that almost infinite time is needed to significantly increase the dry matter content during expression of extremely compressible solids, and that the filtrate flux becomes independent of the applied pressure. For practical purposes, this may explain why dewatering of biological sludge becomes time-consuming, and renders sludge cakes low in dry matter content, e.g. 25-30 %. The skin identifies a very concrete technical challenge. Finding a way of breaking it may greatly increase the obtainable dry matter content in the biological sludge cake.

ACKNOWLEDGEMENTS

This research was carried out at the Environmental Engineering Laboratory, Aalborg University, Denmark. The Danish Technical Research Council (Grant. 5.26.09.12) is gratefully acknowledged for economical support to this work.

NOTATION

C_e	Modified consolidation coefficient, m^2/s.
C_{rd}	Diffusive Courant number.
D	Dispersion coefficient, m^2/s.
e	Volume of liquid per volume of solid (void ratio).
e_s	Void ratio in the suspension.
e_0	Void ratio when the solids are in contact and $p_s=0$ (void ratio at filter cake surface during filtration).
e_{wc}	Void ratio at filter cake surface.
F	The system of equations in the numerical solution

	scheme.
s	Summation number.
I	Number of grid points in the main solution scheme.
i	Index for space location in the solution scheme.
J	Jacobean matrix for F.
j	Index for time location in the solution scheme.
k	Iteration number.
n	Form factor for the compressibility with respect to specific resistance.
P	Applied pressure, Pa.
p_a	Scaling factor, Pa.
p_l	Liquid pressure taken as an average over the cross section area, Pa.
p_{lm}	Liquid pressure at the cake/medium interface, Pa.
p_s	Solid pressure (contact pressure) taken as an average over the cross section area, Pa.
p_{sm}	Contact pressure at the medium/cake interface,Pa.
q	Liquid flux relative to absolute coordinates, m/s.
q_s	Solid flux relative to absolute coordinates, m/s.
R_m	Resistance in filter medium, 1/m.
SRF	Specific Resistance to Filtration, kg/m
t	Time, s.
Δt	Time step used in the solution scheme, s.
u	Liquid flux relative to the solids, m/s.
ú	u value estimated as central approximation between e_I^{j+1} and e_{I+1}^{j+1}, m/s.
$\overline{u}_c$	The average value of u in the filter cake, m/s.
u_m	Liquid flux through the medium (filtrate flux), m/s.
w	Material coordinate (solid volume per cross section area), m^3/m^2.
w_c	Total solid volume per cross section area in the filter cake, m^3/m^2.
w_{tot}	Total solid volume per cross section area, m^3/m_2.
Δw	Space interval used in the solution scheme, m^3/m^2.
$\Delta w1$	Space interval used in the solution scheme at the cake surface, m^3/m^2.
$\Delta(\Delta w1)$	Increase in $\Delta w1$ during one time step, m^3/m^2.

X	Vector for the values of e and u.
ΔX	Correction of X during one iteration step.
x	Absolute space coordinate (distance from filter medium), m.
x_c	Cake thickness in absolute space coordinates, m.
x_{tot}	Total thickness of suspension and cake in absolute space coordinates, m.
z	Distance, m.
Δz	Distance interval, m.

Greek Letters

α	Specific resistance, $1/m^2$.
α_0	Specific resistance when the solids are in contact and $p_s=0$ (specific resistance at the cake surface during filtration), $1/m^2$.
β	Form factor for the compressibility with respect to the porosity.
ε	Porosity.
ε_0	Porosity when the solids are in contact and $p_s=0$ (porosity at the cake surface during filtration).
μ	Viscosity of liquid, kg/ms.
τ	Integration variable, s.

LITERATURE CITED

Atsumi, K., and T. Akiyama, (1975), "A Study of Cake Filtration - Formulation as a Stefan Problem", *J. Chem. Eng. Japan*, Vol. 8, No. 6, pp. 487-492.

Bierck, B.R., and R. I. Dick, (1990), "In Situ Examination of Effects of Pressure Differential on Compressible Cake Filtration", *The International Association on Water Pollution Research and Control, 1990 Sludge Management Conference at Los Angeles California.*

Cunge, J. A., F. M. Holly, and A. Verwey, (1980), "Aspects of Computational River Hydraulics", *Pitman.*

Harlow, F. H., and J. E. Welch, (1965) "Numerical Calculation of

Time-Dependent Viscous Incompressible Flow of Fluid with Free Surface", *The Physics of Fluids*, Vol. 8, No. 12, pp. 2182-2189.

Leu, W., (1981),"Cake Filtration", Ph. D. Dissertation, Univ. of Houston.

Moldrup, P., J. Aa Hansen, D. E. Rolston, and T. Yamaguchi, (1993), "Improved Simulation of Unsaturated Soil Hydraulic Conductivity by the Moving Mean Slope (MMS) Approach", *Soil Science*, Vol. 155, No. 1 (in press).

Moldrup, P., T.Yamaguchi, J.Aa.Hansen, and D.E.Rolston, (1992), "An Accurate and Numerically Stable Model for One-Dimensional Solute Transport in Soils", *Soil Science*, Vol. 153, No. 4, pp. 261-273.

Risbud, H. M., (1974), "Mechanical Expression, Stress at Cake Boundaries, and New Compression-Permeability Cell,"Ph.D. Dissertation, Univ. of Houston.

Ruth, B. F., (1946), "Correlating Filtration Theory with Industrial Practice", *Industrial and Engineering Chemistry*, Vol. 38, No. 6, pp. 564-571.

Satoh, T., and K. Atsumi, (1970), "Forced Expression of Liquid from Pasty Mixture of Liquid and Fine Solid Particles and its Numerical Solution by Method of Moments", *J. Chem. Eng. Japan*, Vol. 3, No. 1., pp. 92-98.

Shirato, M., M. Sambuichi, H. Kato, and T. Aragaki, (1969), "Internal Flow Mechanism in Filter Cakes", *AIChE J.* Vol. 15, No. 3, pp. 405-409.

Shirato, M., T. Murase, H. Kato, and S. Fukaya, (1970), "Fundamental Analysis for Expression under Constant Pressure", *Filtration & Separation*, Vol. 7, pp. 277-282.

Shirato, M., T. Murase, M. Negawa, and H. Moridera, (1971); "Analysis of Expression Operations", *J. Chem. Eng. Japan*, Vol. 4, No. 3, pp. 263-268.

Sørensen, P. B., and J. Aa. Hansen, "Extreme Compressibility in Biological Sludge Dewatering", *Wat. Sic. Tech* (submitted june 1992).

Tiller, F. M., (1955), "The Role of Porosity in Filtration, Part 2. Analytical Equations for Constant Rate Filtration", *Chemical Engineering Progress*, Vol. 51, No. 6., pp. 282-290.

Tiller, F. M., and T. C. Green, (1973), "Role of Porosity in Filtration IX Skin Effect with Highly Compressible Materials", *AIChE J.* Vol. 19, No. 6., pp. 1266-1269.

Tiller, F. M., and W. F. Leu, (1980), "Basic Data Fitting in Filtration", *Journal of The Chinese Institute of Chemical Engineers*, Vol. 11, pp. 61-70.

Tiller, F. M. and C. S. Yeh, (1987),"The Role of Porosity in Filtration, Part XI: Filtration Followed by Expression", *AIChE J.*, Vol. 33, No.8., pp. 1241-1256.

Tosun, I., (1986), "Formulation of Cake Filtration", *Chem. Eng. Sci.*, Vol. 41, No. 10, pp. 2563-2568.

Wakeman, R. J., (1978), "A Numerical Integration of the Differential Equations Describing the Formation of and Flow in Compressible Filter Cakes", *Trans IChemE*, Vol. 56., pp. 258-265.

Wells, S. A., and R.I.Dick, (1989), "Mathematical Modelling of Compressible Cake Filtration", *Proceedings of the 1989 Specialty Conference, Austin, Texas, July 10-12.*

Yeh, S., (1985), "Cake Deliquoring and Radial Filtration", *Ph. D. Dissertation, Univ. of Houston.*

FIGURE LEGENDS

Figure 1: Principle of the physical system, a) formulated in absolute space coordinates, b) formulated in material coordinates.

Figure 2: Numerical modelling principle and applied solution scheme.

Figure 3: Local values of liquid flux in the cake during filtration and expression of a moderately compressible solids, a) liquid flux relative to the solids (u) as a function of w, b) liquid flux relative to absolute coordinates (q) as a function of x.

Figure 4: Local values of liquid flux in the cake during filtration and expression of extremely compressible solids, a) liquid flux relative to the solids (u) as a function of w, b) liquid flux relative to absolute coordinates (q) as a function of x.

Figure 5: Local values of the void ratio (e) in the cake during filtration and expression of moderately compressible solids.

Figure 6: Local values of the void ratio (e) in the cake during filtration and expression of extremely compressible solids.

Figure 7: Local values of the liquid pressure (p_l) in the cake during filtration and expression of extremely compressible solids.

Figure 8: The filtrate flux (u_m) as a function of time, calculated in case of expression of extremely compressible solids using the unified numerical model (Eqs. 9, 10, 24 and 25) and the semi-analytical solution (Eq. 46), respectively.

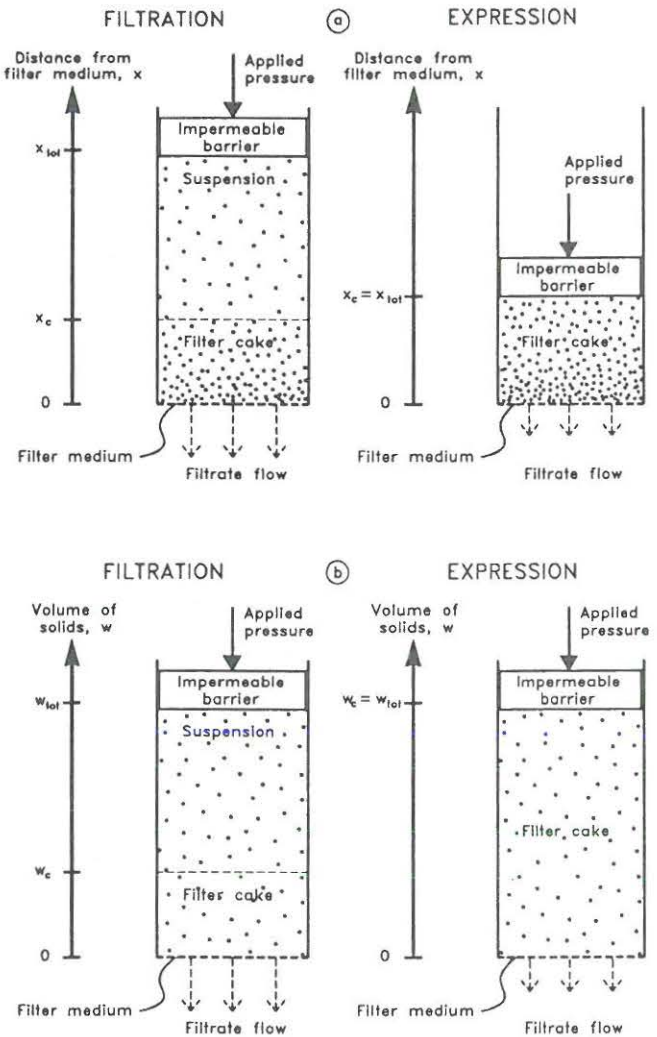

PBS0001
fig1

Figure 1

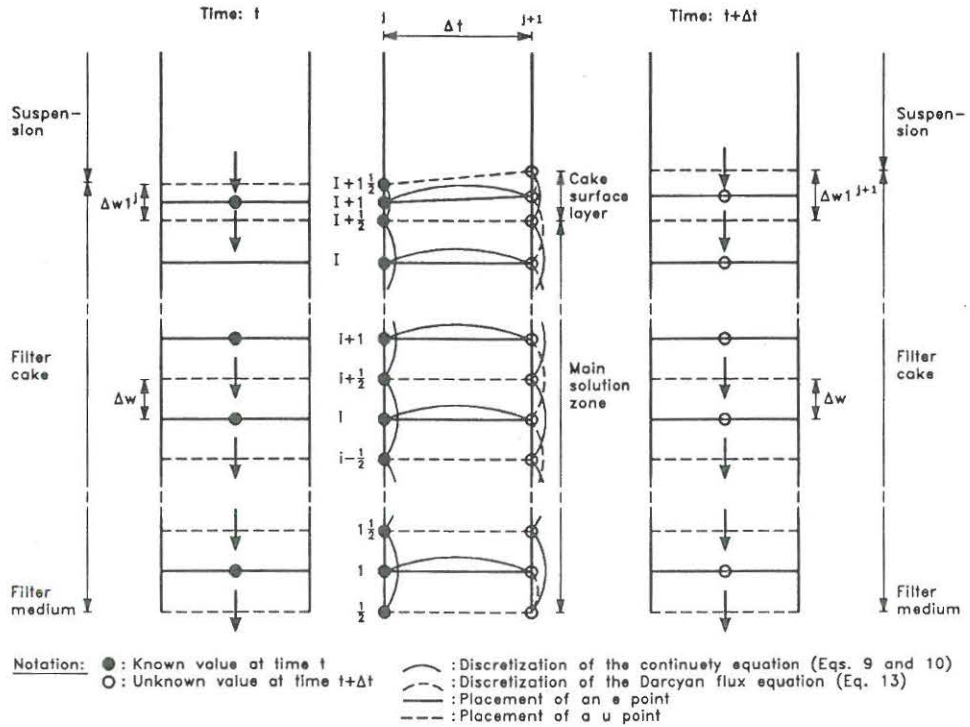

Fig2
PBS0002

Figure 2

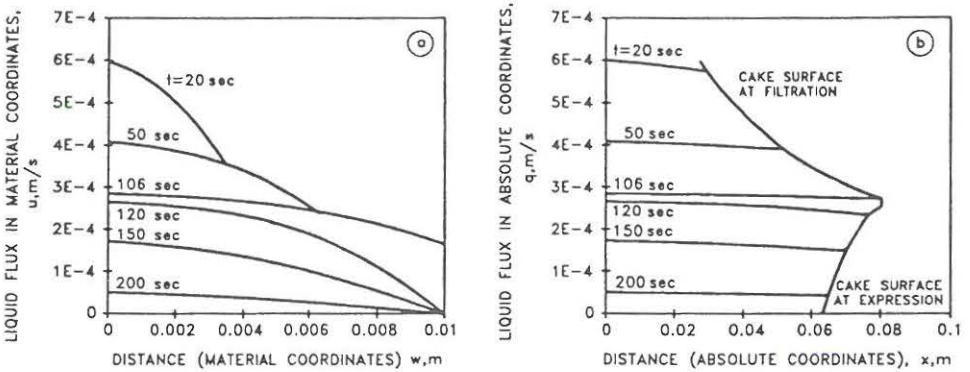

PBS0003
fig3

Figure 3

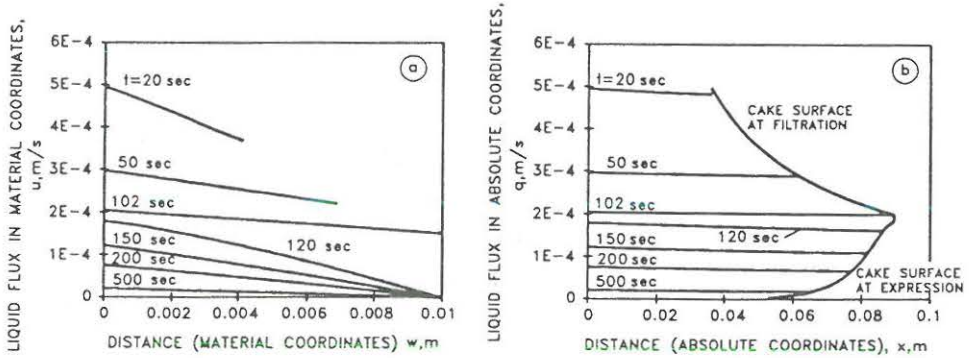

PBS0004
fig4

Figure 4

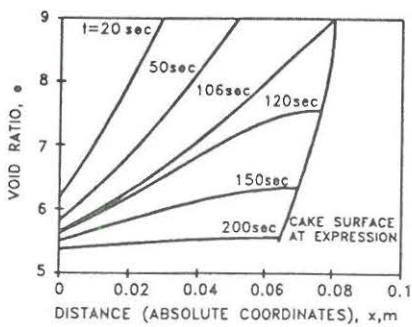

PBS0005
fig5

Figure 5

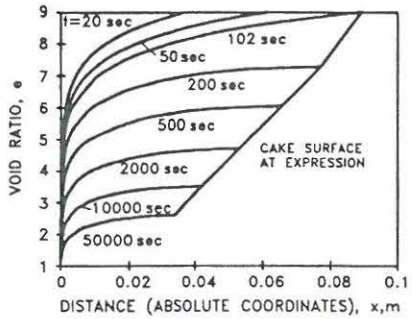

Figure 6

PBS0006
fig6

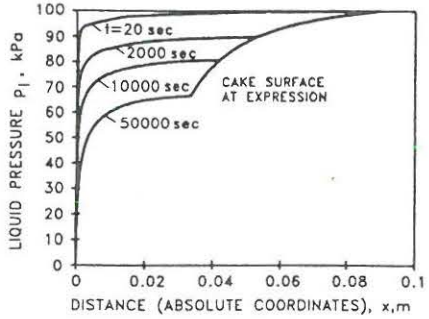

Figure 7

PBS0007
fig7

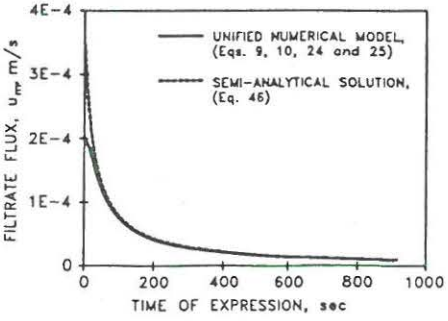

Figure 8

PBS0008
fig8

Extreme Compressibility in Biological Sludge Dewatering

II

EXTREME SOLID COMPRESSIBILITY IN BIOLOGICAL SLUDGE DEWATERING

Peter B. Sørensen and Jens Aage Hansen

Environmental Engineering Laboratory, Aalborg University
Sohngaardsholmsvej 57, DK-9000 Aalborg, Denmark

KEY WORDS

Mechanical sludge dewatering, Filtration/Expression modelling, Biological sludge, Compressibility, Theoretical filtration analysis.

ABSTRACT

The degree of compressibility in the filter cake structure associated with mechanical dewatering of a polyelectrolyte conditioned biological sludge is investigated. Filtration/expression tests are carried out using both an $Al(OH)_3$ and a biological sludge. A numerical model for filtration/expression is established and used to simulate liquid pressure development. A comparison between measurements and calculations shows that the compressibility of the biological sludge is extremely high. Using filtration theories, the degree of compressibility is shown to be so high that a thin skin which accounts for nearly all the hydraulic pressure drop across the filter cake is likely to be formed just above the medium. This extreme compressibility behaviour suggests a reconsideration of the usual power law description of the relations between solid contact pressure, porosity and specific flow resistance. An equation showing the effect of the compressibility on the relation between filtrate flow and applied pressure during filtration is derived, and it is concluded that for extremely compressible solids, the filtrate flow

becomes independent of the pressure applied.

INTRODUCTION

A particle/liquid or solid/liquid distinction is normally used for describing mechanical dewatering of a biological sludge in the form of theories for filtration and expression. These theories contain constitutive relationships between local water content, flow resistance and solid contact pressure. The degree of changes in water content and flow resistance in relation to a change in solid contact pressure is denoted the degree of compressibility. The theories have mostly been verified using inorganic materials which differ significantly from biological sludges. Biological sludges do show some accordance to the theory for filtration using constant applied pressure in that the inverse flow rate of filtrate normally is linearly related to filtrate volume. It would be expected that the biological sludge solids are very compressible compared to typical inorganic solids.

The compressible behavior is investigated for a polyelectrolyte conditioned biological sludge. First, a biological sludge and an inorganic sludge ($Al(OH)_3$) are used in a filtration/expression test where deformation and liquid pressure under the piston are recorded. The compressibility characteristics are formulated as power law functions and deformation and liquid pressure variation during expression are modelled numerically, in order to investigate the degree of compressibility. Second, a simplified theory for filtration, developed by Tiller and Yeh (1987), is used for a provisional determination of the degree of compressibility of the biological sludge. In this analysis the power law functions are still used for describing compressibility. Third, theoretical considerations for filtration are made where the power law functions are replaced by two more basic assumptions regarding void ratio and flow resistance. From this analysis an attempt is made to better assess and model filtration and expression.

FILTRATION/EXPRESSION EXPERIMENT

A laboratory device for one-dimensional filtration/expression is used in characterizing mechanical sludge dewatering. The sludge sample is placed in a cylinder where a filter medium (Whatman #41 filter paper) at the bottom allows an outflow of water and a piston at the top transmits the applied pressure. The principle for the set up is shown in figure 1 and notation in figure 2.

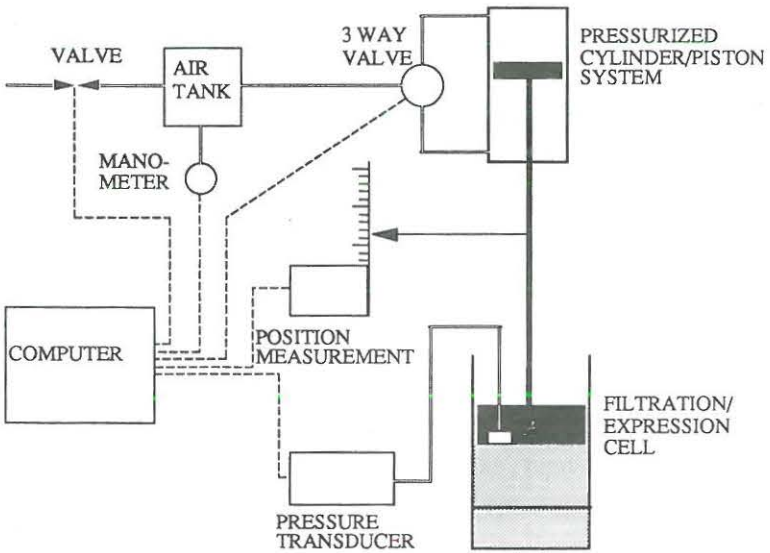

Fig. 1. Laboratory device for filtration/expression experiments. Details of the filtration/expression cell are shown in figure 2.

Data collected are sample deformation (h), defined as the difference between the initial and the actual thickness of the sludge sample, time (t) and liquid pressure at the top of the sample ($p_{l,top}$). The applied pressure is kept constant, so during filtration a plot of $\Delta t/\Delta h$ vs h is linear until, at expression, an upward curvature starts. $p_{l,top}$ is nearly constant during filtration and decreases during expression. Small changes in $p_{l,top}$ during filtration indicate the influence from friction at the piston/wall interfaces.Two different types of sludge were investigated, an $Al(OH)_3$ suspension and a biological sludge. The $Al(OH)_3$ suspension was produced in the laboratory according to Christensen and Dick (1985). The biological sludge was activated sludge from Aalborg East Wastwater Treatment Plant concentrated by sedimentation and stored

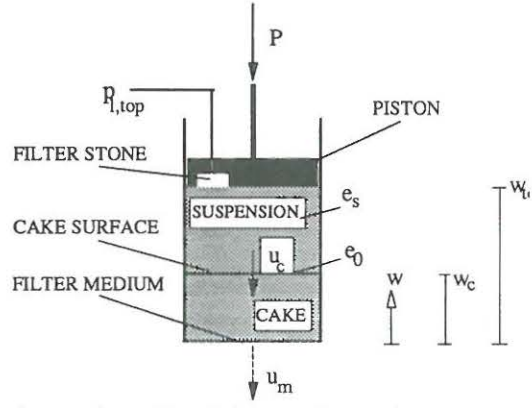

Fig. 2. The filtration/expression cell and the notation used.

anaerobically for about one month. Before dewatering the biological sludge was conditioned using polyelectrolyte (Zetag 57) at dosages of 7 kg dry polymer per ton dry sludge solids.

Results for the $Al(OH)_3$ are shown in figure 3, and it is seen that the non-linear behaviour of the $\Delta t/\Delta h$ vs. h relationship starts at the same time as the drop in $p_{l,top}$. Measurements using the biological sludge are shown in figure 4. $\Delta t/\Delta h$ is linear during the filtration period and raises drastically upwards during expression. But in this case $p_{l,top}$ shows only a very weak tendency for decrease during expression, in contrast to $Al(OH)_3$. This difference in tendency between $Al(OH)_3$ and biological sludge may be attributed to different solid compressibility. In the following, this difference will be investigated using a newly developed numerical filtration/expression model.

INVESTIGATION OF COMPRESSIBLE BEHAVIOR BY FILTRATION/EXPRESSION MODELING

The tendency in the curvature of $p_{l,top}$ for $Al(OH)_3$ and biological sludge is investigated by a numerical model for simulation of filtration/expression as described in Sørensen et al. (1993). The numerical solution is based on local conditions in the particle/liquid system, and formulated as basic equations described briefly in the following. For notation please refer to figure 2. The equations are one dimensional and all the involved parameters are, therefore,

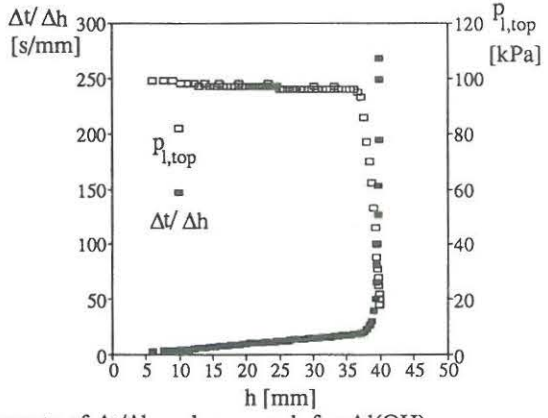

Fig. 3. Measurements of $\Delta t/\Delta h$ and $p_{l,top}$ vs. h for $Al(OH)_3$

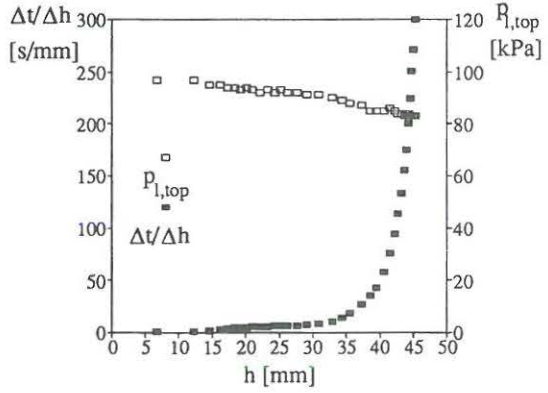

Fig. 4. Measurements of $\Delta t/\Delta h$ and $p_{l,top}$ for biological sludge.

defined relative to the cross section area. In order to describe the local properties in the filter cake, a material coordinate system is used. In this w expresses the volume of solids between a given position in the filter cake and the filter medium. The local continuity of liquid is expressed by the equation

$$\frac{\partial e}{\partial t} = \frac{\partial u}{\partial w} \qquad (1)$$

where e is void ratio and u is the liquid flux relative to the solids velocity, taken as an average over the cross section area. u is determined by Darcy's Law

$$u = \frac{-1}{\mu\alpha}\frac{\partial p_s}{\partial w} \qquad (2)$$

where μ is viscosity of liquid, α local specific resistance and p_s solid contact pressure. The

connection between the solid contact pressure and the liquid pressure is determined by the force balance

$$P=p_l+p_s \tag{3}$$

where P is the externally applied pressure and p_l the liquid pressure. The boundary condition at the filter medium is

$$u_m=\frac{1}{\mu R_m}p_{lm} \tag{4}$$

where u_m is liquid flux through the medium, R_m medium resistance and p_{lm} liquid pressure at the cake/medium interface. If the medium resistance is insignificant (R_m=0), eq. (4) is replaced by the condition: p_{lm}=0. During filtration the cake thickness w_c is determined by

$$\frac{dw_c}{dt}=\frac{u_c}{e_s-e_0} \tag{5}$$

where u_c is the liquid flux relative to the solids velocity at the cake surface, e_0 the void ratio at the cake surface and e_s the void ratio in the suspension. w_c is constant and u_c zero during expression.

The constitutive relationships between e, α and p_s need to be established before the equations become operational for use. Power law functions are chosen according to Tiller and Leu (1980)

$$(1-\varepsilon)=(1-\varepsilon_0)\left(1+\frac{p_s}{p_a}\right)^{\beta} \tag{6}$$

$$\alpha=\alpha_0\left(1+\frac{p_s}{p_a}\right)^{n} \tag{7}$$

where ε is the porosity (ε=e/(1+e)), ε_0 and α_0 the porosity and specific resistance when the solids are just in contact and p_s=0 (at the cake surface during filtration), p_a a scaling factor, and β and n compressibility constants characterizing the sensitivity of ε and α to changes in p_s. Table 1 shows the values of β and n suggested by Leu (1981).

u_m is equal to $\Delta h/\Delta t$ and the value of h is expressed by

$$h=w_{tot}(e_s-\bar{e}_{tot}) \tag{8}$$

where w_{tot} is total solid volume in the sample divided by cross section area and $\bar{e}_{tot}$ is the

average void ratio in the sludge column determined by

$$\bar{e}_{tot} = \frac{1}{w_{tot}} \left(e_s (w_{tot} - w_c) + \int_0^{w_c} e\,dw \right) \qquad (9)$$

TABLE 1. The Relation Between n, β and Compressibility (p_a=5 kPa) (Leu, 1981).

Degree of compressibility	Slight	Moderate	High
n	0.20	0.60	1.20
β	0.05	0.15	0.30

Calculation results for moderate solid compressibility are shown in figure 5. (w_c=2x10^{-2} m, e_s=24, R_m=0, ε_0=0.9, β=0.15, α_0=5.5x10^{14} s/m^2, n=0.6, p_a=5 kPa). It is seen that the tendency in curvature for $p_{l,top}$ looks more like $Al(OH)_3$ (figure 3) than biological sludge (figure 4). Calculation results for high compressibility are shown in figure 6 (β=0.25 and n=1.25; all other parameter values are unchanged except for α_0 which is chosen to 2x10^{14} s/m^2 to make u_m in the same range as in the moderate compressibility case).The drop in $p_{l,top}$ during expression in figure 6 is a little less drastic than in figure 5. However, for β and n corresponding

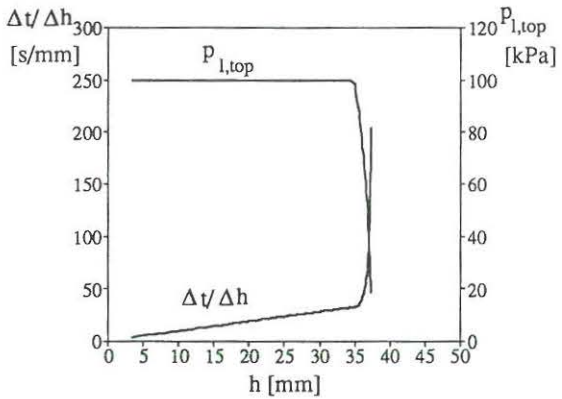

Fig. 5. Calculation of Δt/Δh and $p_{l,top}$ for assumed moderate solid compressibility, cf. table 1.

to a high degree of compressibility, the calculation results still resemble the $Al(OH)_3$ measurements much better than the biological sludge measurements (compare figures 3,4 and 6). The sludge, therefore, is not likely to be characterized adequately by the classification

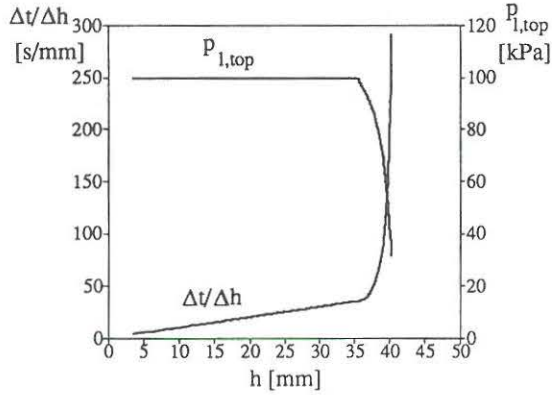

Fig. 6. Calculation of $\Delta t/\Delta h$ and $p_{l,top}$ for assumed high solid compressibility, cf. table 1.

system defined by Leu (1981). A method is needed, for better determination of the degree of compressibility. A method based on simplified modeling, and covering only filtration, is suggested here.

SEEKING BETTER SLUDGE SOLID COMPRESSIBILITY CHARACTERIZATION

In order to study solid compressibility, a method developed by Tiller and Yeh (1987) is used. They use the filtration theory for determination of the relationship between filtrate flux (u_m) and applied pressure (P).

The average liquid flux in the cake ($\bar{u}$) is

$$\bar{u}=\frac{1}{w_c}\int_0^{w_c} u\,dw \qquad (10)$$

Substitution of eq.(2) into eq.(10), and assuming zero medium resistance ($R_m \approx 0$) and uniform cake flux profile ($u_m \approx \bar{u}$), gives

$$u_m=\frac{1}{\mu w_c}\int_0^{P} \frac{1}{\alpha}\,dp_s \qquad (11)$$

Use of eq. (7) in eq. (11) yields

$$u_m w_c \mu=\frac{p_a}{\alpha_0 (1-n)}\left[\left(1+\frac{P}{p_a}\right)^{1-n}-1\right] \qquad (12)$$

From this it is seen that u_m becomes nearly independent of P, if P is sufficiently large for n>1. If u_{mP} denotes u_m at P and $u_{m\infty}$ denotes u_m at an infinitely high value of P, then the ratio $u_{mP}/u_{m\infty}$ is determined using eq. (12),

$$\frac{u_{mP}}{u_{m\infty}} = 1 - \frac{1}{(1+\frac{P}{P_a})^{n-1}} \qquad (13)$$

given n>1 and w_c is independent on the value of P. The assumptions of uniform u profile and constant w_c make the calculations independent of eq. (6), and n is therefore the only factor for characterizing the compressibility in this context.

It is now possible to investigate the compressible behavior of the sludge solids by constant pressure filtration experiments. An SRF apparatus similar in principle to the one applied by Christensen et. al. (1993) is used for experimentation. Time (t) and filtrate volume (V_{mes}) are recorded. The inner diameter of the cylinder is 10 cm and a Whatman #41 filter paper is used as filter medium. The SRF apparatus is used instead of the filtration/expression apparatus shown in figure 1, because it allows for series of experiments to be completed more quickly.

Polymer conditioned biological sludge is filtered by compressed air at different pressures (P) or by drainage where P is equal to the sample depth in the cylinder. P decreases during drainage as the sample depth decreases, and in this case the value of P is estimated to be equal to the mean depth during the experiment (approximately 0.4 kPa). The filtrate flux through the filter medium (u_m) is determined by $\Delta V_{mes}/\Delta t \cdot A$, where A is the filter medium area. Three filtration experiments were made for each P value and the average used to determine u_{mP}; except for P=100 kPa, where only two experiments were successful.

u_{mP} at fixed filtrate volumes is found constant for all the pressure filtration tests, $u_{m\infty}$ is therefore estimated using an average of all the pressure filtration tests. So, the ratio $u_{mP}/u_{m\infty}$ is about one for all the values of P in the pressure filtration tests, as shown in figure 7. The deviation from one is caused by experimental errors, which are mainly due to the conditioning process and the fact that flow of filtrate is very quick so the filtration takes only a few minutes. The only significant deviation in the ratio occurs at 0.4 kPa, but this is mainly caused by the medium resistance, which is significant for so low values of P. Eq.(13) is used to fit

the results in figure 7, and it is seen that n needs to be about 5 or larger to obtain agreement between theory and experiments.

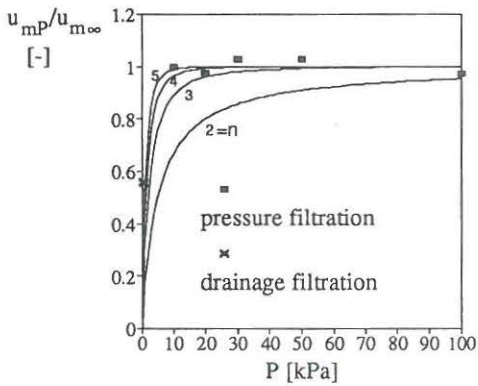

Fig. 7. The ratio u_{mP} / $u_{m\infty}$ at different values of the applied pressure for filtration of the biological sludge. The curves are calculated using eq. (13) and the numbers denote the values of n.

In order to get an impression of the liquid pressure profile in the sludge filter cake, the profile of contact pressure (p_s) in the cake during filtration is calculated using eq.(7) in eq.(11) and integrating with respect to p_s (Leu, 1981):

$$p_s = p_a \left[\left(\left(\left(1+\frac{P}{p_a}\right)^{1-n} - 1 \right) \left(1-\frac{w}{w_c}\right) + 1 \right)^{\frac{1}{1-n}} - 1 \right] \qquad (14)$$

The relative liquid pressure distribution (p_l / P) is calculated by using eq. (14) and the relationship $p_l = P - p_s$ and is shown in figure 8 for n=5, p_a=5 kPa and different values of P. It is seen that nearly all of the pressure drop takes place in a very thin layer just above the filter medium.

All these considerations are based on the constitutive equation (eq.(7)), but the extreme value of n tells that the simple power law relationship is questionable. Therefore, in the following, a new relation between u_m and P will be derived using only the assumption of uniform flow profile ($u_m \approx \bar{u}$) and no medium resistance ($R_m \approx 0$) as above and replacing eqs. (6) and (7) by two very basic assumptions regarding void ratio and flow resistance as functions of contact pressure between solids. u_m is determined as a function of P by eq. (11) where w_c is dependent on the average void ration in the cake ($\bar{e}$) according to the mass balance

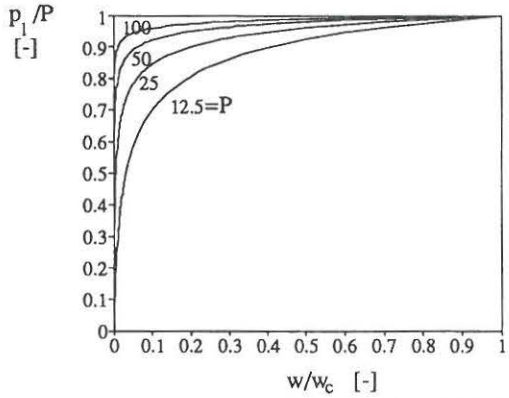

Fig. 8. Calculated relative liquid pressure profile in the cake during filtration for n=5. The numbers give values of applied pressures in kPa.

$$w_c = \frac{V}{e_s - \bar{e}} \tag{15}$$

where V is filtrate volume per cross section area. $\bar{e}$ is expressed by the equation

$$\bar{e} = \frac{1}{w_c}\int_0^{w_c} e\,dw \tag{16}$$

The assumption of uniform flow profile and the use of eq. (2) to substitute dw with dp_s in eq. (16) gives

$$\bar{e} = \frac{1}{\mu w_c u_m}\int_0^P \frac{e}{\alpha}\,dp_s \tag{17}$$

Eq.(11) is used in eq.(17) to obtain

$$\bar{e} = \frac{\int_0^P \frac{e}{\alpha}\,dp_s}{\int_0^P \frac{1}{\alpha}\,dp_s} \tag{18}$$

From this it is seen that $\bar{e}$ depends only on P during filtration. Use of Leipnitz rule for determination of $d\bar{e}/dP$ gives

$$\frac{d\bar{e}}{dP} = \frac{\int_0^P \frac{1}{\alpha}\,dp_s\,(e)_{p_s=P} - \int_0^P \frac{e}{\alpha}\,dp_s}{(\alpha)_{p_s=P}\left(\int_0^P \frac{1}{\alpha}\,dp_s\right)^2} \tag{19}$$

Use of eq. (18) in eq. (19) yields

$$\frac{d\bar{e}}{dP} = \frac{(e)_{p_s=P} - \bar{e}}{(\alpha)_{p_s=P}\int_0^P \frac{1}{\alpha}\,dp_s} \tag{20}$$

From eq.(11) and eq. (15), $\partial u_m/\partial P$ is found by use of Leibnitz Rule

$$\frac{\partial u_m}{\partial P}=\frac{1}{\mu V}\left[\frac{e_s-\bar{e}}{(\alpha)_{p_s=P}}-\frac{d\bar{e}}{dP}\int_0^P\frac{1}{\alpha}dp_s\right] \tag{21}$$

Combining eq.(20) and eq. (21) yields

$$\frac{\partial u_m}{\partial P}=\frac{e_s-(e)_{p_s=P}}{\mu V(\alpha)_{p_s=P}} \tag{22}$$

For void ratio and flow resistance the following assumptions can be made:

1. e is a positive and decreasing function of p_s
2. α is a positive and increasing function of p_s i.e.

$$\lim(\alpha)_{p_s=P}\to\infty \quad \text{for} \quad P\to\infty$$

Use of these assumptions in eq.(22) reveals that

$$\lim\frac{\partial u_m}{\partial P}\to 0 \quad for \quad P\to\infty \tag{23}$$

$$\frac{\partial u_m}{\partial P}>0 \tag{24}$$

So, as P increases, u_m becomes less and less sensitive to the actual value of P, and this tendency is more and more marked as the compressibility increases. But, it is impossible for u_m to decrease as P increases, no matter how compressible the cake is. This is a verification of the result derived from eq. (13) for n>1. All experiments to date give results that are in agreement with eq. (24).

The relationship between Specific Resistance to Filtration (SRF) and applied pressure (P) is described in the literature using the equation

$$SRF=SRF_0\cdot P^m \tag{25}$$

where SRF_0 is a constant and m a compressibility related number. A conflict appears when in the literature, m larger than one is reported. This corresponds to a decreasing filtrate flow as the applied pressure is increased. The theoretical basis for the SRF is equal to the assumptions used in the derivation of eq. (22). Therefore, m greater than one will indicate that this parameter is questionable as a theoretical dewatering characterization parameter in the specific experiment.

CONCLUSION

Investigations of liquid pressure variations during time at filtration/expression and investigation of filtrate flow variations as a function of the applied pressure, show that the filter cake structure for polyelectrolyte conditioned biological sludge is extremely compressible.

When, according to usual filtration theory, the degree of compressibility is assumed extremely high, calculations for filtration using power law functions as constitutive relationships show that nearly all the liquid pressure drop happens in the lowest few per cent of the cake, just above the medium. So, in a dewatering situation where the cake thickness typically is a few centimeters, the main part of the liquid pressure drop in the cake occurs in a few tenths of a millimeter. This suggests the formation of a filter skin that must be further studied and manipulated, e.g. to improve dewatering performance.

When biological sludge compressibility is characterized by the usual power law functions (eq. (6) and eq. (7)), the values of the parameters in these need to be set at extreme values in order to obtain coincidence between measured and calculated results. The usual power laws therefore seem questionable if not inadequate for biological sludge dewatering. Experiments are planned to investigate the actual liquid pressure distribution during pressure filtration and expression.

When the power law functions are replaced by two more basic assumptions regarding void ratios and flow resistance, the theoretical considerations for filtration show that extreme compressibility results in a filtrate flow which is independent of the applied pressure. Experimental data on filtration are in complete agreement with this theoretical prediction. It is demonstrated that during filtration it is impossible for the filtrate flow to decrease as the applied pressure is increased, no matter how extreme the compressibility is. In the literature, however, a compressibility factor for the Specific Resistance to Filtration (SRF) larger than one is reported, which means that the filtrate flow should decrease as the applied pressure is increased. The parameter SRF is theoretically defined by the same considerations for filtration as used in this investigation. Therefore, in case of a compressibility factor for SRF larger than one, the SRF parameter is not theoretically well defined.

LEGENDS

A	Filter medium area [m^2]
e	Volume liquid per volume solids (void ratio) [-].
$\bar{e}$	Average void ratio in the cake [-].
e_s	Void ratio in suspension [-].
e_0	Void ratio when the solids are in contact and p_s=0 [-].
$\bar{e}_{tot}$	Average void ratio in the sludge column [-].
h	Sample deformation [mm].
n	Form factor for the compressibility with respect to specific resistance [-].
m	Compressibility factor for the relationship between SRF and P [-].
P	Applied pressure [Pa].
$P_{l,top}$	Liquid pressure at the top of the sample [kPa].
p_a	Scaling factor [Pa].
p_l	Liquid pressure taken as an average over the cross section area [Pa].
p_{lm}	Liquid pressure at the cake/medium interface [Pa].
p_s	Average pressure of solid (contact pressure) [Pa].
R_m	Resistance in medium [1/m].
SRF	Specific Resistance to Filtration [kg/m].
SRF_0	Constant in eq.(25) [-].
t	Time [s].
u	Liquid flux relative to the solids velocity [m/s].
u_c	Liquid flux relative to the solids velocity at cake surface [m/s].
$\bar{u}$	Average liquid flux relative to the solids velocity in the cake [m/s].
u_m	Liquid flux through the medium [m/s]
u_{mP}	Filtrate flux related to the applied pressure P [m/s].
$u_{m\infty}$	Filtrate flux related to a infinite high applied pressure [m/s].
V	Filtrate volume per cross section area [m].
V_{mes}	Filtrate volume measured [m^3].
w	Solid volume per cross section area [m^3/m^2].
w_c	Total solid volume per cross section area in the cake [m^3/m^2].
w_{tot}	Total solid volume in the sample per cross section area [m^3/m^2].

α	Specific resistance [$1/m^2$].
α_0	Specific resistance when the solids are in contact and p_s=0 [$1/m^2$].
β	Form factor for the compressibility with respect to the porosity [-].
ε	Porosity [-].
ε_0	Porosity when the solids are in contact and p_s=0 [-].
μ	Viscosity of liquid [kg/ms].

ACKNOWLEDGEMENTS

This research was carried out at Environmental Engineering Laboratory, Aalborg University, Denmark. The authors would like to thank Henrik Koch because he was the main force in the construction of the filtration/expression device. The Danish Technical Research Council (Grant 5.26.09.12) is gratefully acknowledged for economical support to this work.

REFERENCES

Christensen, G. L., and Dick, R. I., (1985), "Specific Resistance Measurements: Methods and Procedures", Journal of Environmental Engineering, ASCE, Vol. 111, No. 3, pp. 258-271.

Christensen, J.R., Sørensen, P.B., Hansen, J.Aa., Christensen, G.L., (1993), "Mechanism for overdosing in sludge conditioning", Journal of Environmental Engineering, ASCE, Vol. 119, No. 1, pp.xx-xx (in press).

Leu, W., (1981),"Cake Filtration",Ph. D: Dissertation, The Faculty of the Department of Chemical Engineering, University of Houston.

Sørensen, P.B., Moldrup, P. and Hansen, J.Aa., (1993), "Unified Modeling of Filtration and Expression by Finite Differences", For submission to AIChE, January 1993.

Tiller, F. M., and Yeh, C. S., (1987), "The Role of Porosity in Filtration, Part XI: Filtration

Followed by Expression", AIChE, Vol. 33, No. 8, pp. 1241-1256.

Tiller, F. M. and Leu, W. F. (1980), "Basic Data Fitting in Filtration", Journal of The Chinese Institute of Chemical Engineers, Vol. 11, pp. 61-70.

Effect of Small Scale Solids Migration in Filter Cakes during Filtration of Wastewater Solids Suspensions

III

Effect of Small Scale Solids Migration in Filter Cakes during Filtration of Wastewater Solids Suspensions

Peter B. Sørensen, Jimmy R. Christensen and Jacob H. Bruus.

ABSTRACT

Upward curved (concave) filtration plots of the inverse filtrate flux as a function of filtrate volume have been investigated using a laboratory-scale filtration device and different wastewater solids suspensions stored anaerobically in the laboratory. Using an empirical approach in which a polynomial expression of abitrary order was applied for regression analysis on filtration data it was shown that a parabolic expression was able to adequately fit all concave filtration plots. Turbidity measurements on supernatant and filtrate evidenced that the concave behaviour of the filtration plots could be explained by migration of small scale solids into the filter cake pores (blinding). The coefficients of the derived parabolic equation characterized the resistance attributed to blinding, basic cake filtration, and the filter medium, respectively. Based on the coefficients of the derived parabolic equation, a physically comprehensible parameter for characterizing the influence of blinding on filtration was defined.

KEYWORDS

blinding, cake filtration, empirical characterization, wastewater sludge.

INTRODUCTION

The **cake filtration theory (CFT)** is normally applied for characterizing the filterability of **wastewater solids suspensions (WWSS)**. A **filtration plot (FP)** is obtained by relating the ratio between accumulated time filtrate volume or the inverse filtrate flux, respectively, to the accumulated filtrate volume. If the assumptions governing the CFT are fulfilled, FPs are linear during filtration. As a result, the specific resistance to filtration (SRF) is constant and may be used for characterizing the filtration properties of WWSS.

Novak et al. (1988) showed that during anaerobic storage of WWSS a decrease in filterability was accompanied by a development of non-linear FPs expressed by a more and more pronounced upward facing (concave) curvature. Concave FP conflicts with CFT in that the *SRF* value is no longer a constant characteristic of the solids suspension being tested. In such cases, at least one of the assumptions governing the CFT is erroneous.

Concave FPs have been observed and analyzed by several investigators, and two explanations accounting for non-linear FPs have been offered: (1) a deposition of suspension solids on the filter cake surface due to **sedimentation** concomitant with filtration (Bockstal et al., 1985), or (2) a penetration and subsequent deposition of small scale solids in the filter cake or medium, thus **blinding** (clogging) the porous structure of the filter cake or the medium (Notebaert et al., 1975; Tiller et al., 1981; Leu and Tiller, 1983; Novak et al., 1988).

It is the objective of this study to further investigate the concave FP, associated with WWSS during anaerobic storage. in order to explain the concave FP and to derive a physical comprehensible parameter characterizing the phenomenon.

GOVERNING EQUATIONS FOR CAKE FILTRATION

Relationships governing *SRF* are derived from the CFT as expressed by Eqs. 1 and 2 (Ruth, 1946).

$$\frac{dt}{dV} = \frac{\mu}{P}[SRF\ C\ V + R_m] \qquad (1)$$

$$\frac{t}{V} = \frac{\mu}{P}[\frac{SRF\ C}{2} V + R_m] \qquad (2)$$

In Eqs. 1 and 2, t is time (s), V filtrate volume per unit cross-sectional area (ml/cm^2), μ viscosity of filtrate (Pa·s), P applied pressure (Pa), *SRF* the specific resistance to filtration

(cm/g), C deposited mass of cake solids on the cake surface per unit filtrate volume and per cross-sectional area (g/ml), and R_m the medium resistance (1/cm).

Eq. 1 is derived using a Darcyan description of the local flow properties prevailing in the filter cake in which the liquid flow profile is assumed uniform. Eq. 2 is the integrated version of Eq. 1 and is traditionally used for determining *SRF*. Filtration plots (FPs) relating the left hand sides of Eqs. 1 or 2 to accumulated filtrate volume yield linear relationships implying that each of the parameters P, μ, *SRF*, C, and R_m are constant during filtration. However, because concave FP develops in the FPs during anaerobic storage of WWSS, at least one of the parameters in Eqs. 1 and 2 is not constant in such cases.

NON-LINEAR FILTRATION BEHAVIOUR

Bockstal et al. (1985) suggested occurrence of simultaneous **sedimentation** and filtration to explain concave curvature due to a continuosly increasing value of C in Eqs. 1 and 2. The deposition of solids on the filter cake surface due to filtration was estimated by the slurry concentration (c). However, this is only a good estimation when the filtrate volume is much larger than the volume of liquid contained in the corresponding filter cake. The deposition due to sedimentation was estimated by assuming a constant Stoke settling velocity of suspension solids in the (v_s). Adopted to the notation used this yields

$$t=\frac{\mu}{P}\left[\frac{1}{6}\frac{\mu}{P}(SRF\ c)^2\ v_s\ V^3+\frac{1}{2}SRF\ c\ V^2+R_m\ V\right] \qquad (3)$$

In Eq. 3 c is slurry concentration (g/ml), and v_s the Stoke settling velocity (cm/s). Differentiation of Eq. 3 with respect to V gives

$$\frac{dt}{dV}=\frac{\mu}{P}\left[\frac{1}{2}\frac{\mu}{P}\ (SRFc)^2 v_s\ V^2+SRF\ c\ V+R_m\right] \qquad (4)$$

Alternativly, Notebaert et al. (1975), Tiller et al. (1981), Leu and Tiller (1983), and Novak et al. (1988) attributed concave FPs to **blinding**. A constant value of *SRF* requires the local flow resistance in the cake only to be a function of the solid stress in the porous structure within the filter cake. In case of blinding, however, the local flow resistance is a function of both solid stress and the amount of small scale solids deposited. Therefore, as the amount of small scale solids deposited increases, the value of *SRF* increases. Similarly, blinding of the filter medium results in an increasing value of R_m. In both cases concave behaviour can occur. All the investigators, however, have only applied empirical approaches to describe the blinding phenomenon.

As deep bed filtration theory (DBFT) describes the deposition of small scale solids in an existing porous structure, this theory might therefore be thought to account for the blinding phenomenon. However, the DBFT operates with an incompressible porous structure in which small scale solids are deposited, whereas the cake associated with CFT is compressible. A unification of the CFT and the DBFT seems possible but would introduce several empirical constants. These might be estimated for well defined inorganic slurries, but the complex structure of WWSS is likely to prohibit an accurate determination of such empirical constants. Therefore, a unification of the CFT and the DBFT to describe the blinding phenomenon was not further investigated and it seems only possible to use an empirical approach in case of WWSS filtration.

EMPIRICAL APPROACHES DESCRIBING BLINDING

Notebaert et al. (1975) and Novak et al. (1988) described the blinding phenomenon by assuming an empirical relationship between *SRF* and *V* as

$$SRF=\alpha V^{\beta} \tag{5}$$

where α and β are empirical coefficients. Combining Eqs. 1 and 5 yields

$$\frac{dt}{dV}=\frac{\mu}{P}[\alpha C V^{\beta+1}+R_m] \tag{6}$$

which may be integrated

$$t=\frac{\mu}{P}[\frac{\alpha C}{\beta+2}V^{\beta+2}+R_m V] \tag{7}$$

Notebaert et al. (1975) and Novak et al. (1988) determined the empirical coefficients, α and β, by using Eq. 7 and log-log plots of t versus V, assuming R_m to be negligible. It seems, however, preferable to use Eq. 6 instead of Eq. 7 because: (1) Eq. 6 is much more sensitive to variations in filtrate flow and (2) asynchronous time and volume registration does not affect data analysis by Eq. 6.

Other empirical expressions than Eq. 6 have been suggested by Tiller et al. (1981) who distinguished between cake and medium blinding. A distinction between cake and medium resistance in relation to blinding requires that the hydraulic pressure drop across the filter medium can be measured as done by Leu and Tiller (1983) using kaolin and attapulgite suspensions. Sørensen and Hansen showed, on the other hand, that wastewater solids exhibit extreme compressible behaviour meaning that the total hydraulic pressure drop through the filter cake in practice occurs within a thin fraction of the cake, defined as a skin, just above the filter medium. The existence of such a skin makes it practically very difficult to distinguish between cake and medium blinding in case of WWSS filtration. Furthermore, the empirically equations derived by Tiller et al. (1981) are rather complicated given their empirical background. Therefore, they will not be used in this study concerning WWSS filtration.

The emipirical approach applied in this study is to analyze the

concave behaviour systematically using a polynomial expression of arbitrary order (n) according to

$$\frac{dt}{dV}=a_n V^n+a_{n-1}V^{n-1}+\ldots+a_1 V+a_0 \qquad (8)$$

where n is the order of the polynomial expression, and a_i a coefficient related to the term of order i. In Eq. 8 no assumptions regarding cake versus medium resistances are made in advance, and it provides a more general empirical approach to examine the concave behaviour than applied by earlier investigators. The minimum value of n necessary for obtaining an adequate fit of filtration data by Eq. 8 determines the order of the polynomium describing the concave FP.

MATERIAL AND EXPERIMENTAL PROCEDURES

Samples of WWSS were collected at Aalborg East and Aabybro wastewater treatment plants both having biological nutrient removal. The WWSS samples were thickened for approximately 1.5 hour and the supernatant was removed. For each WWSS sample a series of filtration tests were carried out after different periods of anaerobic storage in the laboratory at room temperature. For some of the series, the filtration tests were accompanied by turbidity measurements on the supernatant (Table 1).

Filtration tests were carried out using a pressurized filtration device similar to the one used by Christensen et al. (1993). WWSS sample volumes for filtration tests varied between 300 and 500 ml. The diameter of the filter medium used in the device was 10 cm. Consequently, the sample volume per unit cross-sectional area varied between 3.82 and 6.37 ml/cm^2, (Table 1). The applied pressure (P) was in all filtration tests 1 bar, and Whatman #41 filter paper was used as filter medium. In some cases, development of air/suspension interfaces at the top of the WWSS samples in the pressurized filtration device was inappropriate and subsequently avoided by installing a nylon piston before the

filtration test was initiated. Usually, the filtrate flow direction was downward. However, when using the nylon piston in the pressurized filtration device, an upward filtrate flow direction could be established simply by turning the filtration device around.

During filtration a time series of the filtrate volume was obtained as $(t_1, V_1), \ldots, (t_i, V_i), \ldots, (t_M, V_M)$, in which M was the total number of volume readings. From such time series, V and dt/dV in Eq. 8 were estimated according to

$$V \approx \frac{1}{2}(V_i + V_{i-1}) \tag{9}$$

$$\frac{dt}{dV} \approx \frac{t_i - t_{i-1}}{V_i - V_{i-1}} \tag{10}$$

Readings of the filtrate volume taken into account were separated according to the criterion: $V_i - V_{i-1} > \Delta V_{min}$. ΔV_{min} was the key parameter regarding filtration data analysis. The value of ΔV_{min} needed to be large enough to secure a denominator of Eq. 10 significantly different from zero to avoid inappropriate fluctuations in the estimations of dt/dV. On the other hand, increasing values of ΔV_{min} adversely affected the number of data points available for the FPs. In this study, a ΔV_{min} of 0.064 ml/cm^2, corresponding to an absolute volume of 5 ml, seemed to provide optimal conditions under the given circumstances.

Turbidity of supernatant and filtrate was characterized by light absorption at 650 nm using a Milton Roy Spectronic 301 spectrophotometer. Supernatant were generated by centrifuging WWSS samples at 2200 rpm in 2 minutes. A series of filtrate samples for turbidity measurements during filtration were obtained by collecting the filtrate in several beakers. In such cases the time used for filtrate collection and the accumulated volume of filtrate were recorded for each beaker in order to determine the corresponding FPs.

RESULTS AND DISCUSSION

Determining the n value in Eq. 8

All data from the filtration series presented in Table 1 have been used for the regression analyses to determine the lowest value of n necessary for establishing agreement between filtration data and Eq. 8. The level of significance (%) needed for acceptance of different values of n are determined by analysis of variance and presented in Table 2. According to Table 2, it is not necessary to use values of n higher than two to adequately fit all filtration data examined in this study. Only two tests suggested n equal to 3 to obtain a 95 % significance level (test series 2, days 1 and 10). However, in both cases only a very small improvement was obtained by increasing the value of n from two to three. In consequence, concave behaviour associated with WWSS filtration may, as shown in Figure 1, be described by the parabolic equation

$$\frac{dt}{dV}=a_2V^2+a_1V+a_0 \qquad (11)$$

Eliminating the sedimentation hypothesis

The relationship between dt/dV and V expressed by Eq. 11 is similar to Eq. 4; that is, supporting the expression for concave behaviour derived by Bockstal et al. (1985) based on the sedimentation hypothesis. However, sedimentation will inevitably develop a liquid phase in the upper part of the WWSS sample in the filtration device. Therefore, in the last period of filtration there is no cake build up and the only contribution to an increasing flow resistance stems from compression of the filter cake. When only liquid is filtered through the cake, the compression of the filter cake structure continuously decreases and approach a steady-state situation in which the flow resistance is constant. As a result, an upward facing curvature in the first part of the FP, as described by Eq. 4, will be succeeded by a downward facing curvature in the last part and approach a horizontal asymptote. Therefore, simultaneous

sedimentation and filtration is more likely to result in S-shaped FPs as suggested by Christensen and Dick (1985) and not concave FP as described by Eqs. 4 and 11 and illustarted in Figure 1.

In order to provide experimental evidence for this claim, filtration experiments were performed using both upward and downward filtrate flow directions. A WWSS sample was collected at the Aalborg East wastewater treatment plant and exposed to three days of anaerobic storage to secure significant concave behaviour in the FPs. Three filtration tests were performed for upward and three for downward filtrate flow directions. All six tests were carried out using the nylon piston in the filtration device. If the parameter a_2 were a result of sedimentation, the value of a_2 would be significantly affected by reversing the filtrate flow direction. However, no such difference in the value of a_2 was exhibited (Table 3). Therefore, the deposition rate of solids on top of the filter cake surface is governed by filtration only, and the concave behaviour is not a result of sedimentation.

Relating Eq. 11 to the blinding hypothesis

A prerequisite for blinding to occur seems to be the existence of solids in at least two size ranges of significantly different orders of magnitude. During anaerobic storage of WWSS, small scale solids in form of free bacteria are released (Rasmussen et al.) which may migrate into the filter cake formed by the larger scale solids (flocs). Therefore, the blinding phenomenon seems to offer an obvious explanation for the concave behaviour examined in this study. Karr and Keinath (1978) fractionated WWSS and suggested the filterability (*SRF*) to be strongly correlated to the so-called supracolloidal particles. However, Karr and Keinath (1978) assumed *SRF* to be constant during the whole filtration experiment also in case of blinding, which seems very questionable. If the blinding hypothesis were correct, the number of free bacteria present in the WWSS liquid phase could be an important factor affecting the concave behaviour.

The characteristics of the liquid phase are assessed by analyzing the supernatant. The number of free bacteria is determined for WWSS collected at Aalborg East wastewater treatment plant using a microscope according to the procedure described by Rasmussen et al. and compared with corresponding turbidity measurements (Figure 2). A rather good correlation is indicated and turbidity measurements presented hereafter are consequently interpreted as evidencing the existence of free bacteria.

Figure 3 shows the relationship between the degree of non-linearity of FPs, characterized by the coefficient a_2 (Eq. 11), and corresponding measurements of supernatant turbidity. Filtration tests of which the parabolic relationship is insignificant (Table 2) are omitted. Even though the characteristics of the WWSS sources vary in form of differences in dry matter content (Table 1), a universal relationship between turbidity and the coefficient a_2 seems to exist. The correlation between the numbers of free bacteria and a_2 is much better than the one for a_1, see Figure 4. In light of Figures 3 and 4 it is concluded that the parameter a_2 is primarily affected by the number of free bacteria and, consequently, describes a blinding phenomenon. The parameter a_1 seems, on the other hand, more related to the resistance of the unblinded cake structure.

Comparison between β and a_2.

Eq. 6 represents an alternative to Eq. 11 and, subsequently, β is an alternative to a_2 as a parameter describing blinding. The β values, shown in Figure 5 as a function of supernatant turbidity, have been estimated using Eq. 6 and the filtration tests associated with Figures 3 and 4. Similar to Notebaert et al. (1975) and Novak et al. (1988), the value of R_m is considered negligible. The relationship between β and supernatant turbidity seems also to be universal. However, the correlation is much better for a_2 (Figure 3) than for β (Figure 5). It is noticed that the value of β for a linear FP is 0.19 (day 0 in test series 1, Table 2) but should have resulted in β=0. This is due to the fact that a small amount of filtrate is released without any

resulting cake build up during application of the WWSS sample in the filtration device. This error in filtrate volume registration do not affect determinations of a_2 value. Consequently, the parameter a_2 seems advantageous to β in describing the blinding phenomenon.

Dramatic deviations from concave behaviour

In some FPs the concave behaviour suddenly changes as a result of a temporarily increasing filtrate flux. Examples of such strange behaviours are shown in Figure 6 in which it is seen that Eq. 11 provides an adequate fit of the FP data until the sudden increase in the filtrate flux. Penetration of air through the filter cake after cease of filtration could explain this phenomenon. But, a similar filtration test was performed by Christensen and Sørensen using WWSS from Aalborg East treatment plant which was conditioned by a very low polymer dose (0.5 kg/tDS). In this test the nylon piston was applied in the filtration device (Figure 7) and the explanation conserning air penetration is rejected because the strange behaviour of the FP is reproduced.

The course of filtrate turbidity during filtration in Figure 7 may provide an explanation of the phenomenon as follows. Initially, the filter cake is very thin and allows most of the small scale solids to penetrate the cake. As filtration advances, the filter cake becomes thicker, and more and more small scale solids are deposited in the cake (cake blinding), whereby the filtrate turbidity decreases. Some deposition of small scale solids may, however, also occur as the filtrate passes the filter medium (medium blinding). This is supported by Tiller et al. (1981) who observed that cloudy filtrates associated with liquefied coal filtration were caused by penetration of small scale solids through the cake and filter medium. The filtrate became less turbid during filtration, thus indicating a deposition of small scale solids in the cake or filter medium (blinding).

Later on, the course of filtrate turbidity with filtrate volume deviates from the general decreasing tendency; in fact a substantial increase is displayed which is accompanied by an increasing filtrate flux. This can be explained by the deposition of small scale solids within the cake structure which locally increases the liquid/solid friction and consequently the solid stress in the filter cake. The resulting decrease in porosity of the cake due to the compressible behaviour increases the hydraulic pressure gradient which then may exert a detaching shear force on the walls of the channels forming the porous structure in the filter cake. Therefore, a situation is feasible whereby locally increasing hydraulic pressure gradients in some sections of the cake cause an erosion of previously deposited small scale solids resulting in increasing filtrate turbidity as well as a temporary reduction in the flow resistance.

The development of strange behaviours identifies the limit of application of any empirical approach for describing FPs exhibiting concave behaviour. Subsequently, it is not recommended to extrapolate fitting results to filtrate volumes larger than associated with a particular filtration test.

Quantifying the influence of blinding on the flow resistance

Eq. 11 can be rewritten in terms of resistances as

$$\frac{P}{\mu}\frac{dt}{dV}=\frac{P}{\mu}a_2V^2+\frac{P}{\mu}a_1V+\frac{P}{\mu}a_0 \qquad (12)$$

The right hand side of Eq. 12 identifies three contributers to the overall resistance to filtration. The unblinded medium resistance is expressed by the coefficient Pa_0/μ. But in the tests performed in this study the values were insignificant, i.e. $a_0=0$. The two remaining contributors, (Pa_2V^2/μ) and (Pa_1V/μ), are assumed to characterize the resistance due to blinding and the basic unblinded cake resistance, respectively. Therefore, the two parameters a_1 and a_2 are designated blinding coefficient and cake filtration coefficient. As expected, the unblinded cake resistance dominates in the initial stages of filtration while the resistance due to blinding dominates at larger accumulated

filtrate volumes, as shown in Figure 8.

Consequently, the filtrate volume per unit cross-sectional area at which the ratio between the resistance due to blinding and the resistance due to unblinded cake is unity (V_b) can be determined as the ratio between the blinding and the cake filtration coefficients, respectively

$$\frac{\frac{P}{\mu}a_2 V_b^2}{\frac{P}{\mu}a_1 V_b}=1 \Rightarrow V_b=\frac{a_1}{a_2} \qquad (13)$$

The parameter V_b is shown in Figure 9 as a function of the anaerobic storage time. Filtration tests of which the parabolic relationship is insignificant (Table 2) are omitted. It is seen in Figure 9 that the blinding influence generally increases during anaerobic storage. After about one week of storage, though, the blinding influence is nearly constant yielding a blinding dominated filtration when about 2 ml/cm^2 filtrate is collected.

The derivation of V_b is based on the assumption that the resistance associated with blinding and the unblinded cake structure, respectively, can be separated according to a_2 and a_1 in Eq. 11. This is, however, a rather unproven assumption. Therefore, V_b must be considered as an interesting concept rather than a real number reflecting the actual physical system. Nevertheless, the fact that the correlation between the number of free bacteria and a_2 is much better than the same correlation for a_1 indicates some physical reality behind V_b.

CONCLUSIONS

Filtration plots (FPs) associated with anaerobically stored WWSS generally display upward facing curvatures (concave behaviour). Regression analyses applying a polynomium of arbitrary order suggest a simple parabolic equation relating the inverse filtrate

flux (dt/dV) to the accumulated filtrate volume (V) for describing concave behaviour.

Turbidity of WWSS supernatant evidences the existence of small scale solids, in form of free bacteria, which are much smaller than the solids forming the filter cake. There is a general, good correlation between the second order parameter identified by the parabolic equation and turbidity measurements, irrespective of the solids concentration of the WWSS being tested. Such a good correlation do not exist between the supernatant turbidity and the linear parameter. This indicates that migration of small scale solids into the filter cake and filter medium during filtration (blinding) is responsible for concave behaviour. Therefore, the second order parameter seems attributed to the resistance associated with blinding while the first order parameter seems related to the resistance of the unblinded filter cake. Consequently, the second order parameter is designated a blinding coefficient while the first order parameter is designated a cake filtration coefficient.

The blinding influence is characterized by a physically comprehensible parameter based on the coefficient of the parabolic equation relating dt/dV to V. This parameter identifies the filtrate volume at which the ratio between the resistance due to blinding equals the resistance due to the unblinded filter cake. The blinding influence increases during the first week of anaerobic storage and approaches a constant value yielding a blinding dominated filtrate flow at filtrate volumes above 2 ml/cm^2.

In some cases FPs display a sudden deviation from the concave behaviour accompanied by a drastic increase in filtrate turbidity. Interactions between the compressible filter cake structure and the deposited small scale solids, in form of erosion of previously deposited small solids, provide a plausible explanation for this strange behaviour. The development of such strange behaviour identifies the limit of application regarding

any empirical equation for describing FPs exhibiting concave behaviour.

ACKNOWLEDGEMENTS

Credits. The Danish Technical Research Council (Grant 5.26.09.12) is gratefully acknowledged for financial support to this study. The authors further wish to thank Lisbeth Wybrandt for technical assistance in the laboratory and Ph.D. student Hanne Rasmussen for performing the bacteria countings and for using data from hers research.

Authors. Peter B. Sørensen and Jimmy R. Christensen are Ph.D. Students at the Environmental Engineering Laboratory, University of Aalborg, Denmark. Jacob H. Bruus is Process engineer (Ph.D.) at APV Pasilac, Aalborg, Denmark. All correspondence regarding this paper should be addressed to Professor Jens Aage Hansen, Head of the Environmental Engineering Laboratory, University of Aalborg, Sohngaardsholmsvej 57, DK-9000 Aalborg, Denmark.

NOTATION

Symbols

a_i	Coefficient in Eq.8 related to the order i (-).
C	Deposited mass of cake solids on the filter cake surface per unit filtrate volume and per unit cross-sectional area (g/ml).
c	Slurry concentration (g/ml).
M	The number of readings in the measured time series of filtrate volume (-).
n	Order of the polynomial expression in Eq.8 (-).
P	Applied pressure (Pa).
R_m	Medium resistance (1/cm).
SRF	Specific Resistance to Filtration (cm/g).
t	Time (s).
V	Filtrate volume per unit cross-sectional area (ml/cm^2).
V_b	Filtrate volume per unit cross-sectional area at which the resistance from blinding equals the unblinded cake resistance (ml/cm^2).
ΔV_{min}	Minimum filtrate volume interval used in the filtration plots (ml/cm^2).
v_s	Stoke settling velocity of suspension solids (cm/s).

Greek letters

α	Empirical coefficient in Eq.5 (-).
β	Empirical coefficient in Eq.5 (-).
μ	Viscosity of filtrate (Pa·s).

Appreviations

CFT	Cake filtration theory.
FP	Filtration plot.
WWSS	Wastewater solids suspension.

REFERENCES

Bockstal, F. *et al.* (1985) Constant Pressure Cake Filtration with Simultaneous Sedimentation. *Filt. & Sep.*, **22**, 255.

Christensen, G.L., and Dick, R.I. (1985) Specific Resistance Measurements: Nonparabolic Data. *J. Env. Eng.*, **111** 243.

Christensen, J.C. *et al.* (1993) Mechanisms for Overdosing in Sludge Conditioning. Accepted for *J. Env. Eng.*, **119** in press.

Christensen ,J.C. and Sørensen, P.B., Controling of Polymer sludge Conditioning, (In prep.)

Leu, W., and Tiller, F.M. (1983) Experimental Study of the Mechanism of Constant Pressure Cake Filtration: Clogging of Filter Media. *Sep. Sci. Tech.*, **18**, 1351.

Notebaert, F.F., *et al.* (1975) A New Deduction with a Larger Application of The Specific Resistance to Filtration of Sludges. *Water Res.*, **9**, 667.

Novak, J.T., *et al.* (1988) The Blinding of Sludges During Filtration. *J. Water Pollut. Control Fed.*, **60**, 206.

Karr, P. R. and T. M. Keinath (1978) Influence of Particle Size on Sludge Dewaterability. *J. Water Pollut. Control Fed.*, **50** 1911.

Rasmussen, H., *et al.* Physical, Chemical and Microbiological Changes in Anaerobically Stored Activated Sludge from a Nutrient Removal Plant: Effects on Dewaterbility. *Water Res.*, (Accepted 1992).

Ruth, B. F. (1946) Correlating Filtration Theory with Industrial Practice. *Ind. Eng. Chem.*, **38**, 564.

Sørensen, P.B., and Hansen, J.Aa. Investigation of the Extreme Compressible Behaviour in Biological Sludge Dewatering.

Wastewater Sludge Dewatering, Specialized Conference, Aalborg, Denmark, *Water Sci. Tech.*, (Accepted October 1992).

Tiller, F.M., *et al.* (1981) Clogging Phenomena in the Filtration of Liquefied Coal. *Chem. Eng. Progress*, **77**, 61.

FIGURE LEGENDS

Figure 1 Filtration data and fitted curves using Eq. 11 for test series 1.

Figure 2 Relationship between turbidity and the number of free bacteria in WWSS supernatant.

Figure 3 Relationship between the non-linear parameter in Eq. 11 (a_2) and turbidity of WWSS supernatant.

Figure 4 Relationship between the linear parameter in Eq. 11 (a_1) and turbidity of WWSS supernatant.

Figure 5 Relationship between the parameter β in Eq. 6 (assuming R_m=0) and turbidity of WWSS supernatant.

Figure 6 Filtration data and fitted curves using Eq. 11 for test series 2 (day 8) and 3 (day 21) showing strange behaviours.

Figure 7 Filtration data and filtrate turbidity associated with strange behaviours; a nylon piston has been used for the filtration test.

Figure 8 The resistance attributed to blinding (Pa_2V^2/μ) and the resistance attributed to unblinded cake filtration (Pa_1V/μ) as a function of accumulated filtrate volume for test series 1, day 14.

Figure 9 Calculated values for V_b as a function of anaerobic storage time.

TABLE 1. The different filtration test series.

Test series number	Wastewater treatment plant for sampling	Date of sampling	Day number associated with anaerobic storage used for filtration tests	Turbidity measurement carried out	Average dry matter content of the WWSS during the storage period (g/l)	Sample volume used for the filtration tests (ml/cm²)
1.	Aalborg East	28/11 1991	0,1,4, 7,11,14	+	8.10	3.82
2.	Aalborg East	13/5 1991	0,1,3, 8,10,14	+	9.95	6.37
3.	Aalborg East	1/7 1991	0,1,2, 3,4,21	-	11.60	5.09
4.	Aabybro	19/8 1991	0,1,3, 8,10,14	+	6.75	3.82

TABLE 2. Results of regression analyses presented by the levels (%) for acceptance of the order (n) in Eq. 8 to be significant.

Day	series No.	n = 1	n = 2	n = 3	n = 4
0	1.	100.00	20.42	22.68	43.34
	2.	100.00	100.00	35.46	90.56
	3.	100.00	99.99	6.76	13.12
	4.	100.00	99.79	83.66	17.30
1	1.	100.00	99.99	54.75	4.42
	2.	100.00	100.00	96.63	88.97
	3.	100.00	100.00	86.55	88.69
	4.	100.00	98.45	24.89	60.04
2	3.	100.00	100.00	15.95	40.89
3	2.	100.00	100.00	92.04	43.81
	3.	100.00	100.00	37.76	26.62
	4.	100.00	100.00	18.05	20.67
4	1.	100.00	100.00	93.11	53.16
	3.	100.00	100.00	38.52	37.15
7	1.	100.00	100.00	21.87	31.63
	4.	100.00	100.00	84.24	28.31
8	2.	100.00	100.00	67.25	47.65
10	2.	100.00	100.00	99.75	53.11
	4.	100.00	100.00	14.37	71.54
11	1.	100.00	100.00	3.91	24.42
14	1.	100.00	100.00	84.78	23.47
	2.	100.00	100.00	90.14	51.22
	4.	100.00	100.00	6.87	13.11
21	3.	100.00	100.00	59.63	26.89

TABLE 3. a_2 values for upward and downward filtrate flow directions.

Test No.	a_{21} (cm^6s/ml^3)	
	Downward filtrate flow direction	Upward filtrate flow direction
1.	78	94
2.	83	77
3.	75	71
Mean value	79	81

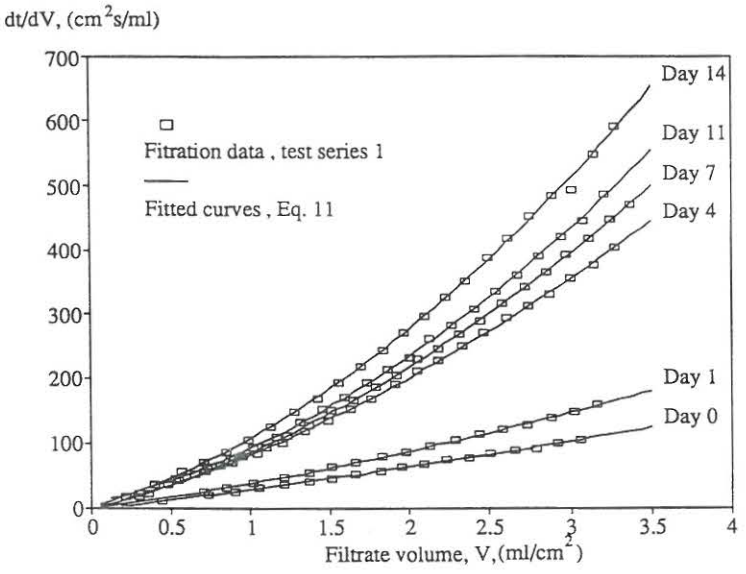

Figure 1

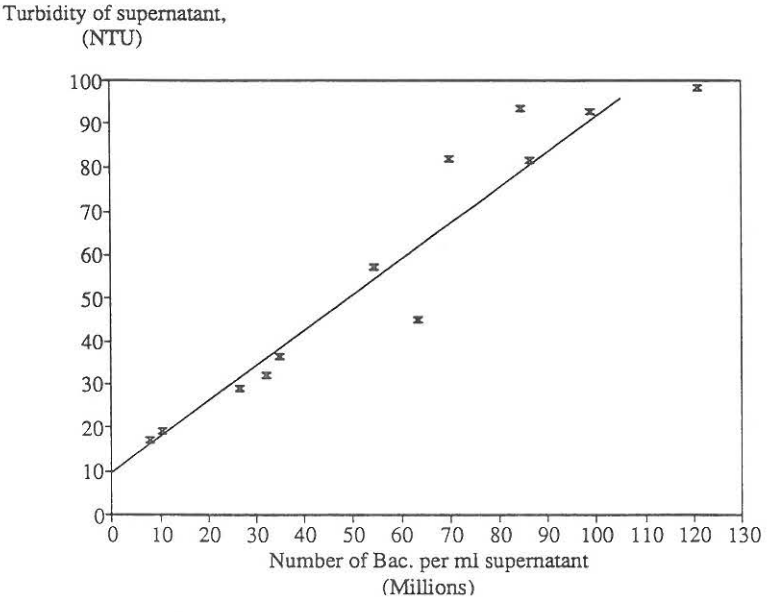

Figure 2

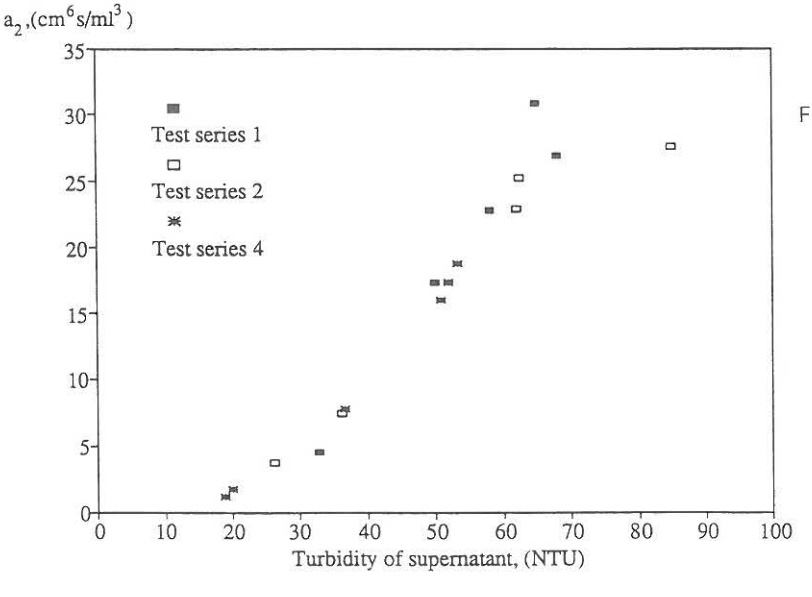

Figure 3

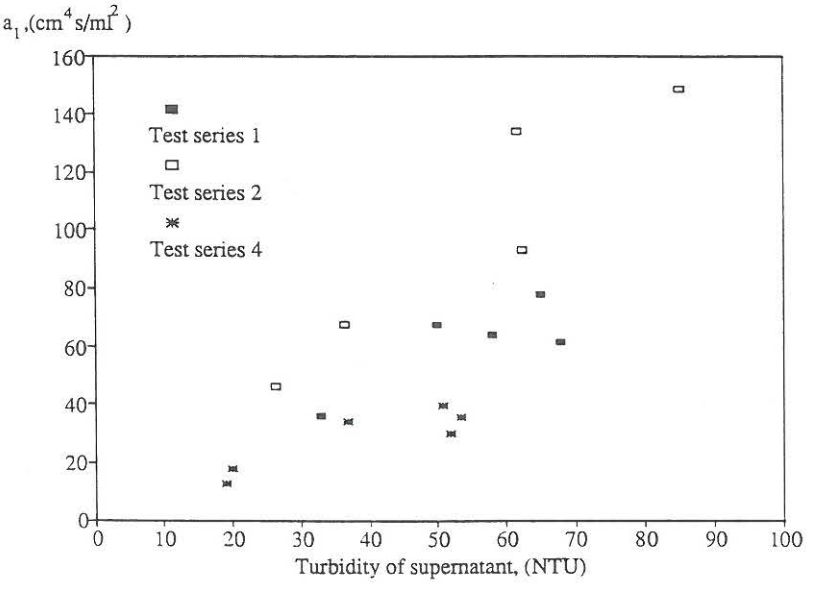

Figure 4

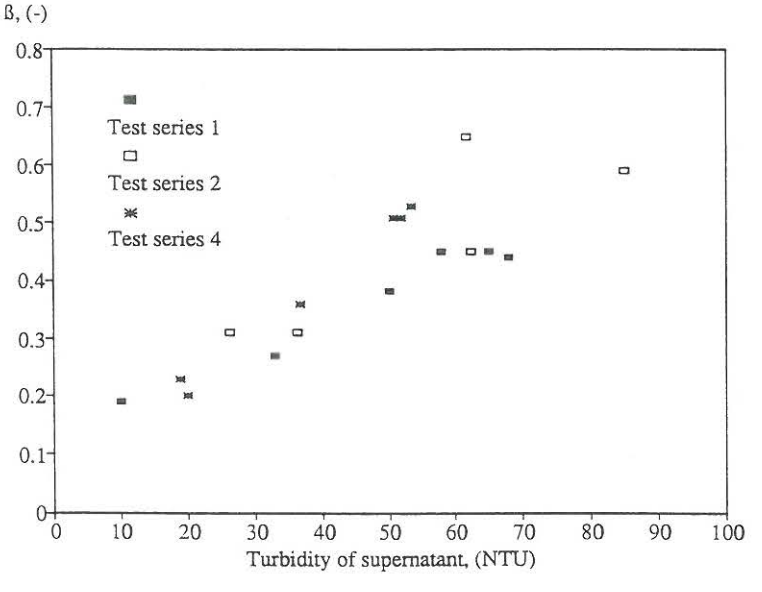

Figure 5

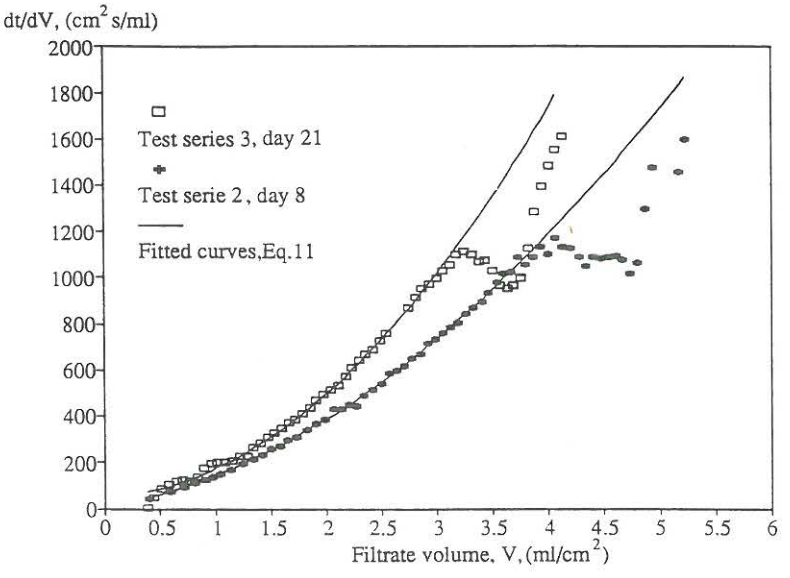

Figure 6

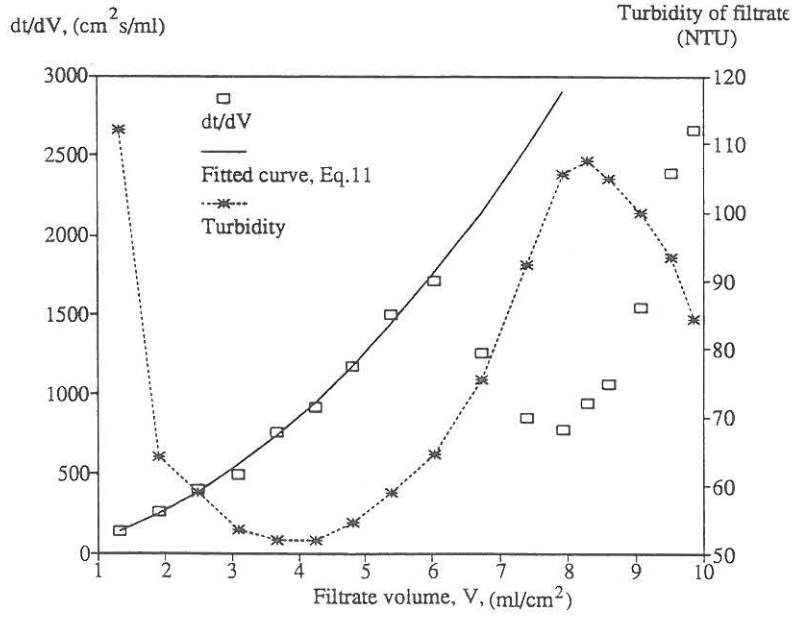

Figure 7

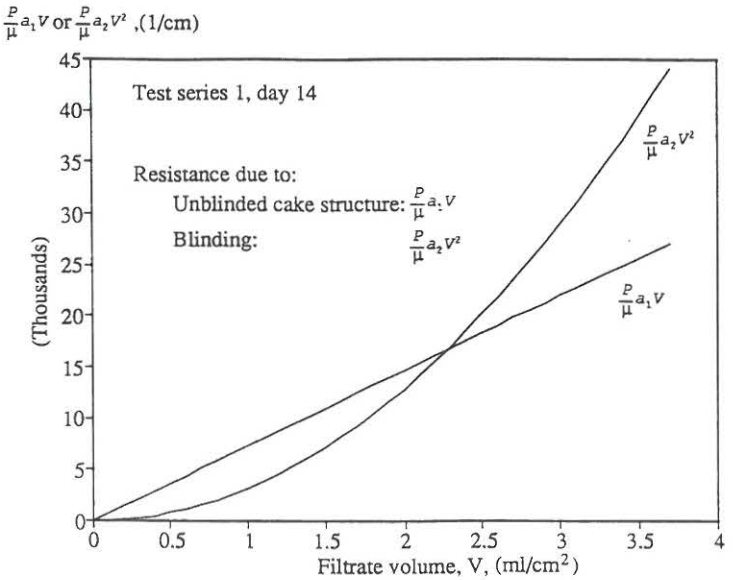

Figure 8

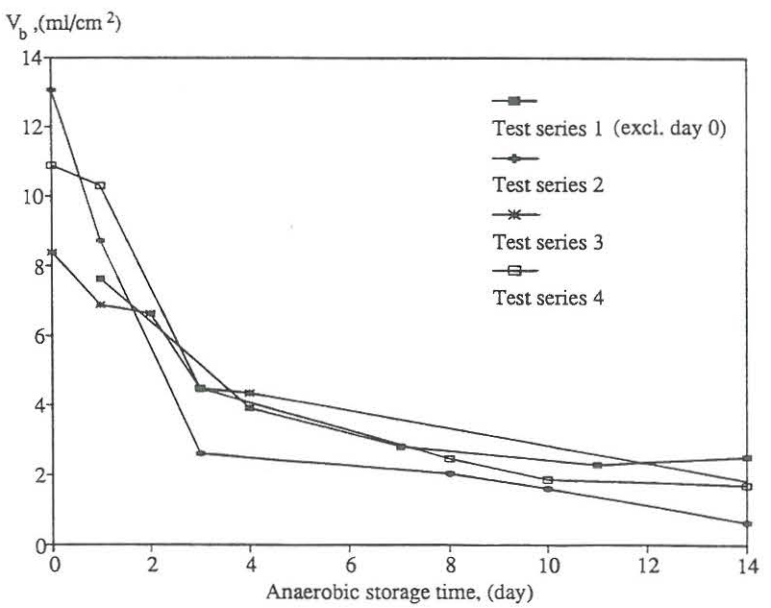

Figure 9

Mechanisms for Overdosing in Sludge Conditioning

IV

Mechanisms for Overdosing in Sludge Conditioning.

By Jimmy Roland Christensen[1], Peter Borgen Sørensen[1],
George Lee Christensen[2], Member ASCE, and Jens Aage Hansen[3].

[1] Ph.D. student, Environmental Engineering Laboratory, University of Aalborg, Sohngaardsholmsvej 57, DK-9000 Aalborg, Denmark.

[2] Professor, Civil Engineering Department, Villanova University, Villanova, PA 19085.

[3] Professor, Environmental Engineering Laboratory, University of Aalborg, Sohngaardsholmsvej 57, DK-9000 Aalborg, Denmark.

ABSTRACT

The mechanisms responsible for overdosing are studied using organic polymers as well as inorganic chemicals as sludge conditioners. Anaerobically stored sludges were used to minimize changes of sludge characteristics due to microbial activity within the period of experimentation. Conditioned sludge is considered as a two-phase system consisting of a liquid phase and a solid phase. Sludge dewaterability is characterized by capillary suction time (*CST*) and specific resistance to filtration (*SRF*), and the sludge liquid phase is characterized separately by its viscosity. Based on the experimental results it is concluded that: overdosing is only associated with polymer conditioning; the traditional use of *CST* and *SRF* does not explicitly account for the mechanisms causing overdosing behaviour; increasing viscosity of the liquid phase, not reduced flocculation performance, is primarily responsible for overdosing as measured by *CST* and *SRF*; and *CST* is incapable of detecting measurable changes in sludge dewaterability within a fairly wide range around the optimal polymer dosage.

INTRODUCTION

Sludges from wastewater treatment plants usually exhibit resistance to mechanical dewatering. Therefore, wastewater sludges are conditioned with chemicals to enhance dewaterability. In sludge conditioning investigations one of the objectives is to determine the effect of different chemical dosages on dewaterability. Dewaterability of conditioned sludge is often characterized exclusively by capillary suction time (*CST*). An optimal dosage of sludge conditioner can be defined as either the amount of added chemicals which yields a distinct optimal dewaterability or the lowest amount of added chemicals which results in an acceptable dewatering performance. When dosages exceed the optimal dosage and dewaterability is reduced simultaneously, the process is described as "overdosed" and vice versa for "underdosed".

Since the introduction of polymeric coagulants, overdosing has been a recognized phenomenon in the coagulation of dilute suspensions in water and wastewater treatment (O'Melia 1972). For example, Pulaski (1968) documented overdosing in experiments on polymeric coagulation of dilute kaolinite suspensions, and Black et al. (1966) provided similar results for dilute clay suspensions. Usually, overdosing in dilute suspensions is attributed to a reduced ability to aggregate the colloidal solids associated with saturation of the colloidal surfaces with polymer. Saturation of the colloidal surface with polymer is usually accompanied by a reversal of the surface charge. The optimal polymer dosage is commonly associated with partial coverage of the colloidal surface which is accompanied by minimum surface charge.

Overdosing of concentrated suspensions (sludges) has also been documented in coagulation processes (sludge conditioning) for water and wastewater sludges. Investigations on the difference between inorganic (ferric chloride and lime) and organic sludge conditioning showed that overdosing only seemed to occur using polymeric coagulants (Christensen and Wavro 1981). Overdosing associated with organic sludge conditioning has been reported by Dentel and Wehnes (1988), Novak and Haugan (1979), and Werle et al. (1984). Nevertheless, not all investigators have

presented data documenting the overdosing phenomenon. For example, Cole and Singer (1986) investigated the effects of different polymers on the *CST* of anaerobically digested sludges, and these investigators did not present any data on overdosing using polymer dosages up to $2 \cdot 10^{-2}$ $kg\,kg^{-1}$ (*kg* dry polymer per *kg* dry sludge solids). Novak (1990) and Tenney et al. (1970) presented data of which some exhibited overdosing while others did not.

Typical sludge concentrations of 1 to 8 % solids lead to relatively broad regions of optimal conditioning with respect to polymer dosage. It seems likely that overdosing in sludge conditioning has not been reported more frequently because the width of the effective coagulation zone, in the dewaterability or turbidity versus polymer dosage curve, is directly related to the solids concentration of the suspension. In many instances, however, sludge conditioning studies have not investigated large enough polymer dosages to produce overdosing.

The specific mechanisms associated with overdosing in polymeric sludge conditioning have not been studied. Most investigators appear to assume the mechanisms are similar to the mechanisms for overdosing in dilute suspensions, (Novak and Haugan 1979; O'Brien and Novak 1977). For example, Novak and Haugan (1979) investigated the effect of polymer dosage on an alum sludge and measured dewaterability (*CST*) of sludge and electrophoretic mobility of supernatant particles as a function of polymer dosage. The results indicated that the polymer dosage for optimal dewaterability coincided with the polymer dosage associated with zero electrophoretic mobility.

The objective of this study is to investigate the mechanisms which are responsible for the overdosing behaviour exhibited by wastewater sludges conditioned with organic polymers, and to compare organic and inorganic sludge conditioning in light of these mechanisms. A two-phase sludge concept is defined which consists of a liquid phase and a solid phase. The commonly used dewaterability measurements *CST* and specific resistance to filtration (*SRF*) are evaluated with respect to the proposed two-phase concept. *CST* and *SRF* are used to characterize sludge dewaterability, and these measurements are supplemented with viscosity and *CST* measurements on the sludge liquid phase. The ability of *CST* and *SRF* to characterize changes in sludge dewaterability and the significance

of the two-phase concept regarding the overdosing behaviour of polymer conditioned sludges are demonstrated. As this study focuses on the phenomenon "overdosing" and the interpretation of dewaterability measurements according to the two-phase sludge concept, only one type of sludge, one type of organic conditioner and one type of inorganic conditioner are used.

THEORY

In order to interpret data on sludge conditioning experiments, certain theoretical topics must be addressed. The following paragraphs address some necessary theoretical aspects of dewaterability analyses of conditioned sludges considered as two-phase systems.

Dewaterability characterization according to the two-phase concept. *SRF* and *CST* represent filtration processes which are special cases of the flow through a solid matrix concept. This concept is based on a two-phase system in which the suspension/slurry to be separated is subdivided into a liquid phase and a solid phase, and where each phase has its own individual characteristics. Thus, the theoretical background exists for assessing the usefulness of *SRF* and *CST* in characterizing conditioned sludges as two-phase systems.

SRF and *CST* characterize a resistance to filtration. This resistance can be subdivided into an apparatus resistance and a sludge resistance. It is the sludge resistance part of *CST* and *SRF* that is of interest in the sludge dewatering context, and it is important that the influence of the apparatus resistance does not mask the influence of the sludge resistance. The sludge resistance, in turn, can be subdivided into resistances associated with the solid phase and the liquid phase to evaluate the effect of each of the two phases on sludge dewaterability.

Specific resistance to filtration (*SRF*). The commonly used relationship governing *SRF* measurements can be derived from the conventional compressible cake filtration theory (Carman 1938; Ruth 1946) (Eq. 1).

$$\frac{t}{V} = \frac{\mu_f \cdot SRF \cdot w}{2 \cdot A^2 \cdot P} \cdot V + \frac{\mu_f \cdot R_m}{A \cdot P} \tag{1}$$

where t is the time in the filtration process $[s]$, V is the filtrate volume $[m^3]$, μ_f is the filtrate viscosity $[Pas]$, SRF is the average specific resistance to filtration $[m kg^{-1}]$, w is the mass of dry cake deposited per unit volume of filtrate $[kg m^{-3}]$, A is the area of the filter medium $[m^2]$, P is the applied pressure $[Pa]$, and R_m is the media resistance $[m^{-1}]$.

The first part of the right hand side of Eq. 1 represents the sludge (filter cake) resistance while the second part represents the apparatus (filter media) resistance which is usually insignificant in a *SRF* test. *SRF* is calculated according to the principles described in Christensen and Dick (1985), and it turns out that *SRF* is inversely proportional to both μ_f (related to the liquid phase) and w (related to the solid phase). Thus, *SRF* relates only to the sludge resistance and can be evaluated according to the two-phase sludge concept. When calculating *SRF*, water viscosity (μ_w) or a constant value equal to $1.1 \cdot 10^{-3}$ *Pas* (Vesilind 1980) is commonly used instead of measured values of μ_f. This procedure has been shown to be erroneous in determining *SRF*, if the actual value of μ_f deviates significantly from the corresponding value for water (Christensen and Dick 1985).

Capillary suction time (*CST*). It is impossible to verify any dewatering theory using the common *CST* apparatus because a single *CST* measurement only records one data pair of time and distance travelled by a filter paper wetting front. This is inadequate for describing the dynamics of the dewatering process taking place in the *CST* test. Tiller et al. (1983) developed a more advanced

CST concept which recorded the wetting front location in the filter paper at several time intervals. Based on this concept, an equation governing the *CST* measurements performed in this study can be expressed by Eq. 2.

$$CST = c_1 \cdot SRF \cdot \mu_f \cdot w + c_2 \cdot \mu_f \tag{2}$$

where c_1 and c_2 are constants associated with the particular *CST* apparatus being used.

Eq. 2 can be divided into two terms analogous to the division described earlier (Eq. 1) for the *SRF* test: a sludge resistance term (the first part) and an apparatus resistance term (the second part). The apparatus resistance is typically much more significant in a *CST* test than in a *SRF* test. The dependency of *CST* on liquid phase viscosity and solids concentration as well as the existence of an apparatus resistance associated with the *CST* apparatus are rarely taken into account when interpreting *CST* measurements. This have lead to a proposal for a modified *CST* value (CST_{mod}).

Modified *CST* (CST_{mod}). To correct for both apparatus resistance and inherent sludge characteristics in a *CST* test it is suggested to subtract *CST* for the liquid phase (CST_f) from the *CST* measurement, and then divide by w and μ_f. These corrections yield a modified *CST* value which relates only to the sludge resistance (Eq. 3) and is in accordance with the two-phase sludge concept.

$$CST_{mod} = \frac{(CST - CST_f)}{w \cdot \mu_f} \tag{3}$$

In Eq. 3 the mass of sludge solids per unit volume of filtrate (w) can be approximated by the sludge solids concentration, while μ_f has to be measured. A *CST* test does not produce any filtrate, but if a *SRF* test or a sedimentation test accompanies the *CST* test, the filtrate or the supernatant can be

used for viscosity and *CST* measurements to determine μ_f and CST_f. This approach assumes that such measurements are representative of the viscosity and *CST* of the liquid phase associated with the *CST* test.

MATERIAL AND EXPERIMENTAL PROCEDURES

Activated sludge from Aalborg East Wastewater Treatment Plant was collected two times during the course of the study (designated #1 and #2 respectively). The sludge was stored anaerobically in the laboratory at room temperature ($20 \pm 1°C$) for approximately ten days before any experiments commenced in order to minimize changes in sludge characteristics due to microbial activity within the experimentation period. The solids concentration of the sludges being tested varied between 1.4 and 1.6 % w/w. Two types of conditioning chemicals were used: a 1 % w/V stock solution of a high molecular weight, high charge density cationic polymer (*Praestol 644 BC*) and 10 % w/V stock solutions of $FeCl_3$ and CaO.

Sludge dewaterability was characterized by specific resistance to filtration (*SRF*) and capillary suction time (*CST* and CST_{mod}). *SRF* tests were performed using a computer assisted filtration device according to the principles presented by Christensen and Dick (1985). The pressurized stainless steel cylinder used for the *SRF* tests had an inner diameter of 0.1 *m*, and the filter medium consisted of Whatman #41 filter paper on top of a fine mesh (23 threads per inch) on top of a course mesh (6 threads per inch). The pressure difference used in this study was 10^5 *Pa*. *CST* measurements were performed using a "Triton 165 Capillary Suction Time Apparatus", a sample cylinder with an inner diameter of 10 *mm*, and Whatman #17 chromatography paper.

Rheological measurements were performed using a "Brookfield LVT-DVII" rotational viscometer. The rheology of the filtrate from the *SRF* test was evaluated by measuring corresponding values of shear stress (τ) and shear rate ($\dot{\gamma}$). $\dot{\gamma}$ was first increased from 0 to 75 s^{-1} and then immediately afterwards decreased from 75 to 0 s^{-1}. The mixing apparatus used for sludge conditioning consisted of a "Heidolph RZR 2051" electronic stirrer, a paddle impeller (5.0 *cm* in diameter and 1.2 *cm* in width), and a mixing vessel which had an inner diameter of 10.5 *cm* and four baffles, each 11 % of the inner diameter. The paddle impeller was operated at 500 *rpm* in each experiment.

Conditioning experiments were performed by pouring a 500 *ml* sludge sample into the mixing vessel. The agitator was started, and a measured volume of conditioning chemical was added to the unconditioned sludge. After 60 *s* of mixing, a sample of the conditioned sludge (approximately 6 *ml*) was withdrawn and used for the *CST* test, and then the agitator was stopped. The remaining conditioned sludge was poured gently into the pressurized cylinder used for the *SRF* test. Finally, viscosity and *CST* of the filtrate from the *SRF* test were measured. All experiments were conducted at room temperature ($20 \pm 1°C$).

In the experiments where sludge was conditioned with polymer, the same volume of polymer/water mixture, but with different concentrations of polymer, was added to a fixed volume of sludge. This procedure produced variations in polymer dosage with constant sludge solids concentrations. Polymer dosages ranged between 10^{-4} and 10^{-1} $kg\,kg^{-1}$. In all experiments where sludge was conditioned with inorganic chemicals ($FeCl_3$ and CaO), the sludge solids concentration was measured. $FeCl_3$ was added a few seconds prior to CaO, and three times as much CaO as $FeCl_3$ was added. Inorganic dosages ranged between 10^{-2} and 1 $kg\,kg^{-1}$. In case of inorganic conditioning, the chemical dosages indicated on the graphs represent the total weight of chemicals added.

RESULTS AND DISCUSSION

Dewaterability of unconditioned sludge. Fig. 1 presents data on modified capillary suction time (CST_{mod}) of the unconditioned sludge during the experimentation period. These data show that CST_{mod} of the sludges being tested was roughly constant during the experimentation period. Therefore, variations in sludge dewaterability reported in this investigation are only due to the effects of the applied chemical conditioners.

Polymer as conditioning chemical. Capillary suction time and specific resistance to filtration measurements on polymer conditioned sludge are shown in Fig. 2 (viscosity of water was used in the *SRF* calculations). Data are plotted in a log-log diagram to provide the best identification of the optimal polymer dosages. These data show distinct, but different, optimal polymer dosages associated with *CST* and *SRF*. The optimal polymer dosage based on minimum *CST* is $3 \cdot 10^{-3}\ kg\,kg^{-1}$, but $10^{-2}\ kg\,kg^{-1}$ based on minimum *SRF*. Overdosing is evident beyond the respective optimal dosages for both *SRF* and *CST*.

Rheological measurements on filtrate from the *SRF* tests on polymer conditioned sludge display Newtonian behaviour in the underdosed region. In the overdosed region, filtrate from *SRF* tests behave as power-law fluids. This non-Newtonian behaviour of filtrate associated with the overdosed region is not shown and is not taken explicitly into account in this study. Values of μ_f presented in Fig. 3 are all determined as the apparent viscosity at a shear rate of $75\ s^{-1}$. In the underdosed region, μ_f seems to be independent of polymer dosage and approximately equal to $1.1 \cdot 10^{-3}\ Pas$ while, in the overdosed region, there is a definite influence of polymer dosage on μ_f. The increasing values of μ_f associated with increasing polymer dosages seem likely to be caused by excess polymer in the liquid phase.

The *SRF* values calculated using μ_w (see Fig. 2) are compared in Fig. 4 to recalculated *SRF* values based on measured values of μ_f. There is practically no difference between corresponding *SRF* values in the underdosed region. But calculations of *SRF* using μ_w produces artificially high *SRF* values in the overdosed region compared to *SRF* values calculated using measured values of μ_f. In light of the results in Figs. 3 and 4, the substantial increase in *SRF* in the overdosed region shown in Fig. 2 seems to reflect the use of incorrectly low values of μ_f more than a resistance change by the solids forming the sludge cake.

Capillary suction time measurements and the difference between *CST* and CST_f are presented in Fig. 5. In a wide range of polymer dosages around $3 \cdot 10^{-3}\ kg\,kg^{-1}$ (the optimal dosage) the difference between *CST* and CST_f is approximately zero. In this range of polymer dosages, it seems that the apparatus resistance controls the *CST* value which is then incapable of detecting measurable differences in sludge resistance. Based on Fig. 5, the optimal polymer dosage identified by *CST* measurements according to Fig. 2 may be far from optimal.

Comparisons between *CST* and modified *CST* values (CST_{mod}) are shown in Fig. 6. Because the sludge solids concentration is constant in the polymer conditioning experiments, a solids correction is not included in the modifications. CST_{mod} show the same pattern as for *SRF* calculated using measured values of μ_f; that is, the significant increase in the *CST* measurements is more dependent on increasing viscosity of the liquid phase than effects associated with the solid phase.

Inorganic conditioning chemicals. Capillary suction time and specific resistance to filtration measurements (calculated using μ_w) at different dosages of inorganic conditioner are shown in Fig. 7. *SRF* of inorganic conditioned sludge exhibits no distinct minimum in contrast to the experiments with polymer conditioned sludge. *CST* values start to increase slightly beyond a chemical dosage of 0.3 $kg\,kg^{-1}$, indicating overdosing effects. Based on Fig. 7, an inorganic dosage of 0.3 $kg\,kg^{-1}$

seems to be a proper choice of optimal dosage associated with both *SRF* and *CST* measurements.

Rheological measurements on filtrate from the *SRF* tests on inorganically conditioned sludge all exhibit Newtonian behaviour. Filtrate viscosity measurements (see Fig. 8) demonstrate that μ_f is constant and practically equal to $1.1 \cdot 10^{-3}$ *Pas*, irrespective of the applied dosage of inorganic conditioner. This result contrasts the experiments on polymer conditioned sludge where μ_f increased sharply to almost five times the value for water in the overdosed region. On the other hand, the constant value of μ_f in Fig. 8 can be seen as consistent with the experiments on polymer conditioned sludge, because with inorganic conditioning overdosing does not seem to occur.

Because μ_f is constant and the changes in sludge solids concentration are already accounted for in the calculations of *SRF*, no corrections to *SRF* are required. As the sludge solids concentration is varying with dosage of inorganic conditioner, *CST* is modified according to Eq. 3 by using sludge solids concentration for w and keeping μ_f constant and equal to $1.1 \cdot 10^{-3}$ *Pas*. *CST* measurements and the corresponding CST_{mod} values are shown in Fig. 9. The increasing tendency of *CST* beyond an inorganic dosage of 0.3 $kg\,kg^{-1}$ is eliminated by modifying *CST*, and the responses in CST_{mod} and *SRF* to increasing dosages of inorganic conditioner (see Figs. 7 and 9) seem similar.

SUMMARY AND CONCLUSIONS

The overdosing phenomenon associated with sludge conditioning and the interpretation of dewaterability measurements according to a two-phase (solid and liquid) sludge concept has been investigated. In order to focus on the overdosing phenomenon, only one sludge type, one organic polymer and one combination of inorganic chemicals were applied. Dewaterability of conditioned sludge was characterized by the commonly used capillary suction time (*CST*) and by specific

resistance to filtration (*SRF*). Further, viscosity and *CST* were measured on filtrate from the *SRF* tests to separate the effects of solids and liquid in the sludge. Apparatus resistance and sludge resistance were distinguished when performing *CST* and *SRF* measurements.

The *SRF* test is originally based on the two-phase sludge concept, and the apparatus resistance is usually insignificant compared to the sludge resistance. However, the apparatus resistance associated with *CST* measurements can not be assumed insignificant compared to the sludge resistance. Therefore, a modification of the *CST* test based on theoretical discussions of capillary suction time by earlier investigators was proposed. In this way the impact on a *CST* measurement associated with the apparatus resistance, the filtrate viscosity and the sludge solids concentration was taken into account. Ideally, *SRF* measurements on sludge should always include correction for viscosity of the liquid phase. And, similarly, *CST* measurements should always include corrections for apparatus resistance, liquid phase viscosity, and solids concentration. By such experimental approach, one can expect to adequately characterize sludge dewaterability rather than characteristics of the laboratory equipment.

For polymer as conditioning chemical, increases of both *CST* and *SRF* occurred at high polymer dosages (overdosing). The rises in both *CST* and *SRF* were accompanied by increasing filtrate viscosities (μ_f). For inorganic conditioning chemicals, there were no signs of overdosing, and μ_f was practically constant and equal to $1.1 \cdot 10^{-3}$ *Pas* irrespective of dosage. This shows that increasing viscosity of the liquid phase is a clear sign of polymer overdosing, and in this study a more significant mechanism for overdosing than reduced flocculation performance, which earlier studies with dilute suspensions and sludges have identified as the primary mechanism for overdosing.

The particular sludge tested in this study showed only small differences in sludge dewaterability measured by *CST* within a fairly wide range of polymer dosages around the optimal dosage, because the apparatus resistance masked the sludge resistance. This means that the optimal polymer dosage determined by a *CST* versus polymer dosage curve may be somewhat artificial, unless the apparatus resistance, liquid phase viscosity (μ_f) and sludge solids concentration have been taken into account.

In this study, *CST* determined a lower optimal polymer dosage than *SRF* which shows that *CST* and *SRF* are not always equivalents in characterizing sludge dewaterability. The inconsistency between *CST* and *SRF* for polymer conditioned sludge may be due to the lack of sensitivity associated with the *CST* measurements near the optimal polymer dosage. However, *SRF* and modified *CST* values responded similarly to varying dosages of inorganic conditioners.

A practical implication of this study is that viscosity measurements on the sludge liquid phase (filtrate or supernatant) may be capable of identifying the optimal polymer dosage, i.e. the polymer dosage above which excess polymer in the liquid phase becomes significant. Such an upper limit for polymer addition seem to coincide with optimal sludge dewaterability measured by *SRF* but exceed the optimal polymer dosage determined by *CST* measurements.

ACKNOWLEDGMENTS

This research was carried out at Environmental Engineering Laboratory, University of Aalborg, Denmark. The authors would like to thank L. Wybrandt for assistance in the laboratory. The Danish Technical Research Council (Grant 5.26.09.12) is gratefully acknowledged for financial support to this work.

APPENDIX I. REFERENCES

Black, A.P., Birkner, F.B., and Morgan, J.J., (1966), "The Effect of Polymer Adsorption on the Electrokinetic Stability of Dilute Clay Suspensions", Journal of Colloid and Interface Science, Vol. 21, pp. 626-648.

Carman, P.C., (1938), "Fundamental Principles of Industrial Filtration (A Critical Review of Present Knowledge)", Transactions Institution of Chemical Engineers, Vol. 16, pp. 168-188.

Christensen, G.L., and Wavro, S.G., (1981), "Some Aspects of Iron and Lime versus Polyelectrolyte Sludge Conditioning", Proceedings of the Thirteenth Mid-Atlantic Industrial Waste Conference, Ann Arbor Science Publishers, Inc., Ann Arbor, Michigan, pp. 404-415.

Christensen, G.L., and Dick, R.I., (1985), "Specific Resistance Measurements: Methods and Procedures", Journal of Environmental Engineering, ASCE, Vol. 111, No. 3, pp. 258-271.

Cole, A.I., and Singer, P.C., (1986), "Conditioning of Anaerobically Digested Sludge", Journal of Environmental Engineering, ASCE, Vol. 111, No. 4, pp. 501-510.

Dentel, S.K., and Wehnes, K.M., (1988), "Use of Streaming Current Detectors in Dewatering", Proceedings CSCE-ASCE Joint National Conference on Environmental Engineering, pp. 254-261.

Novak, J.T., and Haugan, B.E., (1979), "Chemical Conditioning of Activated Sludge", Journal of the Environmental Engineering Division, ASCE, Vol. 105, No. EE5, pp. 993-1008.

Novak, J.T., (1990), "The Effect of Mixing on the Performance of Sludge Conditioning Chemicals", Water Supply, Vol. 8, Jönköbing, Sweden, pp. 53-60.

O'Brien J.H., and Novak, J.T., (1977), "Effects of pH and Mixing on Polymer Conditioning of Chemical Sludges", Journal of the American Water Works Association, Vol. 69, pp 600-605.

O'Melia, C.R., (1972), Physicochemical Processes for Water Quality Control, Ed. by Weber Jr., W.J., John Wiley & Sons, New York.

Pulaski, J.C., Jr., (1968), "The Effect of Calcium Ions and pH on the Destabilization of a Dilute Kaolinite Suspension by Synthetic Polymers", unpublished master's report, Department of Environmental Sciences and Engineering, University of North Carolina, Chapel Hill, N.C.

Ruth, B.F., (1946), "Correlating Filtration Theory with Industrial Practice", Industrial and Engineering Chemistry, Vol. 38, No. 6, pp. 564-571.

Tenney, M.W., Echelberger Jr., W.F., Coffey, J.J., and McAloon, T.J., (1970), "Chemical Conditioning of Biological Sludges for Vacuum Filtration", Journal Water Pollution Control Federation, Vol. 42, No. 2, Part 2, pp. R1-R20.

Tiller, F.M., Leu, W., and Nguyen, C., (1983), "Determining Flow Resistance of Compressible Cakes: Capillary Suction Method", Department of Chemical Engineering, University of Houston, Houston, Texas.

Vesilind, P.A., (1980), Treatment and Disposal of Wastewater Sludges, Ann Arbor Science Publishers, Inc., Ann Arbor, Michigan.

APPENDIX II. NOTATION

The following symbols are used:

A = area $[m^2]$

P = applied pressure $[Pa]$

R = resistance $[m^{-1}]$

t = time $[s]$

V = volume $[m^3]$

w = mass of dry cake deposited per unit volume of filtrate $[kg\,m^{-3}]$

Greek letters.

$\dot{\gamma}$ = shear rate $[s^{-1}]$

μ = absolute viscosity $[Pas]$

τ = shear stress $[Pa]$

Subscripts.

$1, 2$ = different constants

f = filtrate

m = media

mod = modified value

w = pure water

Abbreviations.

CST = capillary suction time $[s]$

SRF = average specific resistance to filtration $[m\,kg^{-1}]$

FIGURE LEGENDS

Fig. 1. *CST* of unconditioned sludge in the experimentation period.

Fig. 2. *SRF* and *CST* versus polymer dosage.

Fig. 3. Filtrate viscosity versus polymer dosage compared to viscosity of water.

Fig. 4. *SRF* based respectively on viscosity of water and viscosity of filtrate.

Fig. 5. *CST* and $(CST - CST_f)$ versus polymer dosage.

Fig. 6. *CST* and CST_{mod} versus polymer dosage.

Fig. 7. *SRF* and *CST* versus dosage of inorganic conditioner.

Fig. 8. Filtrate viscosity versus dosage of inorganic conditioner compared to viscosity of water.

Fig. 9. *CST* and CST_{mod} versus dosage of inorganic conditioner.

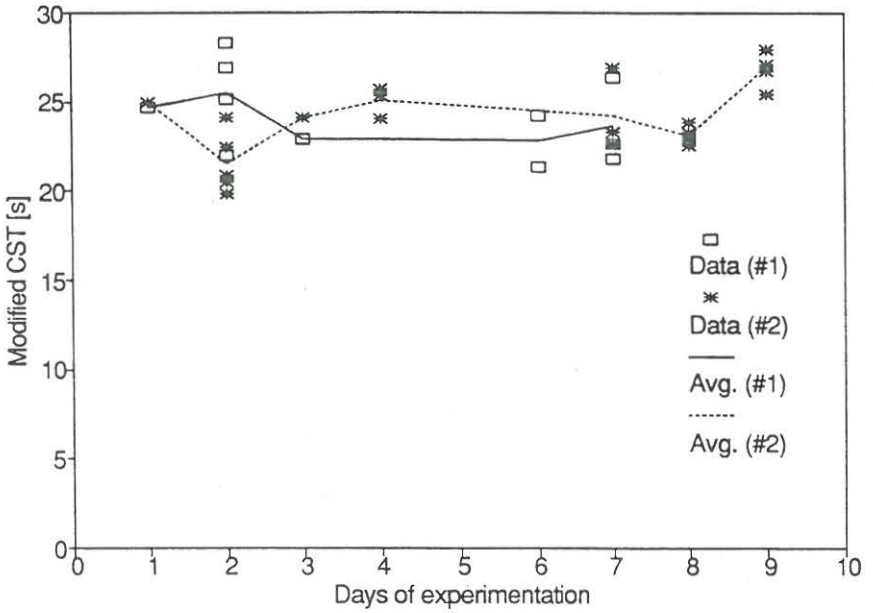

Figure 1

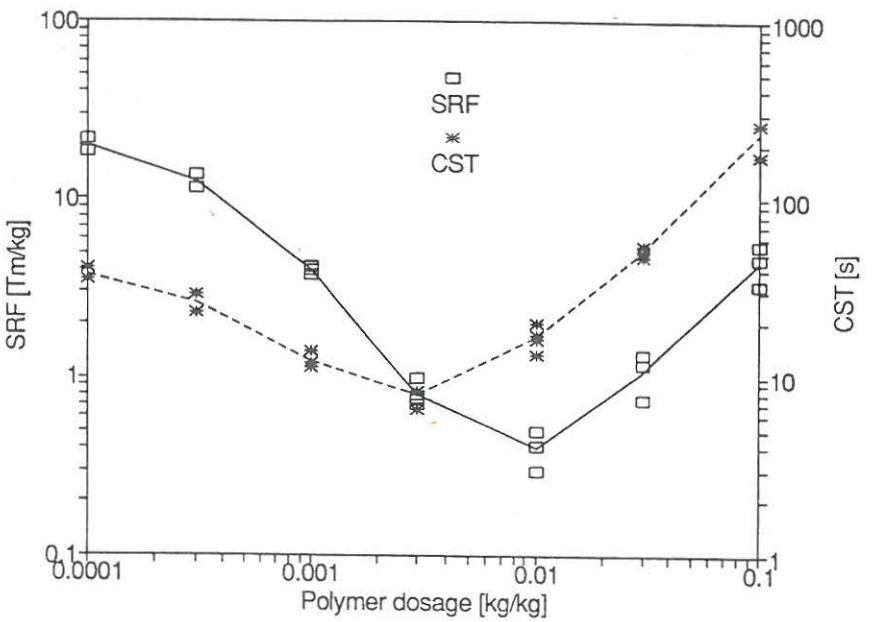

Figure 2

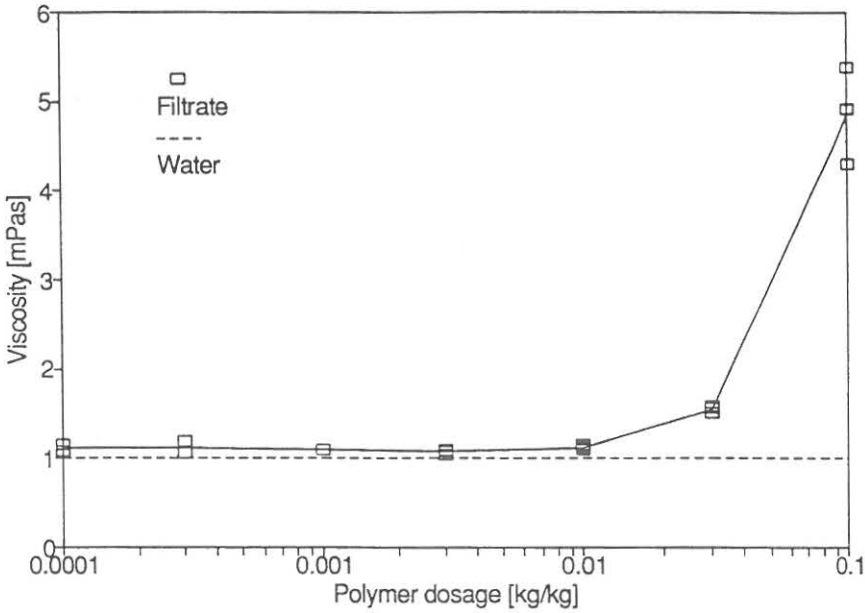

Figure 3

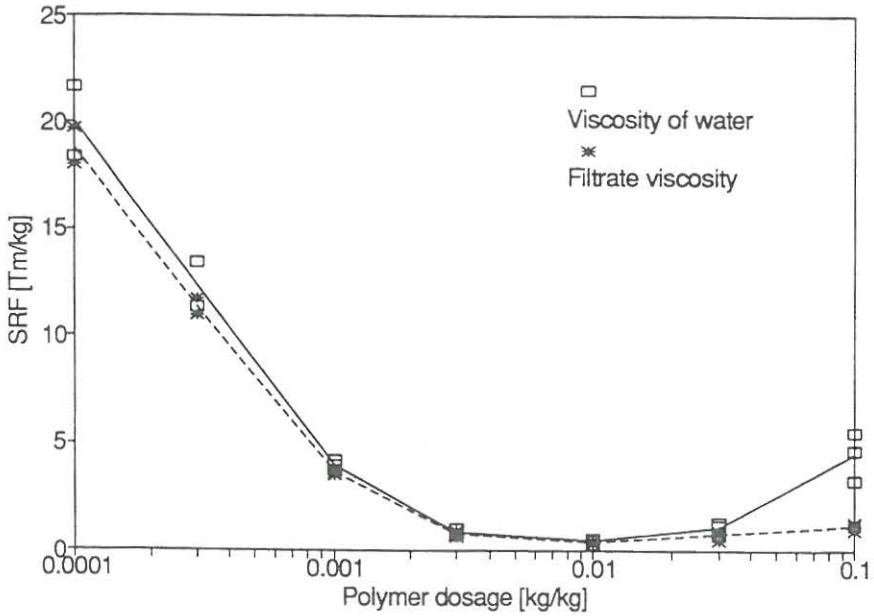

Figure 4

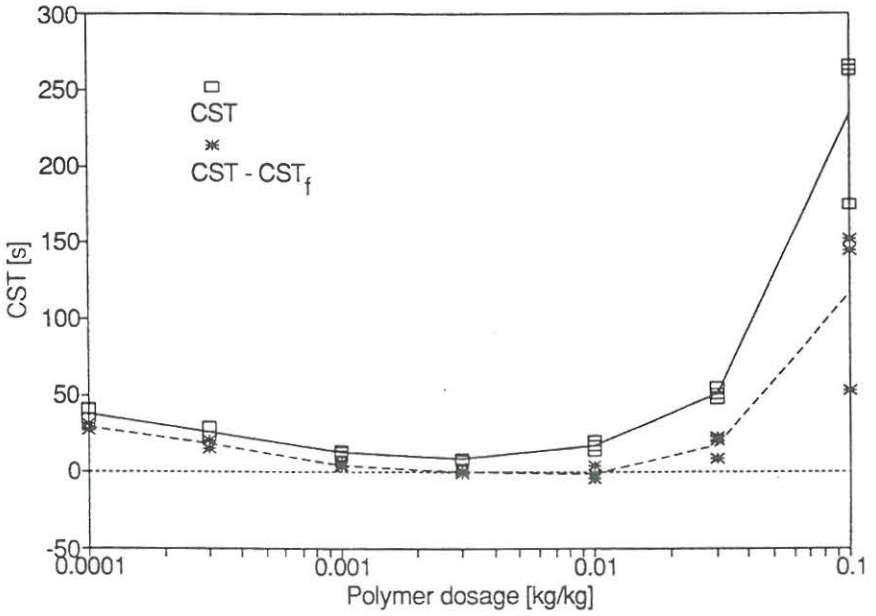

Figure 5

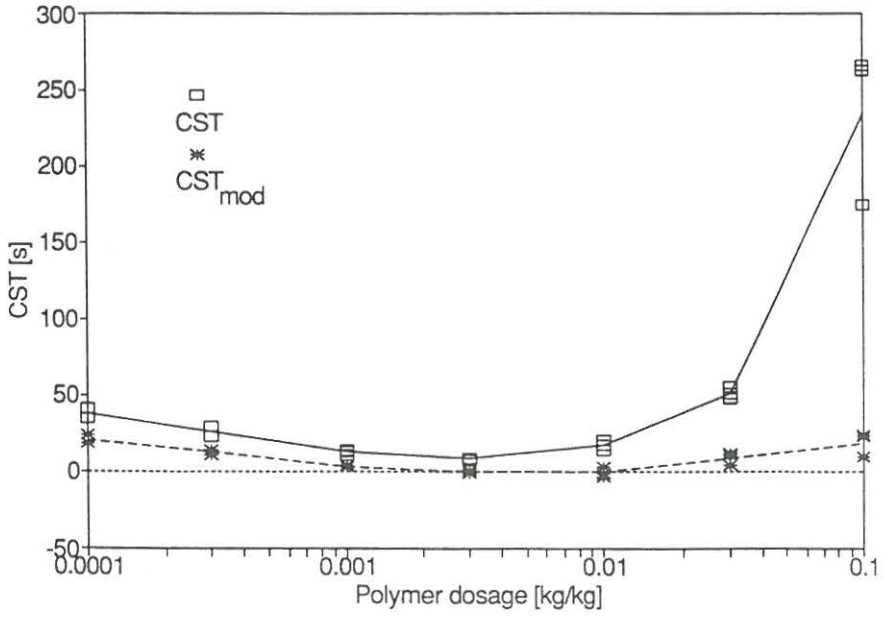

Figure 6

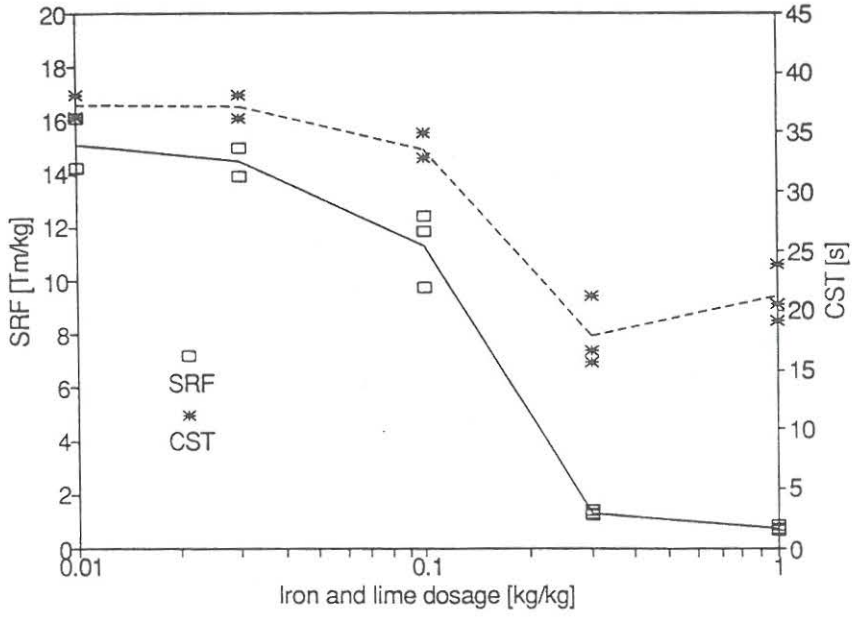

Figure 7

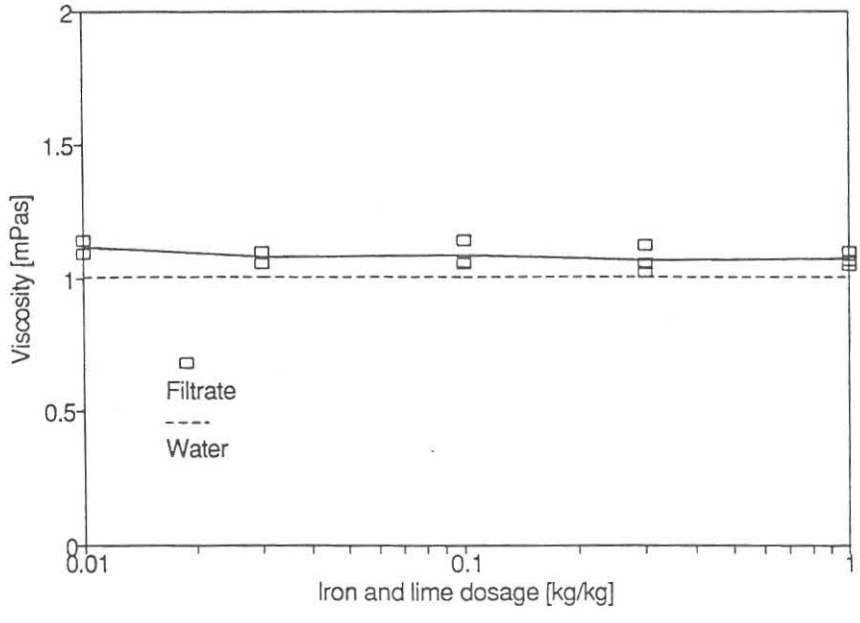

Figure 8

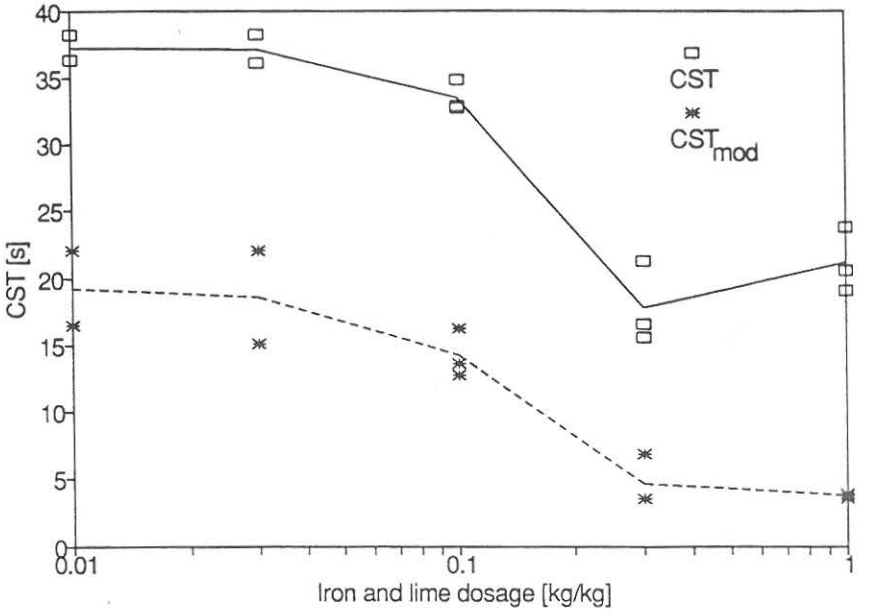
40
35
30
25
20
15
10
5
0
CST [s]
0.01
0.1
1
Iron and lime dosage [kg/kg]
CST
CST$_{mod}$

Figure 9

Control of Polymer Sludge Conditioning

V

Control of Polymer Sludge Conditioning

Jimmy R. Christensen and Peter B. Sørensen

Environmental Engineering Laboratory
Department of Civil Engineering
Aalborg University
Denmark

ABSTRACT

Laboratory-scale polymer conditioning of sludges from different wastewater treatment plants has been investigated. A general response to polymer sludge conditioning was exhibited by different sludges examined: (1) the polymer dosage yielding optimal sludge filterability provided also the highest solids capture, (2) in the underdosed region, improvement of conditioned sludge filterability was closely related to decreasing filtrate turbidity, and (3) in the overdosed region, the deterioration of conditioned sludge filterability was closely related to increasing filtrate viscosity. If the sludges were not optimally conditioned with polymer, non-linear filtration data was shown to more the rule than the exception. A parabolic equation could adequately fit any such non-linear filtration curves. The second order coefficient of the parabolic equation was positive if the sludges were underdosed, but negative if the sludges were overdosed. Based on these findings, two different methodologies for controlling optimal polymer conditioning were suggested: (1) obtaining a second order coefficient of zero, and (2) achieving minimum filtrate turbidity and viscosity. Of these, the latter seemed most promising with respect to establishing automatic, on-line control of optimal full-scale polymer conditioning prior to sludge dewatering. However, further practical developments were necessary before the application of this methodology could be evaluated in full-scale.

INTRODUCTION

The objectives of full-scale sludge dewatering and management are to separate the sludge liquid and solid phases to a desired level, and to secure proper ultimate disposal or utilization of the dewatered sludge. The expenses associated with sludge dewatering and management on two wastewater treatment plants (WWTPs) in Aalborg (Denmark) are summarized in Table 1. Both plants apply the activated sludge process for wastewater treatment performing biological removal of organic matter, nitrogen and phosphorous. At the Aalborg East WWTP only secondary sludge is dewatered while both secondary and anaerobically digested primary sludge are dewatered at the Aalborg West WWTP. In both cases, however, cationic organic polymers are used as conditioning chemicals, belt filter presses are applied for sludge dewatering, and dewatered sludge is deposited close to the plant on land dedicated for this particular purpose.

According to Table 1, approximately 30% of the costs associated with WWTP operation are attributed to sludge dewatering and management. Consumption of conditioning chemicals, in turn, is responsible for approximately 50% of the cost items associated with sludge dewatering. As these costs are significant compared with overall plant operation, incentives for an economical optimization of sludge dewatering are obvious. Commonly suggested constituents of optimization methodologies regarding full-scale sludge dewatering are: (1) minimum use of conditioning chemicals, in this case polymers, (2) minimum volumes of dewatered sludge cake (maximum solids concentration of the cake), (3) maximum yield of dewatering equipment, and (4) maximum solids capture ("cleanest" return flow).

Currently, however, the optimization of full-scale sludge conditioning and dewatering operations are in most cases empirically based, and only in a few cases automatic control of sludge conditioning has been successfully applied (e.g. Crawford, 1989). Therefore, it is the objective of the present study to examine laboratory-scale sludge dewatering in order to identify appropriate characteristic parameters which, ultimately, may be used for achieving automatic control of optimal polymer sludge conditioning. The present study is, however, primarily confined to dewatering by filtration.

EXPERIMENTAL PROCEDURES

Sludge and polymer source.

Samples of activated sludge were collected at Aalborg East, Asaa, and Aabybro WWTPs. Aalborg East and Aabybro WWTPs, having sludge ages above 30 days, perform biological removal of organic matter, nitrogen and phosphorous. Asaa WWTP, of which the sludge age is below 10 days, is only performing biological removal of organic matter. A high molecular weight, high charge density cationic polymer (Praestol 644 BC) was used as sludge conditioner in all experiments. Polymer solutions of 1% w/V were prepared approximately one hour before use each day of experimentation.

Sludge conditioning and dewatering tests.

Sludge conditioning was carried out using impeller agitation in a baffled, cylindrical mixing vessel. The paddle impeller used was operated at a constant rotational speed of 500 *rpm*, and 60 *s* of mixing was applied following polymer addition. More detailed information regarding the mixing arrangement is provided elsewhere (Christensen et al., 1993). In the present study, relatively broad ranges of polymer dosages were applied in order to examine certain phenomena in extreme situations and not with the purpose of matching full-scale conditions. Sludge dewatering properties were assessed by filterability and settleability measurements. Sludge filterability was characterized by Specific Resistance to Filtration (*SRF*) based on filtration tests performed using a pressurized cylinder and a computerized data acquisition system (Christensen et al., 1993). The applied pressure was always 10^5 *Pa*. Sludge settleability was characterized by the Initial Settling Rate (*ISR*) of settling tests which were carried out in a 1 *l* graduated cylinder.

Filtrate characterization.

Filtrate generated during filtration tests was characterized by its viscosity and turbidity. Viscosity measurements were performed using a Brookfield LVT-DVII concentric cylinder rotational viscometer having inner cylinder (spindle) rotation. The spindle was operated at a rotational speed of 60 *rpm* which corresponded to a Newtonian shear rate of approximately 75 s^{-1}. The gap between the two concentric cylinders was approximately 1 *mm*. Turbidity was characterized as the light absorption at a wavelength of 650 *nm* using a Milton Roy Spectronic 301 spectrophotometer.

RESULTS AND DISCUSSION

Filtrate quality related to sludge filterability.

Because the objective is to relate filtrate characteristics to filtration properties of conditioned sludge, only filtrate turbidity and viscosity is considered. However, other filtrate characteristics relating to wastewater treatment might be relevant as well, e.g. *COD*, nitrogen and phosphorous concentrations.

Corresponding measurements of *SRF* and filtrate turbidity and viscosity are shown in Figs. 1 to 4. Even though the sludge samples are from three different WWTPs, a general relationship between minimum *SRF* and minimum filtrate turbidity is indicated. That is, optimal filterability and highest solids capture are obtained at the same polymer dosage. Similarly to the results presented by Christensen et al. (1993), the filtrate viscosity increases in the overdosed region; in fact, the filtrate viscosity seems to increase slightly just before optimal sludge filterability is obtained. However, the viscosity measurements are generally not as accurate and responses to increasing polymer dosages not as pronounced as for the turbidity measurements.

Figs. 2 and 3 represent measurements on the same original sludge source (Asaa WWTP) but at different periods of anaerobic storage in the laboratory. By comparing fresh activated sludge (Fig. 2) and stored sludge (Fig. 3) it is seen that the optimal polymer dosage increases with respect to *SRF* as well as solids capture (minimum filtrate turbidity) during anaerobic storage. Apparently, the polymer conditioning mechanisms resulting in optimal filterability and highest solids capture seem to be identical.

Filtrate characterization during filtration and expression.

Viscosity and turbidity are measured several times during filtration/expression experiments in order to investigate the variations of these variables. Generation of filtrate for such measurements is accomplished using a slightly modified version of the *SRF* device described earlier in that a nylon piston is inserted on top of the sludge sample in the pressurized cylinder (Sørensen et al.). This procedure makes it possible to investigate both filtration and expression stages as established in full-scale filter presses, in the same time avoiding shrinkage effects (Bierck and Dick, 1990).

The application of the piston in the pressurized filtration device slightly reduces the actual pressure difference for filtration/expression compared with the applied pressure. However, because polymer conditioned sludge exhibits extremely compressible behaviour, the filtrate flow rate during filtration and most of expression is independent on the actual pressure difference (Sørensen and Hansen). This claim is experimentally supported by comparing *SRF* calculations based on filtration tests in which pressurized air and a piston, respectively, provide the driving dewatering force. The influence on filtrate characteristics are also evaluated, and to secure filtrate viscosities significantly different from that of water, a very high polymer dosage (50 *kg/tDS*) is applied for these tests. Further, to compare viscosity and turbidity of filtrate and supernatant, respectively, settling tests are performed at the same polymer dosage. Mean values and standard deviations of four replicates are presented in Table 2, according to which there is no statistical

evidence for a difference between neither the two set of *SRF* values nor between viscosity and turbidity of filtrate and supernatant. In addition, a good reproducibility of all tests and measurements are evidenced.

The filtrate from the piston filtration tests is collected in several 50 *ml* beakers. The content of these beakers are weighed on an electronic balance to supply data for filtration plots (Fig. 5) and samples for viscosity and turbidity measurements (Figs. 6 and 7). Cease of filtrate generation recorded in one minute is the arbitrary stop criterion used for the filtration/expression tests.

All filtration plots (Fig. 5) are more or less non-linear. In such cases, the cake filtration theory governing *SRF* does not apply, because this theory requires linear filtration plots. As a consequence, *SRF* is not valid. The most pronounced non-linear filtration behaviour is associated with the lowest applied polymer dosage. Sørensen et al. attributed such filtration behaviour, and the corresponding filtrate turbidity curve in Fig. 6, to complex interactions between a compression of the porous cake structure and deposition of small-scale solids, designated strange filtration behaviour. Less pronounced strange filtration behaviour may be the reason for filtrate turbidity measurements (Fig. 6) having no general tendency during filtration besides the definite drop in the initial stages of filtration. Even when the separation process changes from filtration to expression (at a filtrate volume of approximately 750 *ml*), no general tendency is exhibited.

Filtrate viscosity measurements (Fig. 7), on the other hand, all show a general tendency towards less viscous filtrate as filtration/expression advances. At the highest polymer dosage (considerably overdosed) there are dramatic changes in viscosity, both within the filtration and the expression stages. Apparently, more and more of the excess polymer associated with the sludge liquid phase, responsible for the overdosing behaviour, is adsorbed to the sludge cake matrix during filtration. This may be explained by a higher deep-bed filtration efficiency associated with the sludge cake build-up during filtration. In addition, the liquid residence time within the sludge cake increases during filtration both as a result of increasing sludge cake depth and decreasing filtrate flow rates.

Average values of filtrate turbidity (Fig. 6) and viscosity (Fig. 7) are presented in Table 3. The most pronounced and significant difference between characteristics of liquid from the filtration

and expression stages is associated with the viscosity of overdosed sludge (50 *kg/tDS*). Differences are also indicated by turbidity measurements, but because the expression stage is only responsible for a minor part of the total production of liquid and the variations of turbidity during filtration/expression are not adequately described, these differences are not considered being significant. Also in this case (Table 3), the polymer dosages yielding optimal filterability (*SRF*) and highest solids capture coincide.

Non-linear filtration data related to sludge liquid phase characteristics.

As illustrated in Fig. 5, it seems to be more the rule than the exception that filtration data associated with *SRF* tests exhibit non-linear behaviour if the sludge is not optimally conditioned with polymer. More accurate *SRF* tests using the computerized data acquisition system confirm this finding (Figs. 8 and 9). Underdosed sludge clearly exhibit a concave filtration behaviour while the curvature associated with overdosed sludge is convex. The distinct non-linear behaviours are of course emphasized by the use of filtration plots constituted by the inverse filtration rate (dt/dV) versus accumulated filtrate volume (V) instead of the more commonly used accumulated time divided by accumulated volume (t/V) versus V. However, the former always provides a more adequate characterization of the dynamics associated with filtration than the latter (Sørensen et al.).

Concave filtration behaviour of unconditioned sludges similar to the ones associated with underdosed sludges is commonly attributed to small-scale solids (turbidity) migration in sludge cakes during filtration, designated "blinding" (Notebaert et al., 1975; Novak et al., 1988; Sørensen et al.). In order to describe non-linear filtration behaviour, Sørensen et al. derived a parabolic equation (Eq. 1) which adequately fitted any non-linear filtration data associated with blinding of unconditioned sludge.

$$\frac{dt}{dV} = a \cdot V^2 + b \cdot V + c \qquad (1)$$

It turns out that Eq. 1 is also able to fit the non-linear filtration curves evident in the underdosed as well as in the overdosed regions of polymer dosages. The second order coefficients (a) and first order coefficients (b) of several filtration curves are determined as a function of a broad range of polymer dosages (Fig. 10) and a more narrow range of polymer dosages (Fig. 11). In both cases, however, a value of a equal to zero approximately corresponds to the minimum value of b and, consequently, this situation yields optimal filterability.

As unconditioned sludge is the extreme case of underdosing, the mechanisms for development of non-linear filtration plots in the underdosed region of polymer dosages is probably similar to the mechanisms responsible for blinding of unconditioned sludge (Sørensen et al.). Because the second order coefficient as well as the filtrate turbidity decrease as the polymer dosage approaches the optimal dosage, this hypothesis is supported. However, filtrate turbidity characterizes the amount of small-scale solids that passes through the sludge cake and not the ones which are deposited within the cake causing blinding. According to Sørensen et al., final evidence for the blinding hypothesis requires a universal relationship between the amount of small-scale solids in the sludge liquid phase, e.g. supernatant, and the blinding coefficient.

In the overdosed region of polymer dosages, on the other hand, the most pronounced effects are on the sludge liquid phase viscosity which increase due to the presence of excess polymer (Christensen et al., 1993). Corresponding filtration data and filtrate viscosity measurements for a considerably overdosed sludge (dosage of 50 *kg/tDS*) is used to compare the actual flow rate (designated "measured") with the flow rate normalized (divided) by filtrate viscosity (designated "corrected") as shown in Fig. 12. By normalizing the filtrate flow rate with filtrate viscosity, the decrease in the specific flow resistance during filtration yielding a negative value of the second order coefficient vanishes; in fact, the specific flow resistance actually increases in the initial stages of filtration.

Because filtrate associated with overdosed sludge may be considered as dilute polymer solutions (Christensen et al., 1993), the non-linearities associated with the "corrected" filtration curve in Fig. 12 may be explained by a pseudoplastic, non-Newtonian behaviour of the sludge liquid phase. During filtration, decreasing flow rates reduce the flow velocity in the cake pores and thereby the velocity gradients. Decreasing velocity gradients, in turn, increase the apparent

viscosity of the sludge liquid phase thereby increasing the specific flow resistance, though most pronounced in the initial stages of filtration. Consequently, the development of non-linear filtration behaviour in the overdosed region of polymer dosages is partly explained by a continuous decrease in sludge liquid phase viscosity due to deep-bed filtration of excess polymer in the sludge cake, partly by a pseudoplastic behaviour of the sludge liquid phase.

Practical perspectives.

When using a laboratory-scale filtration device, the polymer conditioning mechanisms yielding optimal filterability and highest solids capture seem similar. Consequently, it may be possible to optimize both the yield (or capacity) of full-scale dewatering equipment and the return flow quality at approximately identical polymer dosages. Based on the discussions above, adjustments of the polymer dosage yielding an optimal situation in full-scale may be controlled in two ways:

* If filtration is the dewatering mechanism to be optimized, second order coefficients of a parabolic equation fitting laboratory-scale filtration data will be positive in the underdosed region but negative in the overdosed region of polymer dosages.

* With respect to dewatering equipment producing return flow continuously, turbidity and viscosity measurements on the return flow will identify both underdosing (high levels of turbidity) and overdosing (high levels of viscosity). Of these, turbidity seems most promising because it is related to the underdosed region of polymer dosages and is more sensitive than viscosity.

In order to make a continuous control of optimal full-scale polymer conditioning operational, the control procedure ought to be based on an automatic, on-line data registration and management to avoid uneconomical requirements for skilled technicians to carry out the tests. It is, however, not immediately obvious how to develop an on-line procedure regarding the filtration tests. In this respect, turbidity (and viscosity) measurements on the return flow seem more promising.

A procedure for an automatic, on-line control of full-scale polymer conditioning based on rheological measurements on conditioned sludge has been shown to work quite well (Crawford, 1989). But, taking the difficulties associated with rheological measurements into account, especially on well-conditioned sludge, it seems more readily accessible to rely on measurements on the more well-defined return flow. Even though return flow is more well-defined than conditioned sludge, there are still practical problems to be met before the suggested polymer control procedure can be expected to work in full-scale. For example:

* The quantities of small-scale solids or excess polymer responsible for underdosing and overdosing, respectively, may in some cases be quite small and as a result difficult to detect and distinguish between in the proximity of the optimal polymer dosage. According to Figs. 6 and 7, this problem may, however, be less serious if turbidity and viscosity are measured as early as possible in the dewatering stage (e.g. the drainage stage of belt filter presses) because such values would be higher than the respective average values associated with the return flow.

* It must be certified that the measured values of turbidity is equivalent to the existence of small-scale solids (Sørensen et al.) and not just some coloured substances with no impact on the dewatering result.

* It must be possible to obtain return flow which is not (strongly) affected by any type of washing water (e.g. in case of belt filter pressing).

CONCLUSIONS

Corresponding measurements of conditioned sludge filterability and filtrate turbidity and viscosity using sludges from three different WWTPs show identical responses. In the underdosed region, increasing polymer dosages simultaneously improve sludge filterability and reduce

filtrate turbidity while in the overdosed region, increasing polymer dosages simultaneously reduce filterability and increase filtrate turbidity as well as filtrate viscosity. The polymer dosage yielding optimal filterability and minimum filtrate turbidity coincides for each sludge source.

If not optimally conditioned with polymer, the assumed straight-line behaviour of filtration data are more the exception than the rule. The development of non-linear filtration plots is caused by sludge liquid phase characteristics. Concave filtration behaviour is attributed to blinding (underdosing) caused by small-scale solids migration in sludge cakes during filtration while the presence of excess polymer in the sludge liquid phase due to polymer overdosing is responsible for convex filtration behaviour.

Because the cake filtration theory governing *SRF* fails to adequately describe such phenomena, a parabolic equation is used to fit non-linear filtration data. With respect to this parabolic equation, a positive second order coefficient reflects blinding (underdosing) while a negative second order coefficient reflects polymer overdosing. In the underdosed region of polymer dosages, improvement of conditioned sludge filterability is accompanied by decreasing filtrate turbidity. In the overdosed region, on the other hand, the deterioration of conditioned sludge filterability is accompanied by increasing filtrate viscosity and turbidity. As a result, a second order coefficient equal to zero corresponds to both optimal filterability and less turbid filtrate.

Based on these general responses, two methodologies for controlling the optimal polymer dosage for sludge conditioning are proposed: (1) using filtration tests to identify the polymer dosage yielding a second order coefficient approximately equal to zero, and (2) using measurements of turbidity and viscosity on the return flow to determine the optimal polymer dosage based on their relation to underdosing (turbidity) and overdosing (viscosity), respectively. However, only the latter seems operational in practice but before this procedure may be applied in full-scale, some practical problems has to be addressed and solved.

REFERENCES

Bierck, B.R., and Dick, R.I., (1990), "Mechanisms of Compressible Sludge Cake Filtration", Journal of Environmental Engineering, ASCE, Vol. 116, No. 4, pp. 168-188.

Christensen, J.R., Sørensen, P.B., Christensen, G.L., and Hansen, J.Aa., (1993), "Mechanisms for Overdosing in Sludge Conditioning", Journal of Environmental Engineering, Vol. 119, No. 1., pp. XX-XX (in press).

Crawford, P.M., (1989), "Optimizing Polymer Consumption in Sludge Dewatering Applications", EWPCA/IAWPRC Conference Preprints, Munich.

Notebaert, F.F., Wilms, D.A., and Van Haute, A.A., (1975), "A New Deduction with a Larger Application of the Specific Resistance to Filtration of Sludges", Water Research, Vol. 9, pp. 667-673.

Novak, J.T., Goodman, G.L., Pariroo, A., and Huang, J.-C., (1988), "The Blinding of Sludges During Filtration", Journal of the Water Pollution Control Federation, Vol. 60, No. 2, pp. 206-214.

Sørensen, P.B., Bruus, J.H., and Christensen, J.R., "Effects of Small Scale Solids Migration in Sludge Cakes during Filtration of Wastewater Solids Suspensions", Water Environment Research (submitted).

Sørensen, P.B., and Hansen, J.Aa., "Extreme Compressibility in Biological Sludge Dewatering", Water Science and Technology (accepted).

FIGURE LEGENDS

Fig. 1. Filtrate turbidity and viscosity compared with *SRF* of conditioned sludge (Aalborg East WWTP).

Fig. 2. Filtrate turbidity and viscosity compared with *SRF* of conditioned sludge (Asaa WWTP - Fresh sludge).

Fig. 3. Filtrate turbidity and viscosity compared with *SRF* of conditioned sludge (Asaa WWTP - Stored sludge).

Fig. 4. Filtrate turbidity and viscosity compared with *SRF* of conditioned sludge (Aabybro WWTP).

Fig. 5. Filtration curves associated with filtrate turbidity and viscosity measurements during filtration/expression. The two lowest polymer dosages relate to the right y-axis.

Fig. 6. Filtrate turbidity versus filtrate volume at different polymer dosages.

Fig. 7. Filtrate viscosity versus filtrate volume at different polymer dosages.

Fig. 8. Filtration curves for polymer conditioned sludge (extreme dosages).

Fig. 9. Filtration curves for polymer conditioned sludge.

Fig. 10. Second order coefficient (a) and first order coefficient (b) for the filtration curves versus polymer dosages. Mechanisms for non-linear filtration behaviour are indicated.

Fig. 11. Second order coefficient (a) and first order coefficient (b) versus polymer dosages.

Fig. 12. Illustration of the impact of liquid phase (filtrate) viscosity on filtration behaviour.

Table 1. Costs associated with sludge dewatering and management at two larger Danish WWTPs (Aalborg East and Aalborg West, 1990).

Treatment plant		EAST (%)	WEST (%)
Wastewater treatment		74	70
Sludge dewatering		15	21
Sludge management		11	9
Dewatering of sludge (100 %)	Wages	31	27
	Machinery	11	15
	Chemicals	52	50
	Electricity	3	6
	Sampling	3	2
Management of sludge (100 %)	Wages	41	40
	Machinery	42	21
	Land	7	37
	Sampling	10	2

Table 2. Comparisons between *SRF* using two procedures for the filtration tests as well as turbidity and viscosity of filtrate and supernatant, respectively.

Param.	*SRF* (air)		*SRF* (piston)		Settling test	
-	mean	st. dev.	mean	st. dev.	mean	st. dev.
SRF [*Tm/kg*]	0.422	0.019	0.414	0.025	-	-
ISR [*mm/s*]	-	-	-	-	0.858	0.041
μ [$mPa \cdot s$]	2.31	0.14	2.37	0.09	2.56	0.06
Turb. [*NTU*]	93	4	101	3	106	18

Table 3. Average values of turbidity and viscosity for the filtration stage (subscript *f*) and for the expression stage (subscript *e*), respectively. Sludge filterability (*SRF*) is presented for comparisons.

Polymer dosage	Filtrate turb.	μ_f	Express. turb.	μ_e	*SRF*
kg/tDS	*NTU*	$mPa \cdot s$	*NTU*	$mPa \cdot s$	*Tm/kg*
0.5	76	1.14	100	1.11	18.37
1	60	1.08	71	1.06	7.40
3	62	1.11	39	1.12	0.52
10	41	1.17	37	1.09	0.22
50	62	2.52	23	1.40	1.52

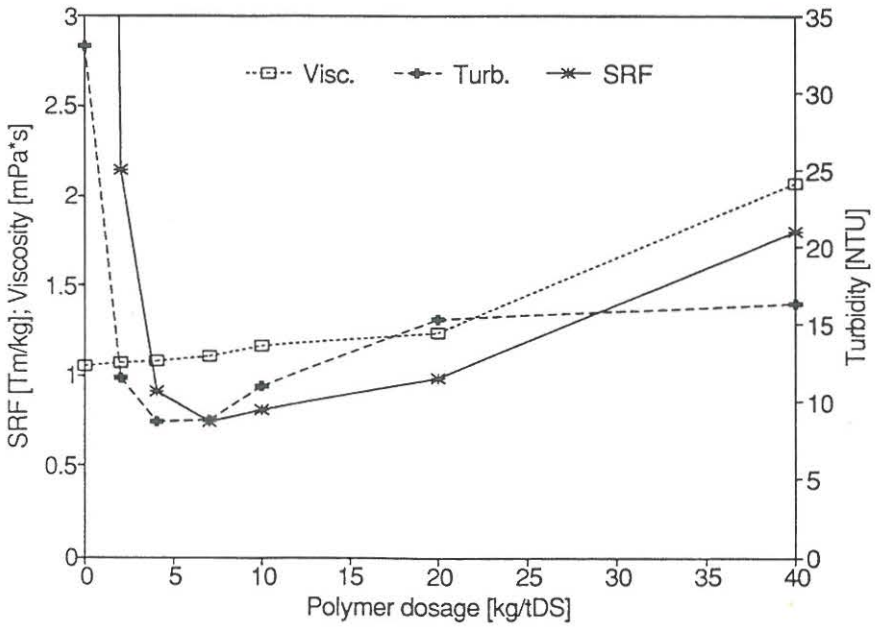

Figure 1

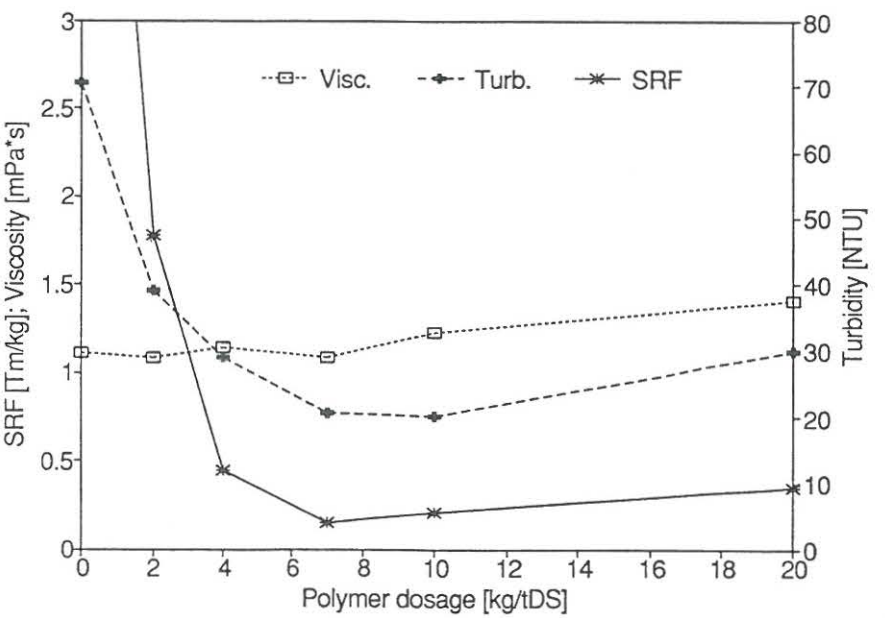

Figure 2

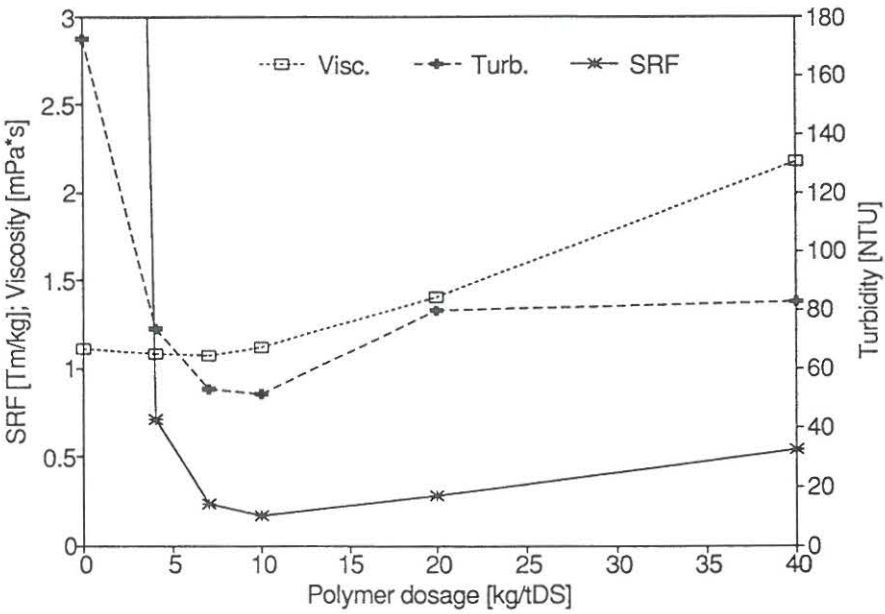

Figure 3

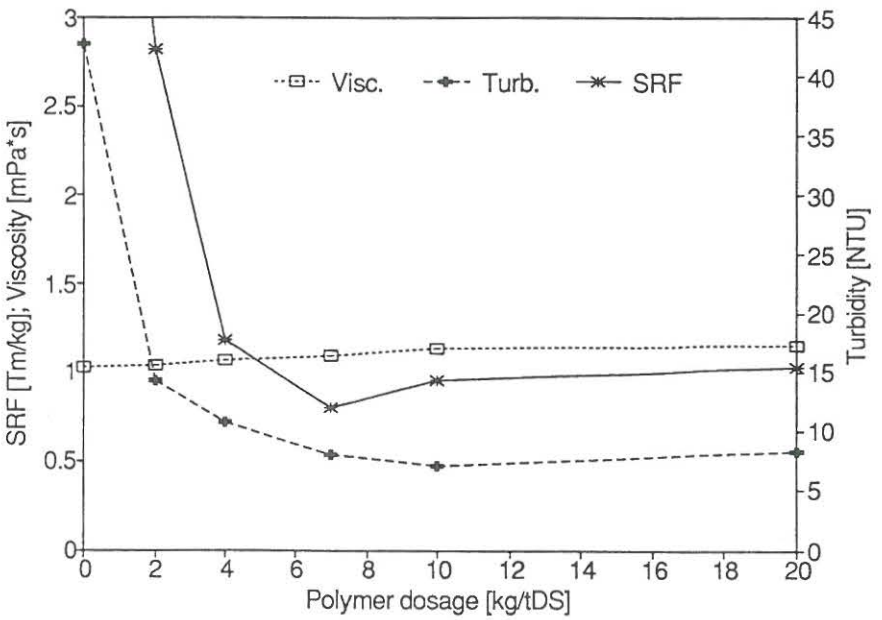

Figure 4

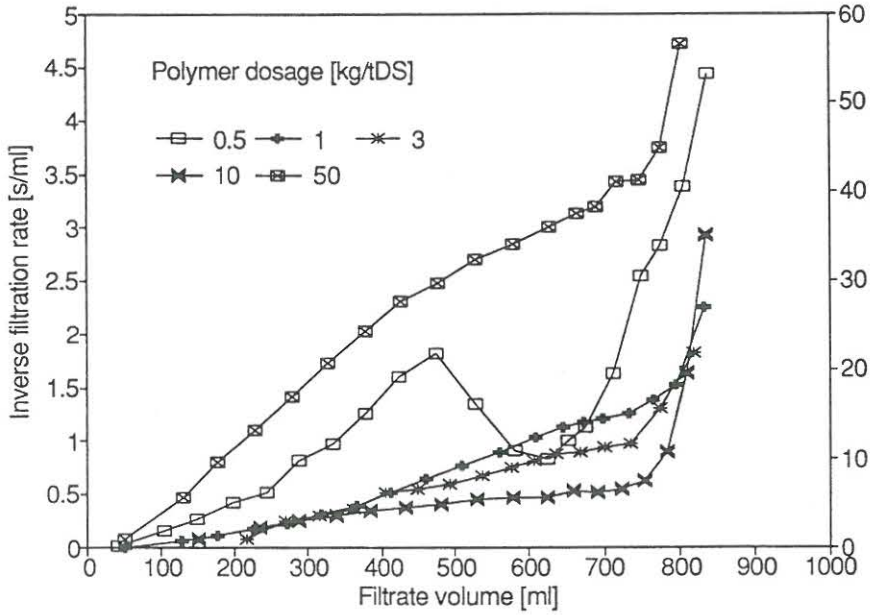

Figure 5

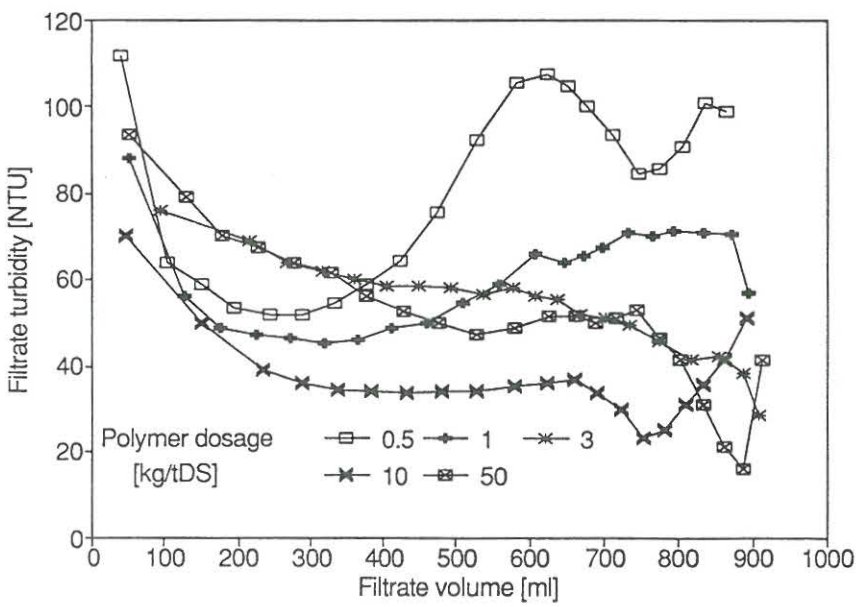

Figure 6

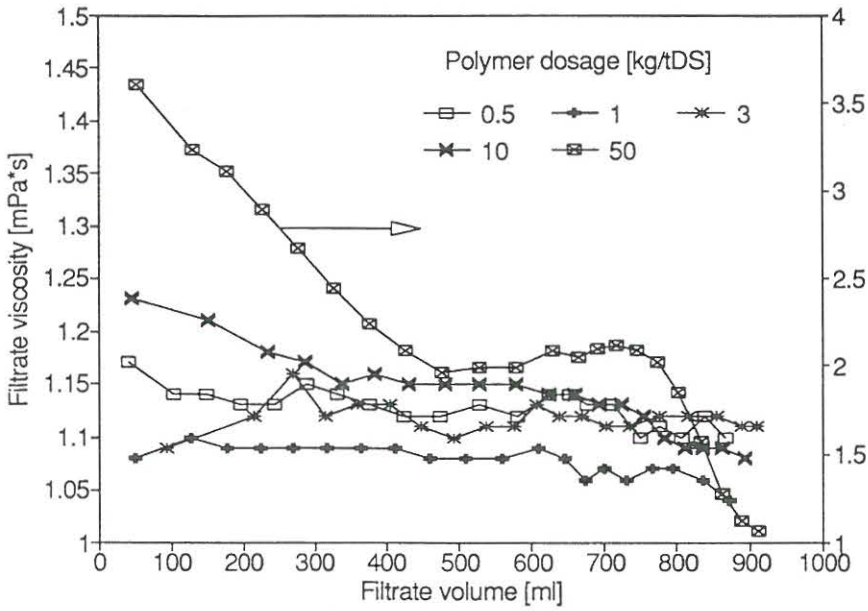

Figure 7

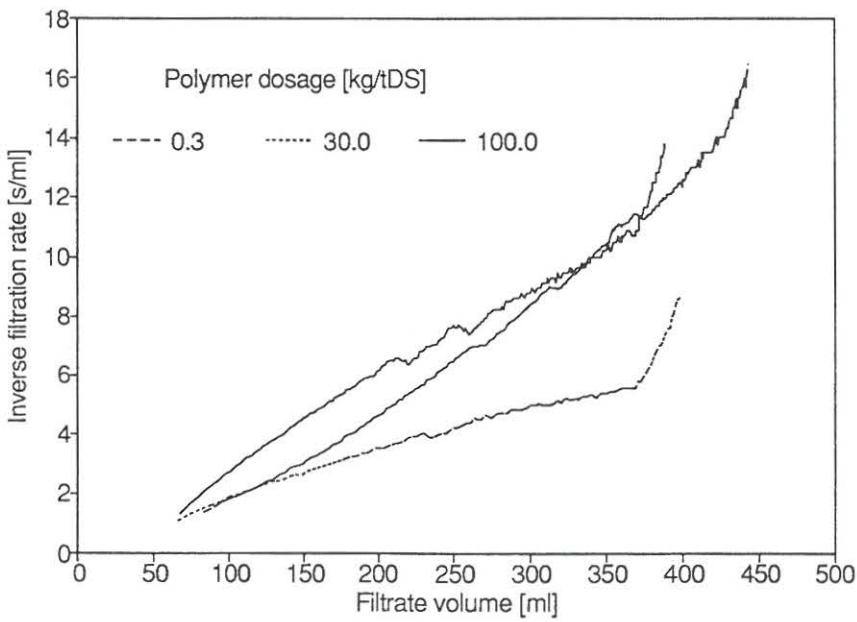

Figure 8

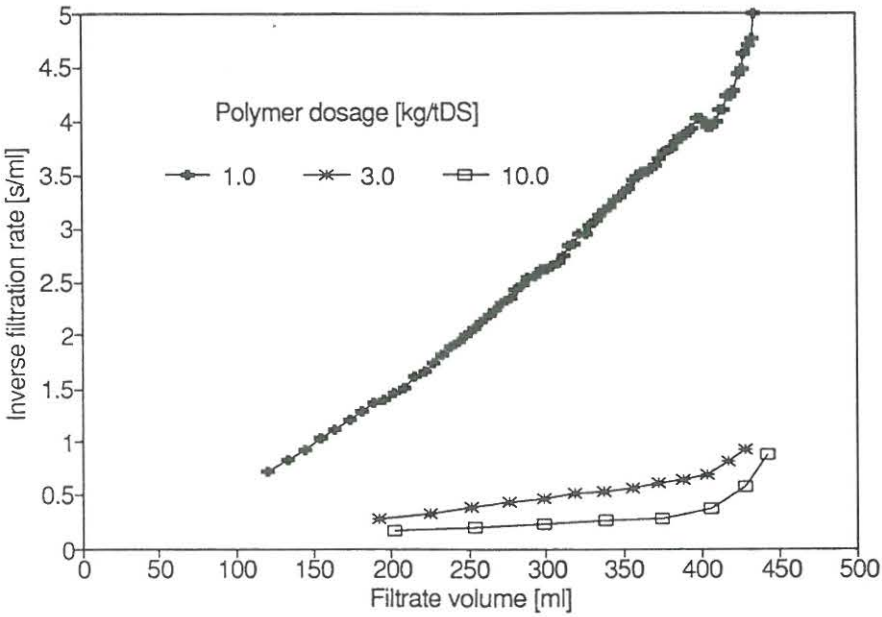

Figure 9

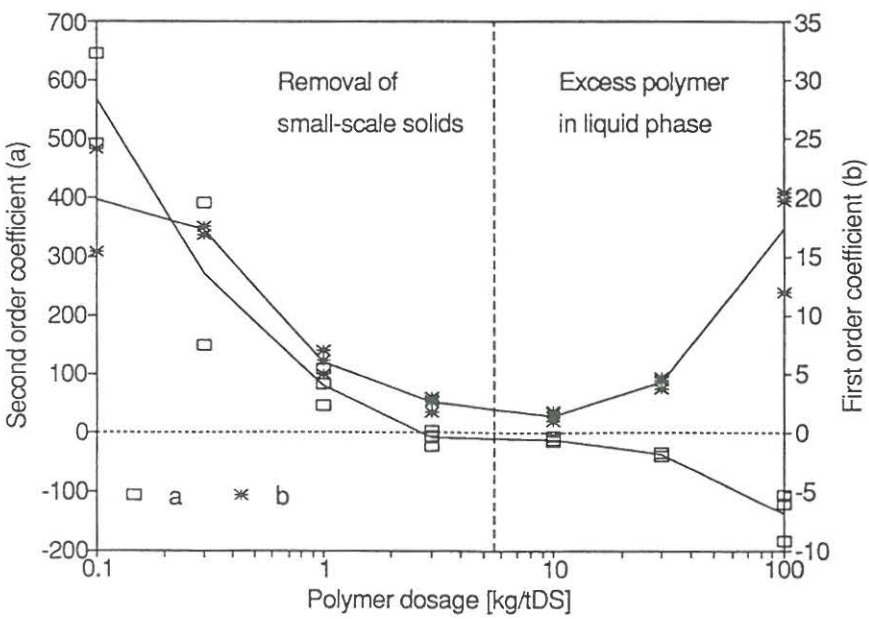

Figure 10

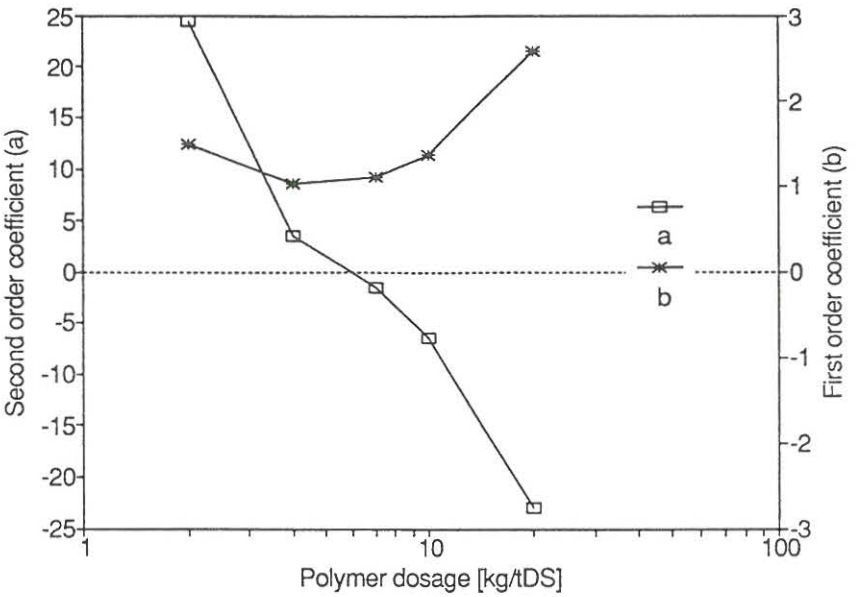

Figure 11

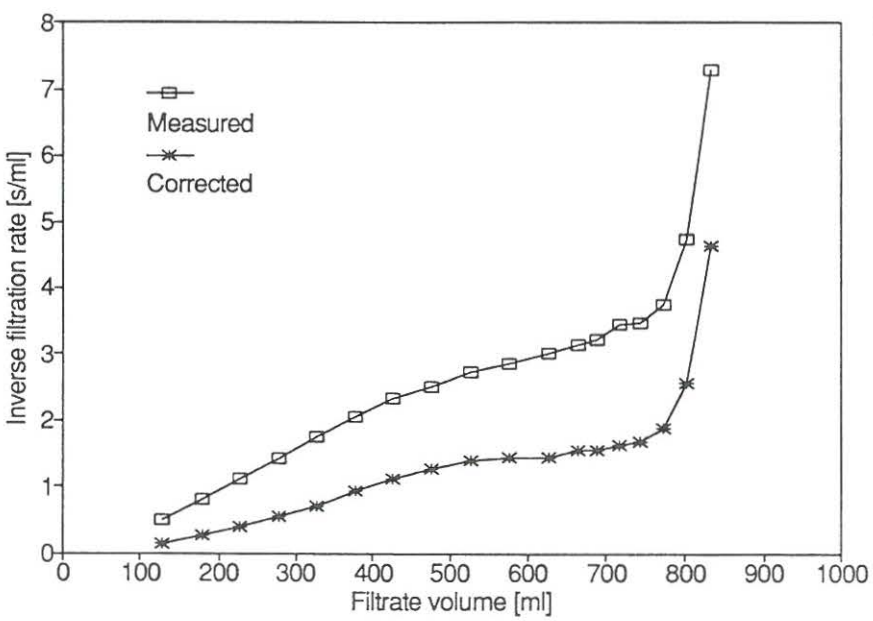

Figure 12

ISBN 87-90033-00-0